Boston University

OpenBU **http://open.bu.edu**

Mechanical Engineering ENG: Mechanical Engineering: Scholarly Papers

1963

Generalized Method of Propeller Performance Estimation 1961-1963

Hamilton Standard. Generalized Method of Propeller Performance Estimation 1961-1963. Windsor Locks, CT: 1963.
https://hdl.handle.net/2144/10454
Boston University

PDB 6101

GENERALIZED METHOD OF PROPELLER PERFORMANCE ESTIMATION

WORCESTER POLYTECHNIC INSTITUTE LIBRARY

This document discloses subject matter in which United Aircraft Corporation has proprietary rights. Neither receipt nor possession thereof confers or transfers any right to reproduce or disclose the document, any part thereof, any information contained therein, or any physical article or device, or to practice any method or process, except by written permission from, or written agreement, with United Aircraft Corporation.

HAMILTON STANDARD

Hamilton Standard DIVISION OF UNITED AIRCRAFT CORPORATION
WINDSOR LOCKS, CONNECTICUT • U.S.A.

June 28, 1963

To: Holders of Hamilton Standard PDB 6101

Subject: Revision 'A' to Hamilton Standard PDB 6101, "Generalized Method of Propeller Performance Estimation"

Gentlemen:

We issued PDB 6101 in early 1961 for use in the preliminary design effort associated with advanced propeller driven aircraft. Since that time, the data contained in PDB 6101 has been expanded to cover a wider range of propeller parameters. In addition, several supplements have been prepared. To make this additional data available to all holders of PDB 6101, we have prepared Revision 'A' which includes the following:

1. Twenty six (26) new performance charts. These include static and flight performance data for 80 and 220 activity factor 3 and 4 bladed propellers as well as static performance data for 120, 160, and 200 activity factor 3 and 4 bladed propellers.

2. Addition of 3 supplements (A, B, and C) presenting methods of weight generalization, noise prediction, and nacelle blocking and compressibility corrections.

In order to incorporate the above into your present manual, the following items are also provided:

a) Revised "Table of Contents"
b) Revised "Introduction"
c) Corrected "Performance Calculation Procedure" and "Sample Computation"
d) Added "Table of Figures"
e) Five (5) index tab sheets
f) Key for re-numbering present charts

The twenty-six (26) new curves have been numbered to provide a systematic arrangement when combined with your present charts. This requires re-numbering of your present charts in accordance with the enclosed key sheet.

HAMILTON STANDARD DIVISION
United Aircraft Corporation

Preliminary Design Group

GENERALIZED METHOD OF PROPELLER PERFORMANCE ESTIMATION

TABLE OF CONTENTS

Title	Page No.
INTRODUCTION	1
PERFORMANCE CALCULATION PROCEDURE	3
TABLE OF FIGURES	6
LIST OF COEFFICIENTS AND SYMBOLS	7
SUPPLEMENTS	

INTRODUCTION

The advent of a new generation of special purpose turboprop aircraft with stringent propulsion requirements has focused increased emphasis on propeller selection and accurate performance assessment during the early stages of defining the aircraft configuration. Since the majority of these new aircraft types are characterized by requiring high propeller performance at the extremities of their flight regime, it is essential that a reliable means of assessing the best propeller compromise be available. Having recognized the deficiencies of existing short-form propeller performance methods for such usage, Hamilton Standard is presenting this manual, which reflects the most recent refinements in propeller aerodynamics in a relatively simple form, for use in the preliminary design effort associated with advanced turboprop aircraft. This manual may also be utilized for conventional free air propeller performance appraisal for both turboprop and reciprocating engine application.

This report provides a generalized performance calculation method for aircraft propellers operating at static and in-flight conditions. The form of method selected was governed primarily by the considerations of ease of usage, and the elimination of the principle deficiency of existing empirical methods -- the deterioration of accuracy at extreme operating conditions and blade geometries. Accordingly, the method incorporates a series of performance maps -- each accurately defining the propeller performance for a specific propeller geometric configuration over the complete range of potential operating conditions. By providing such charts for a systematic variation of each major propeller shape parameter, simple interpolation between charts will define performance for any desired propeller configuration.

Data is presented to cover both three and four way propellers with blade activity factors ranging from 80 to 220 and blade integrated design lift coefficients ranging from 0.150 to 0.700. The data is limited to conditions when the compressibility effects are small; however, if these limits are exceeded, a compressibility correction procedure is provided in Supplement B.

Most recent refinements in the strip analysis method have extended the data to cover the static operating regime. Separate curves covering the static regime are also included. For each in-flight performance map there is a static performance curve for that same propeller configuration. Additional static performance curves are included for intermediate activity factor levels.

In addition to the basic charts, the manual also provides optimum or ideal performance curves for both static and flight operation simply for use as a measure of degree of compromise by permitting a comparison of actual performance levels of the chosen propeller to the ideal level. The optimum or ideal performance curves represent the performance of propellers with minimum induced losses and zero profile losses for a finite number of blades. Thus, an actual propeller design can never equal the optimum, but by careful tailoring for the degree condition it is possible to approach the optimum or ideal performance.

The performance in this report has been based on a constant velocity through the propeller disc since the blocking effects (viz; the actual velocity through the propeller disc) varies greatly from installation to installation. These blocking effects do have an influence on the absolute levels of performance; however they do not change the comparative performance levels of propellers of different designs; therefore the elimination of blocking effects from the procedure will not detract from the usefulness of the method. In general, blocking also has the same affect on the optimum or ideal efficiency as on the calculated efficiency. Generalized nacelle blocking corrections for typical scoop and annular inlets are included in Supplement B.

Also included are Supplements A and C which provide means of estimating weight and noise levels.

PERFORMANCE CALCULATION PROCEDURE

The method of calculating the static and flight performance as described in the Introduction is presented below. A sample computation form is included at the end of this section; a vellum, Figure 60, is also included and may be used for making copies of the form for computations.

With the airplane flight and engine conditions given, and the propeller blade characteristics known, the procedure as outlined on the sample computation sheet is as follows:

(A) From known data, complete the top of the computation sheet. Identify airplane, engine, and gear ratio, and Items 2 through 5 which are numbers of blades, propeller diameter, activity factor and integrated design C_L.

(B) Determine items numbered 6 through 10 from the airplane flight and engine conditions which have been selected for analysis as explained below:

Item No.		
6.	Attitude	Identifying flight condition
7.	BHP	Engine shaft - brake horsepower
8.	Engine RPM	N_e - Engine Speed (rev./min/)
9.	Pressure Altitude	Feet
10.	V_K	Airplane forward velocity (knots, true air speed)

(C) Calculate items numbered 11 through 17:

11.	ρ_o/ρ	Density ratio
12.	f_c	Ratio of speed of sound at standard day sea level to speed of sound at operating conditions.
13.	N	Propeller speed = Engine RPM x G.R.

14. Mach No. — Airplane Mach Number

$$\frac{V_k f_c}{662}$$

15. $ND \times f_c$ — Propeller speed x Propeller diameter x f_c

Items 14 and 15 are used in reading a maximum integrated design C_L from Figure 1. Since the static performance method is limited to the case of small or no compressibility losses, the integrated design C_L (Item 5) cannot exceed the maximum integrated design C_L (Figure 1). For flight performance conditions where compressibility is encountered, corrections are provided in Supplement B.

16. C_P — Power coefficient =

$$\frac{BHP\ (\rho o/\rho)}{2{,}000 \left(\frac{N}{1{,}000}\right)^3 \left(\frac{D}{10}\right)^5}$$

17. J — Propeller advance ratio $101.4\ V_K/ND$

(D) The following items are read from curves or calculated.

18. For $V_K > 0$, the performance is presented on a propeller efficiency basis. The propeller efficiencies are read from curves which span 3 and 4 bladed propellers for 80, 100, 140, 180 and 220 activity factors and .150, .300, .500, and .700 integrated design C_L's. These curves are included in the sections titled "Flight". Performance for other propeller configurations can be obtained by interpolating among these curves. Refer to Supplement B for corrections due to blocking and compressibility.

19. C_T/C_P

For $V_K = 0$, performance presented in the form of C_T/C_P are read from Figures 2 through 17. These curves span the same propeller configurations as the propeller efficiency maps with additional curves for intermediate activity factor levels.

20. Thrust

Thrust in pounds per propeller are computed as follows:

$$V_K = 0 \quad T = (C_T/C_P) \frac{BHP}{ND} \; 33,000$$

$$V_K > 0 \quad T = \frac{326 \; (\eta) \; (BHP)}{V_K}$$

(E) Figures 18 and 39 present the optimum or ideal efficiencies for velocities greater than zero. For the static case, the optimum curves are presented on each individual static curve.

TABLE OF FIGURES

Activity Factor	Static 3-Blade	Static 4-Blade	Flight 3-Blade	Flight 4-Blade
80	2	10	19-22	40-43
100	3	11	23-26	44-47
120	4	12		
140	5	13	27-30	48-51
160	6	14		
180	7	15	31-34	52-55
200	8	16		
220	9	17	35-38	56-59

The numbers in the above table represent the figure numbers covering performance for the specified propellers for static and flight conditions. For flight, 4 numbers are specified as separate figures are provided for various Integrated Design C_L.

HAMILTON STANDARD GENERALIZED PROPELLER PERFORMANCE

Airplane Mythical 1 | Date 2/3/61 | Calc. No. 2396

Engine Hypothetical | G. R. 12:1 | Sheet No. 1

Reference Sample Problem | Calc. By M. M. M. | Checked By S. S.

1	Figure No.	5	5	5	27	28	29	27	28	29
2	No. of Blades	3	→	→	3	→	→	3	→	→
3	Diameter	17'	→	→	17'	→	→	17'	→	→
4	AF	140	→	→	140	→	→	140	→	→
5	Int. Des. C_L	.150	.300	.500	.150	.300	.500	.150	.300	.500
6	Attitude	T. O.	→	→	T. O.	→	→	Cruise	→	→
7	BHP	2500	→	→	2600	→	→	1000	→	→
8	Engine RPM	12,000	→	→	12,000	→	→	10,000	→	→
9	Altitude	S. L.	→	→	S. L.	→	→	25,000	→	→
10	V_{Knots}	0	→	→	100	→	→	300	→	→
11	ρ_o/ρ	1.00	→	→	1.00	→	→	2.232	→	→
12	f_c	1.00	→	→	1.00	→	→	1.10	→	→
13	N	1000	→	→	1000	→	→	833	→	→
14	Mach No.	0	→	→	.151	→	→	.498	→	→
15	ND x f_c	17,000	→	→	17,000	→	→	15,600	→	→
16	C_P	.0880	→	→	.0915	→	→	.1360	→	→
17	J	0	→	→	.596	→	→	2.148	→	→
18	η				.718	.745	.752	.894	.892	.820
19	C_T/C_P	1.805	1.965	2.110						
20	Thrust	8,760	9,540	10,240	6,085	6,310	6,370	971	969	890

LIST OF COEFFICIENTS AND SYMBOLS

AF	Blade activity factor $\frac{100,000}{16}\int_{.15}^{1.0}\left(\frac{b}{D}\right) x^3\, dx$
b	Blade section width, feet
BHP	Shaft - brake horsepower
C_{LD}	Blade section design lift coefficient
C_{Li}	Integrated design C_L $4\int_{.15}^{1.0} C_{LD}\, x^3\, dx$
C_P	Power coefficient $= \frac{P}{\rho n^3 D^5} = \frac{BHP\ (\rho_o/\rho)}{2000\left(\frac{N}{1000}\right)^3\left(\frac{D}{10}\right)^5}$
C_T	Thrust coefficient $= \frac{T}{\rho n^2 D^4}$
D	Propeller installed diameter, feet
f_c	Ratio of speed of sound at standard day sea level to speed of sound at operating condition
G. R.	Gear ratio, propeller speed/engine speed
J	Propeller advance ratio $101.4\, V_K/ND$
M. N.	Airplane Mach Number $V > 0$ M. N. $= \frac{f_c\ V_K}{662}$ $V = 0$ M. N. $= \frac{ND\ f_c}{21,400}$
n	Propeller speed, revolutions per second
N	Propeller speed, revolutions per minute
N_e	Engine speed, revolution per minute
P	Power, foot pounds/second

r	Radius at blade element, feet
R	Blade radius at propeller tip, feet
T	Propeller thrust, pounds

$$V_K = 0 \qquad T = C_T/C_P \times \frac{BHP}{ND} \times 33,000$$

$$V_K > 0 \qquad T = \frac{326 \times \eta \times BHP}{V_K}$$

V_K	Flight velocity, Knots - true air speed
x	Fraction of propeller tip radius, r/R
η	Propeller efficiency, J (C_T/C_P)
θ 3/4	Propeller blade angle at x = 3/4, degrees
ρ	Mass density of air, slugs per cubic foot
ρ_o/ρ	Ratio of density at sea level to density at operating condition.

February 1, 1961

FIGURE 1

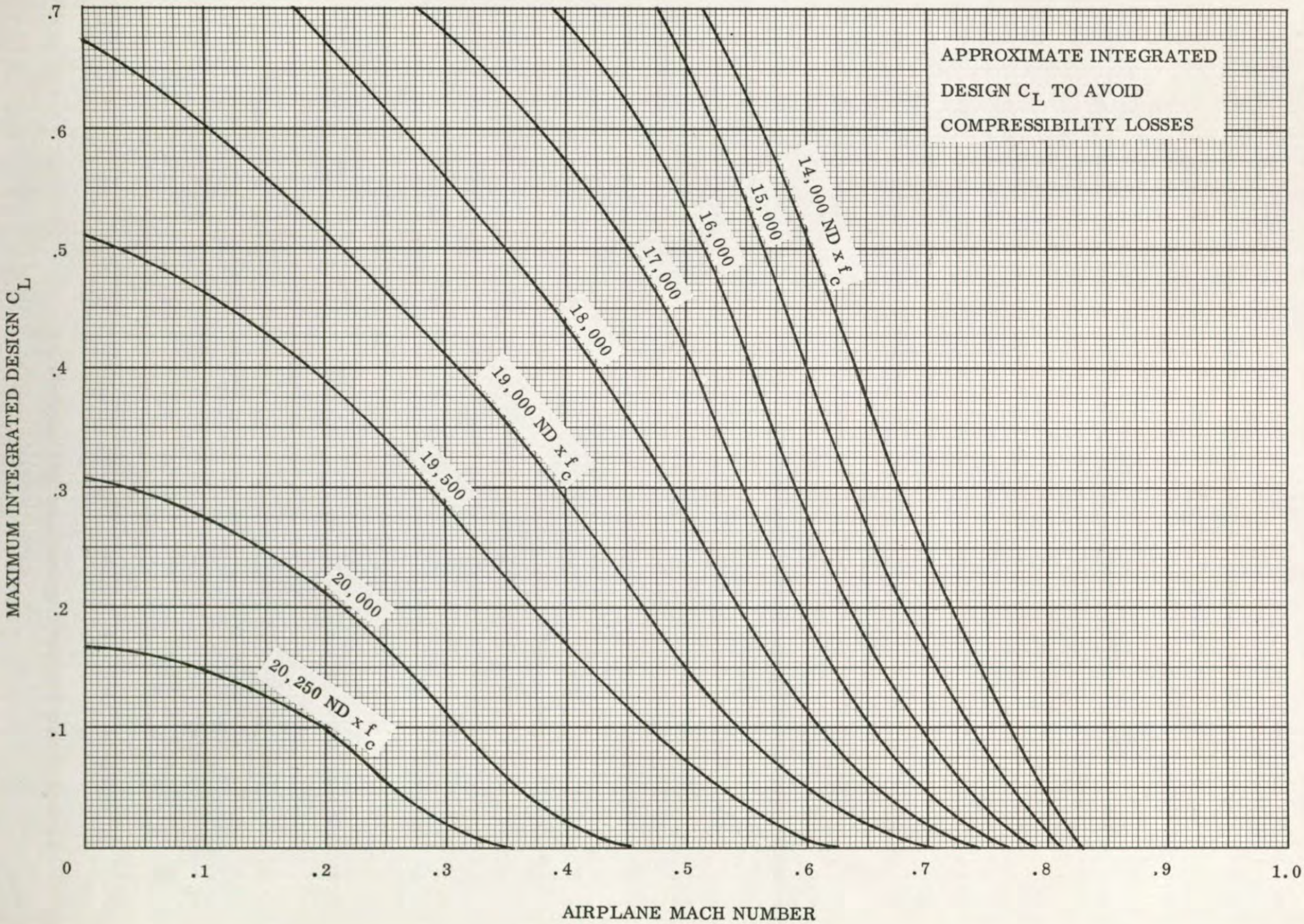

3 BLADE - STATIC

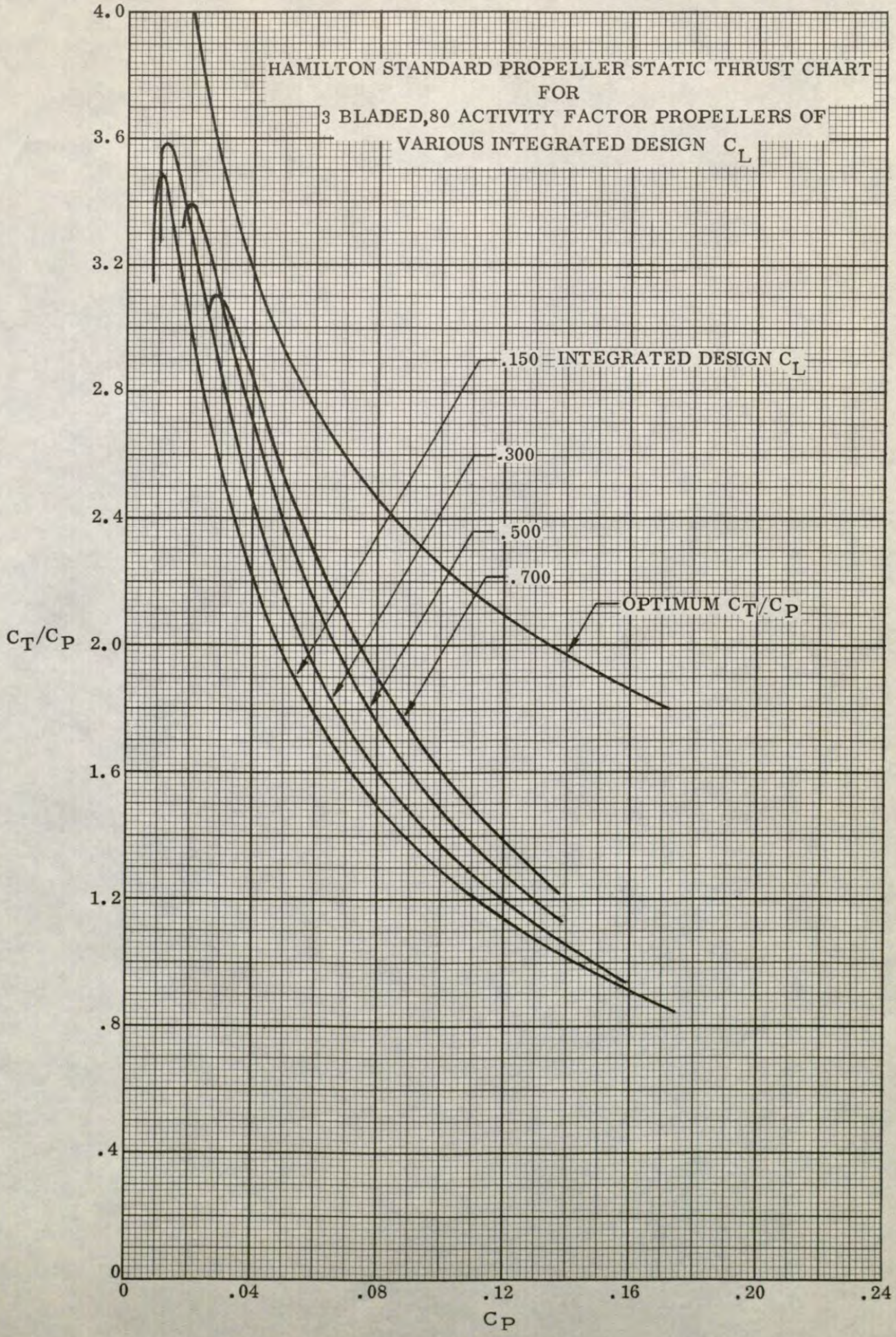
HAMILTON STANDARD PROPELLER STATIC THRUST CHART
FOR
3 BLADED,80 ACTIVITY FACTOR PROPELLERS OF
VARIOUS INTEGRATED DESIGN C_L
.150 INTEGRATED DESIGN C_L
.300
.500
.700
OPTIMUM C_T/C_P
C_T/C_P
4.0
3.6
3.2
2.8
2.4
2.0
1.6
1.2
.8
.4
0
0
.04
.08
.12
.16
.20
.24
C_P

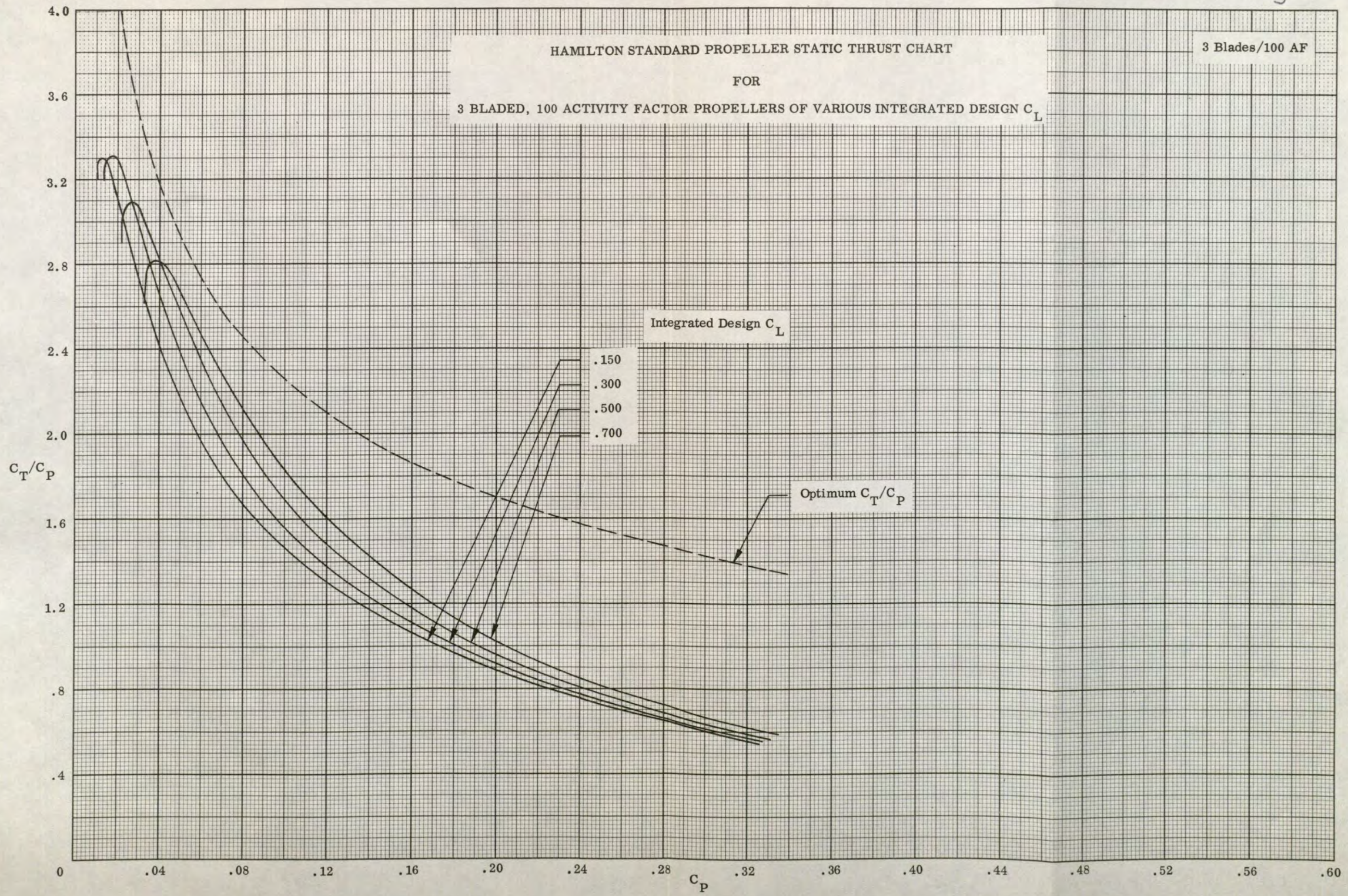
HAMILTON STANDARD PROPELLER STATIC THRUST CHART
FOR
3 BLADED, 100 ACTIVITY FACTOR PROPELLERS OF VARIOUS INTEGRATED DESIGN C_L
3 Blades/100 AF
Integrated Design C_L
.150
.300
.500
.700
Optimum C_T/C_P
C_T/C_P
C_P
4.0
3.6
3.2
2.8
2.4
2.0
1.6
1.2
.8
.4
0
.04
.08
.12
.16
.20
.24
.28
.32
.36
.40
.44
.48
.52
.56
.60

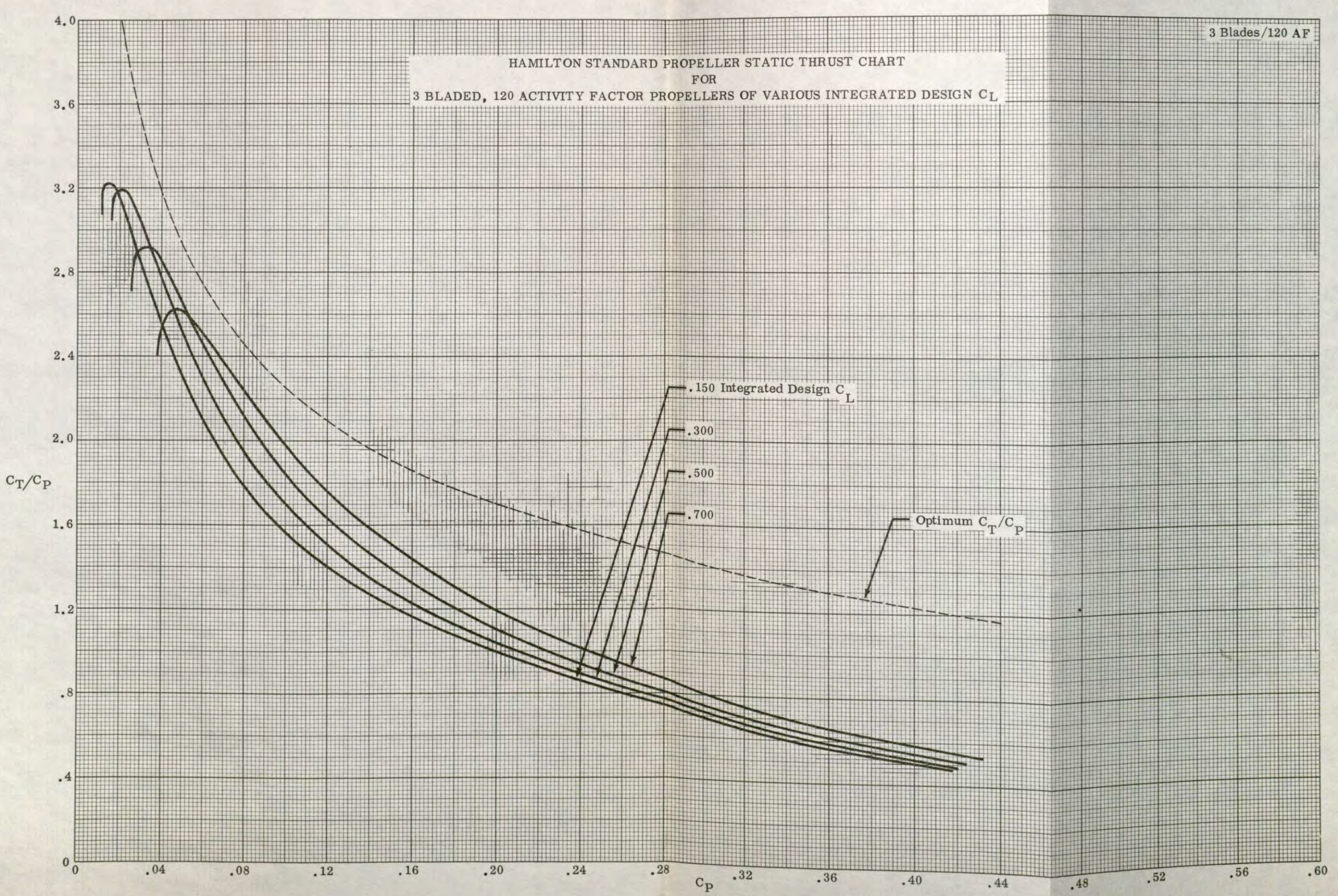
3 Blades/120 AF
HAMILTON STANDARD PROPELLER STATIC THRUST CHART
FOR
3 BLADED, 120 ACTIVITY FACTOR PROPELLERS OF VARIOUS INTEGRATED DESIGN C_L
.150 Integrated Design C_L
.300
.500
.700
Optimum C_T/C_P
C_T/C_P
C_P
4.0
3.6
3.2
2.8
2.4
2.0
1.6
1.2
.8
.4
0
.04
.08
.12
.16
.20
.24
.28
.32
.36
.40
.44
.48
.52
.56
.60

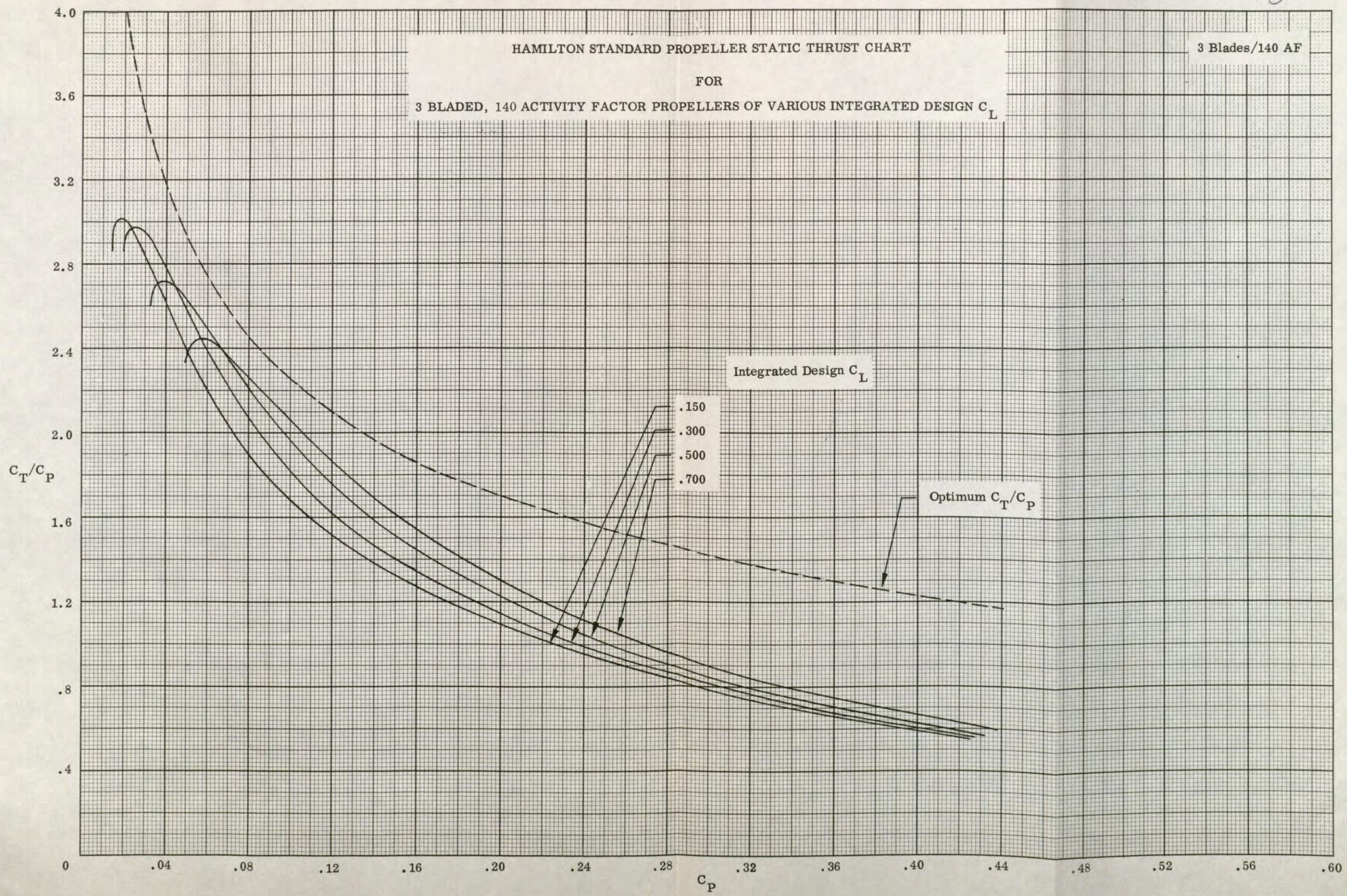
HAMILTON STANDARD PROPELLER STATIC THRUST CHART
FOR
3 BLADED, 140 ACTIVITY FACTOR PROPELLERS OF VARIOUS INTEGRATED DESIGN C_L
3 Blades/140 AF
Integrated Design C_L
.150
.300
.500
.700
Optimum C_T/C_P
C_T/C_P
C_P
4.0
3.6
3.2
2.8
2.4
2.0
1.6
1.2
.8
.4
0
.04
.08
.12
.16
.20
.24
.28
.32
.36
.40
.44
.48
.52
.56
.60

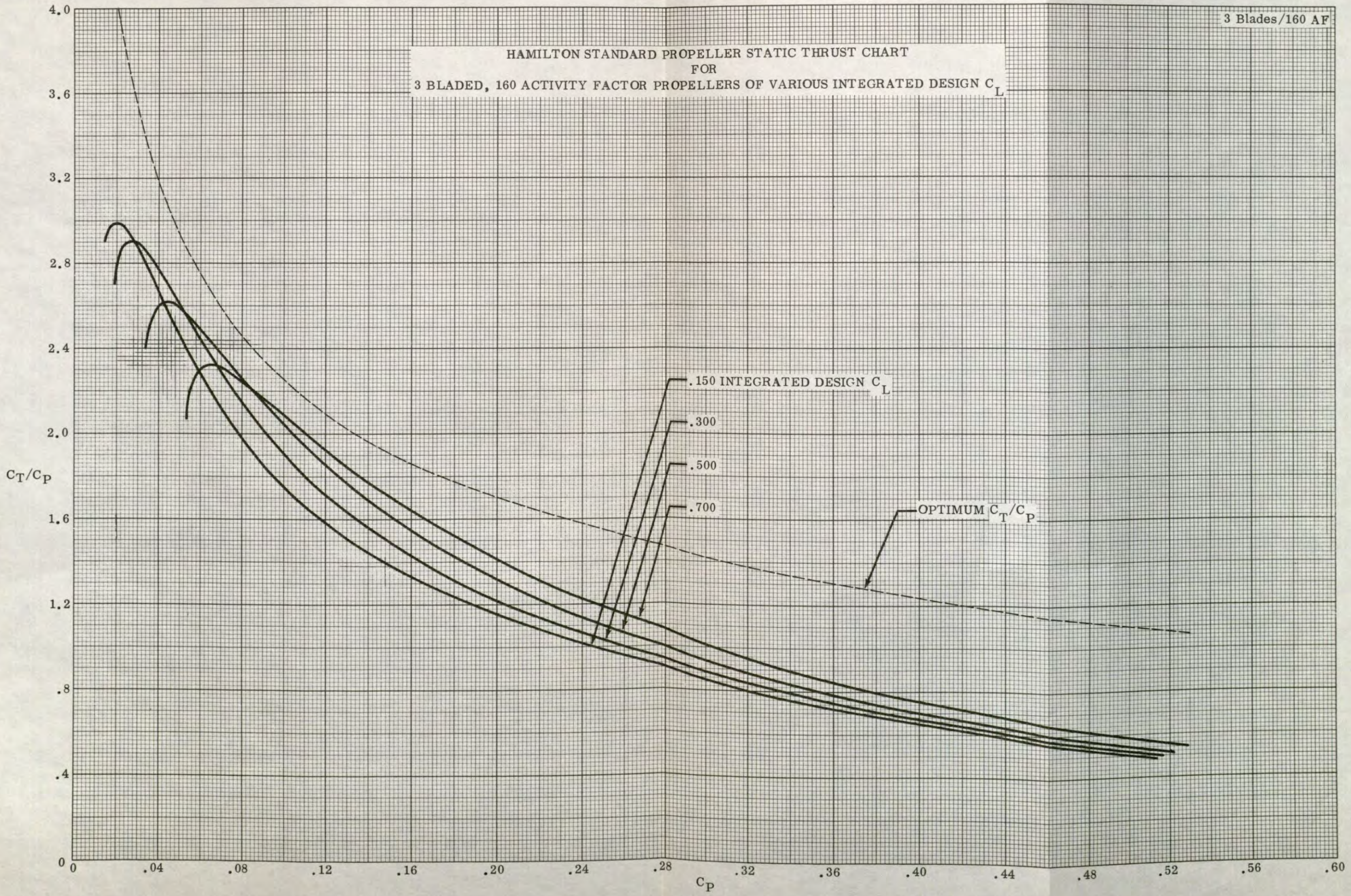
3 Blades/160 AF
HAMILTON STANDARD PROPELLER STATIC THRUST CHART
FOR
3 BLADED, 160 ACTIVITY FACTOR PROPELLERS OF VARIOUS INTEGRATED DESIGN C_L
.150 INTEGRATED DESIGN C_L
.300
.500
.700
OPTIMUM C_T/C_P
C_T/C_P
C_P
4.0
3.6
3.2
2.8
2.4
2.0
1.6
1.2
.8
.4
0
.04
.08
.12
.16
.20
.24
.28
.32
.36
.40
.44
.48
.52
.56
.60

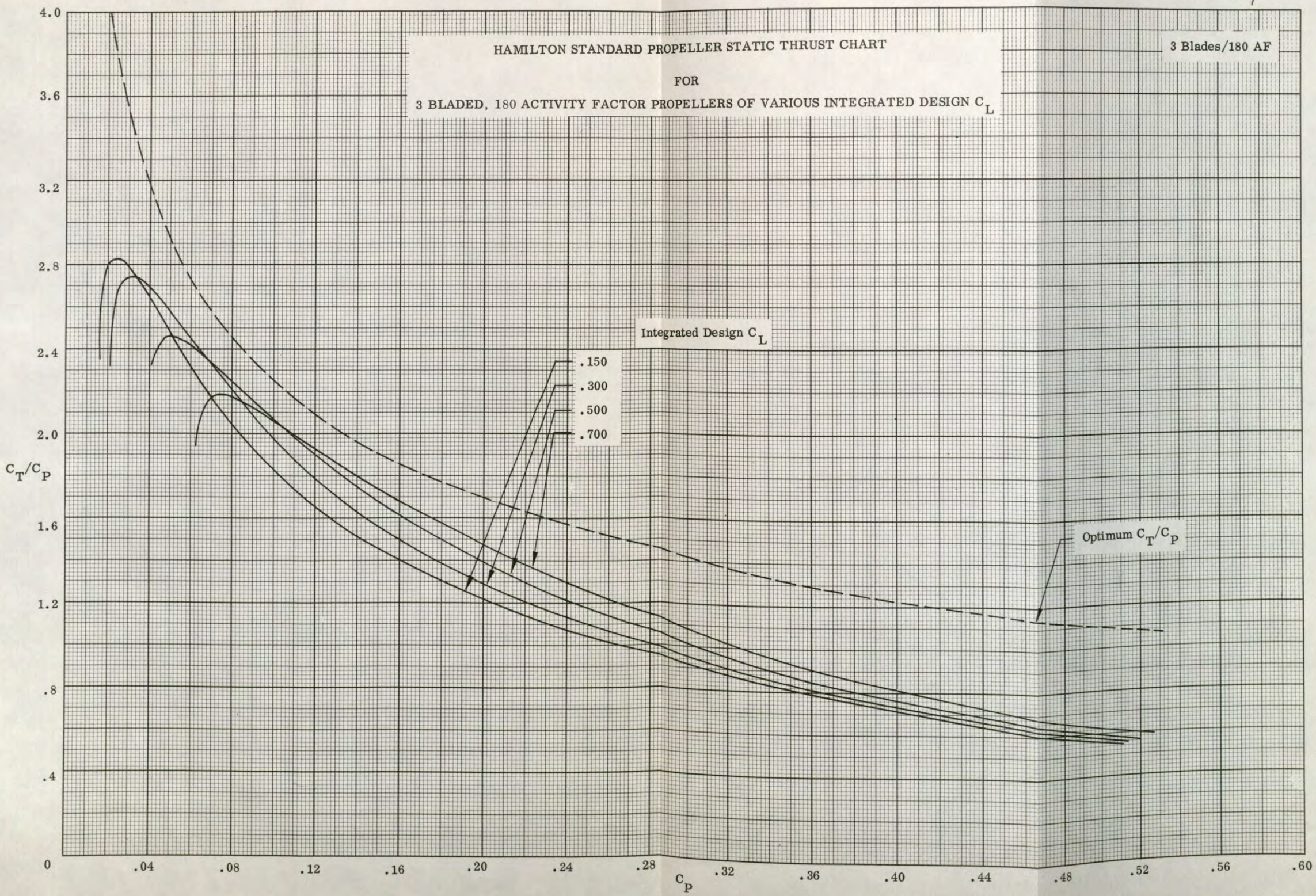
HAMILTON STANDARD PROPELLER STATIC THRUST CHART
FOR
3 BLADED, 180 ACTIVITY FACTOR PROPELLERS OF VARIOUS INTEGRATED DESIGN C_L
3 Blades/180 AF
Integrated Design C_L
.150
.300
.500
.700
Optimum C_T/C_P
C_T/C_P
C_P
4.0
3.6
3.2
2.8
2.4
2.0
1.6
1.2
.8
.4
0
.04
.08
.12
.16
.20
.24
.28
.32
.36
.40
.44
.48
.52
.56
.60

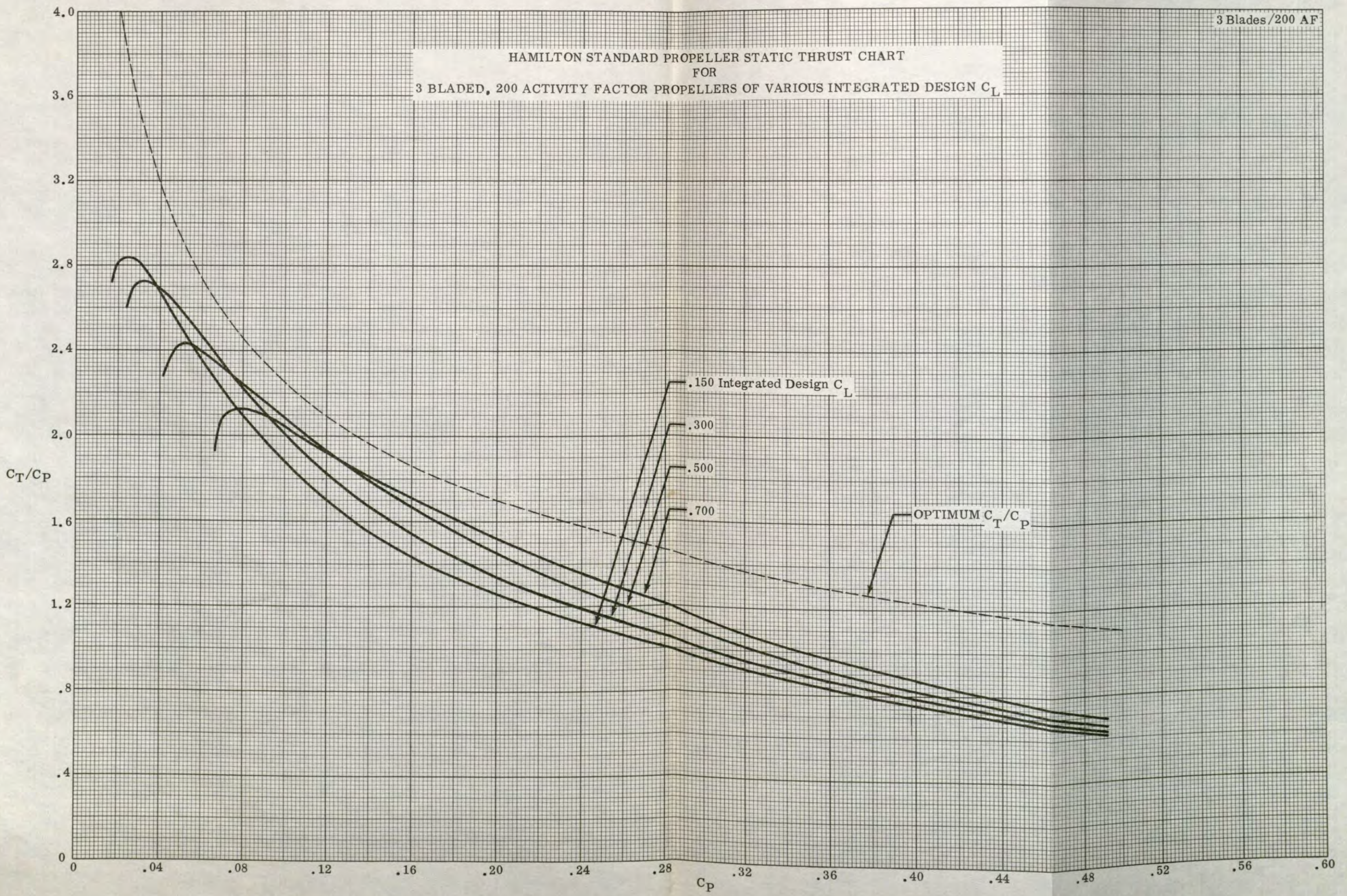
3 Blades/200 AF
HAMILTON STANDARD PROPELLER STATIC THRUST CHART
FOR
3 BLADED, 200 ACTIVITY FACTOR PROPELLERS OF VARIOUS INTEGRATED DESIGN C_L
.150 Integrated Design C_L
.300
.500
.700
OPTIMUM C_T/C_P
C_T/C_P
C_P
4.0
3.6
3.2
2.8
2.4
2.0
1.6
1.2
.8
.4
0
0
.04
.08
.12
.16
.20
.24
.28
.32
.36
.40
.44
.48
.52
.56
.60

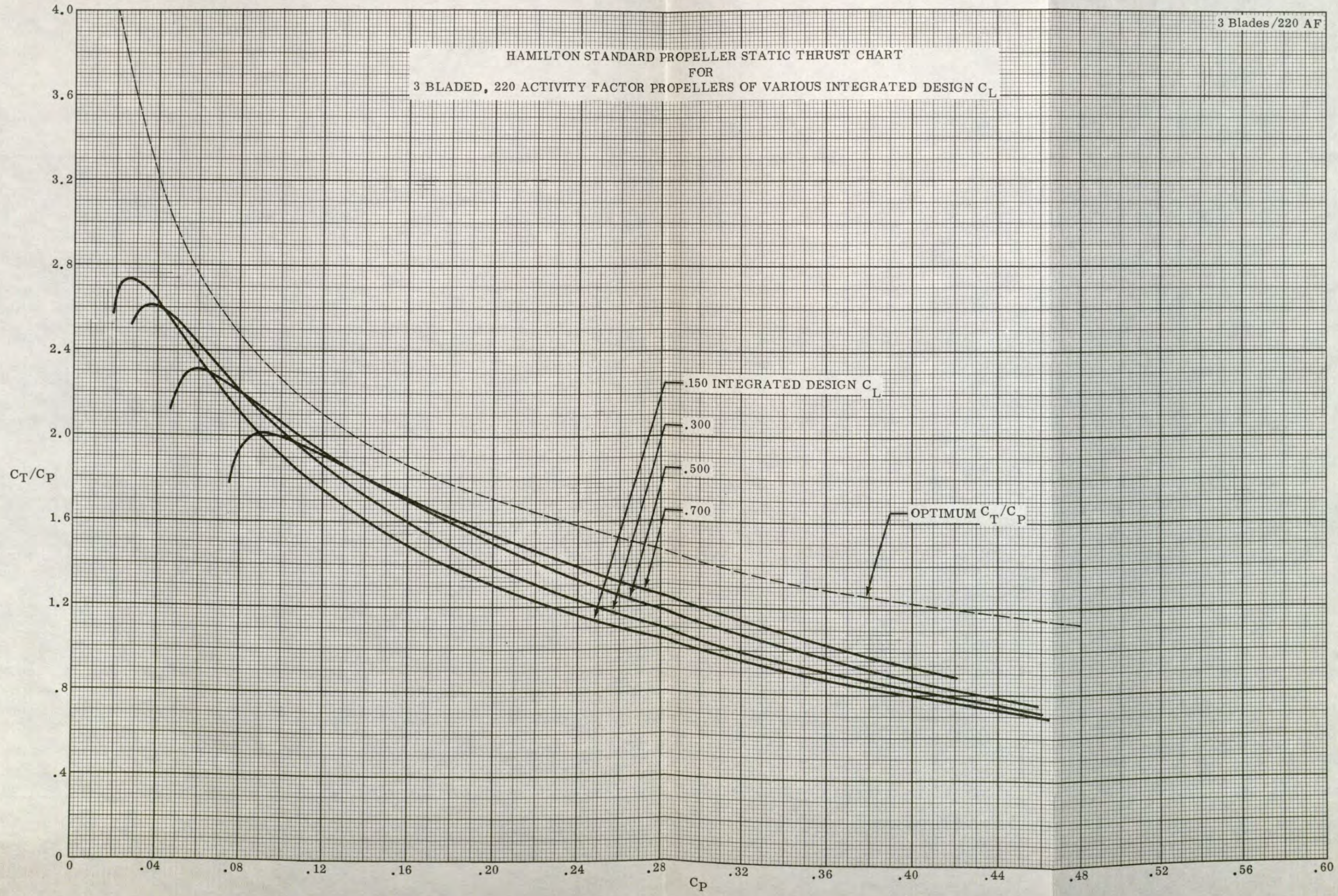
3 Blades/220 AF
HAMILTON STANDARD PROPELLER STATIC THRUST CHART
FOR
3 BLADED, 220 ACTIVITY FACTOR PROPELLERS OF VARIOUS INTEGRATED DESIGN C_L
.150 INTEGRATED DESIGN C_L
.300
.500
.700
OPTIMUM C_T/C_P
C_T/C_P
C_P
4.0
3.6
3.2
2.8
2.4
2.0
1.6
1.2
.8
.4
0
0
.04
.08
.12
.16
.20
.24
.28
.32
.36
.40
.44
.48
.52
.56
.60

4 BLADE - STATIC

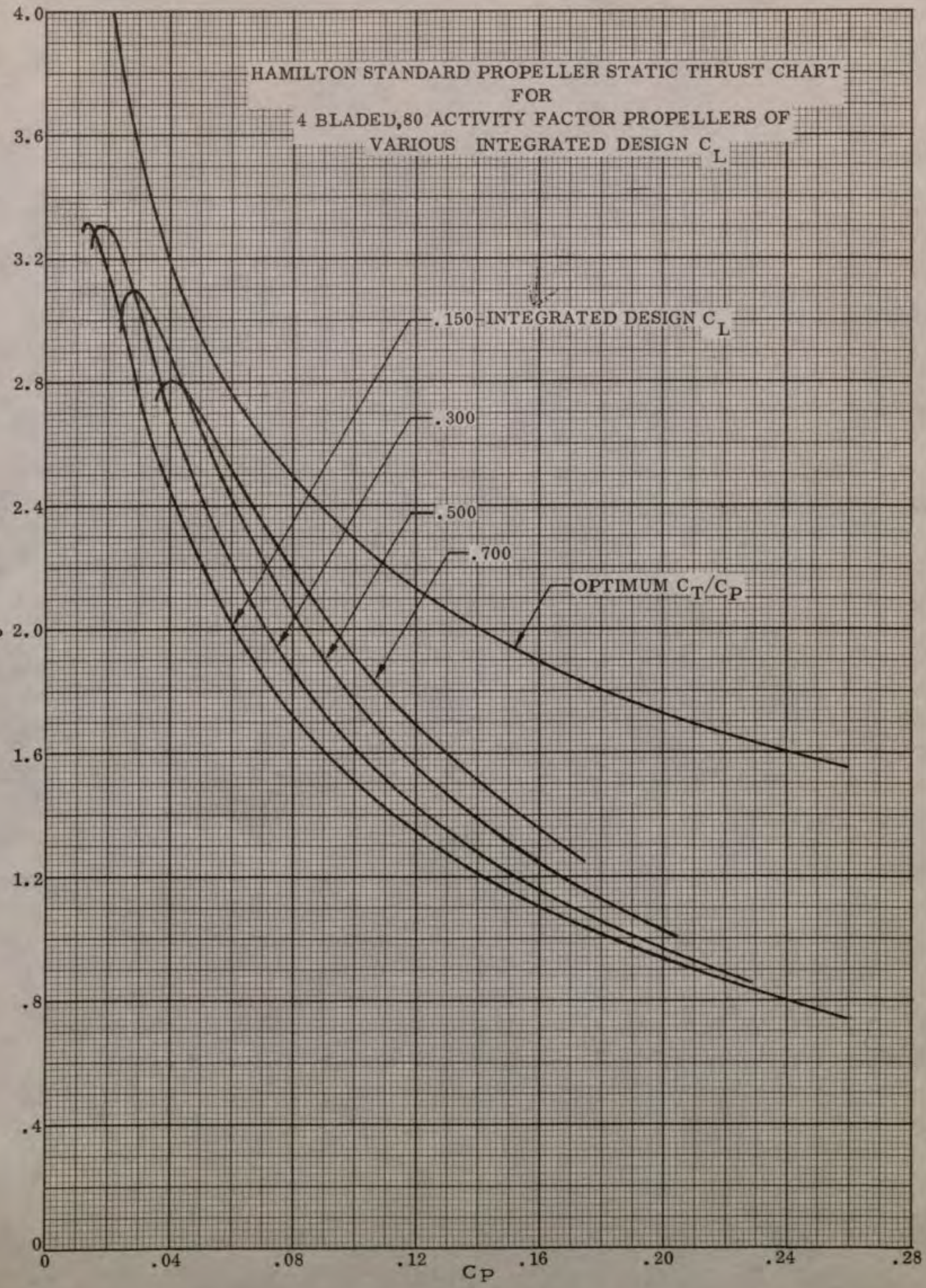
HAMILTON STANDARD PROPELLER STATIC THRUST CHART
FOR
4 BLADED, 80 ACTIVITY FACTOR PROPELLERS OF
VARIOUS INTEGRATED DESIGN C_L
.150-INTEGRATED DESIGN C_L
.300
.500
.700
OPTIMUM C_T/C_P
C_T/C_P
C_P
4.0
3.6
3.2
2.8
2.4
2.0
1.6
1.2
.8
.4
0
0
.04
.08
.12
.16
.20
.24
.28

February 1, 1961

FIGURE 5/11

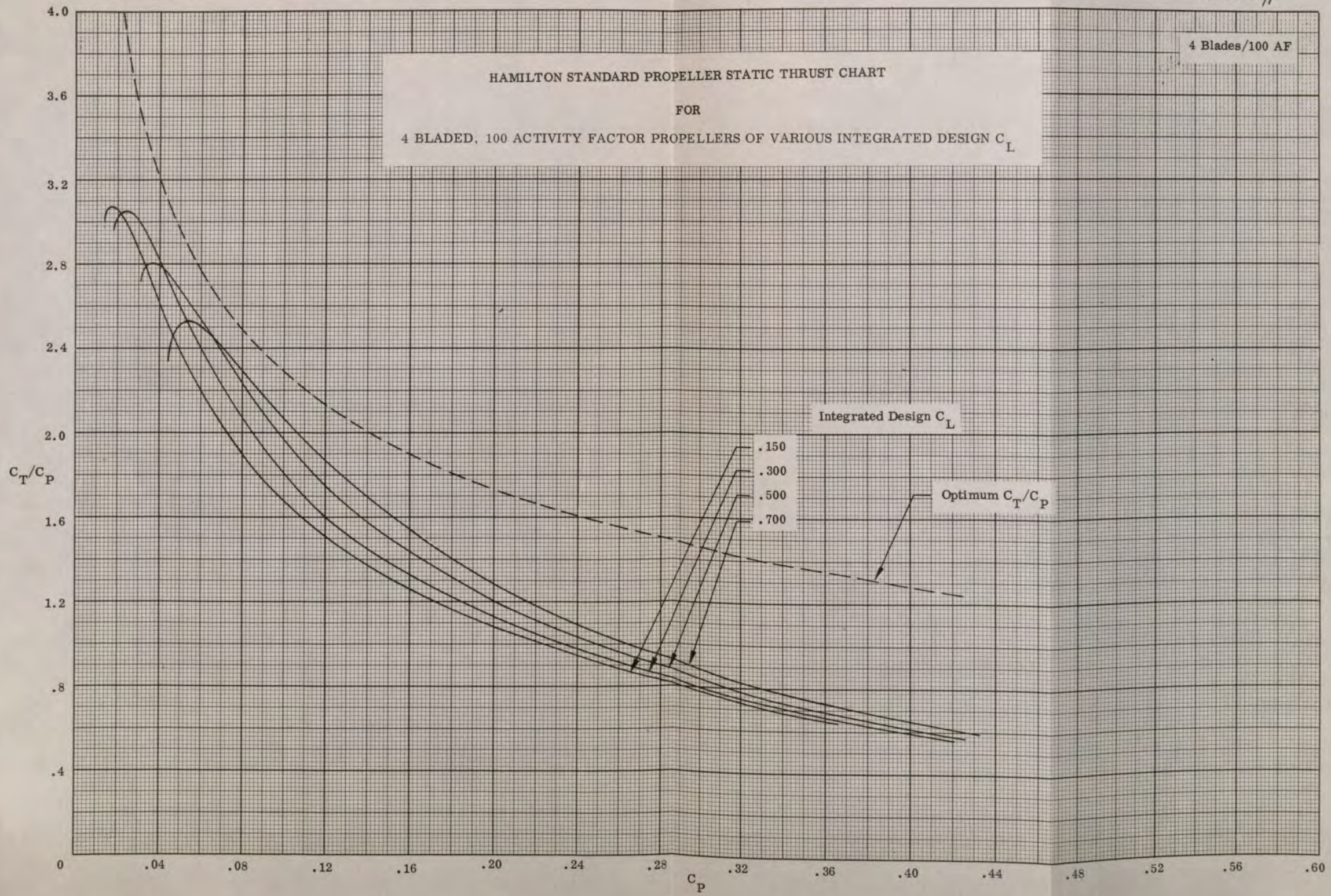

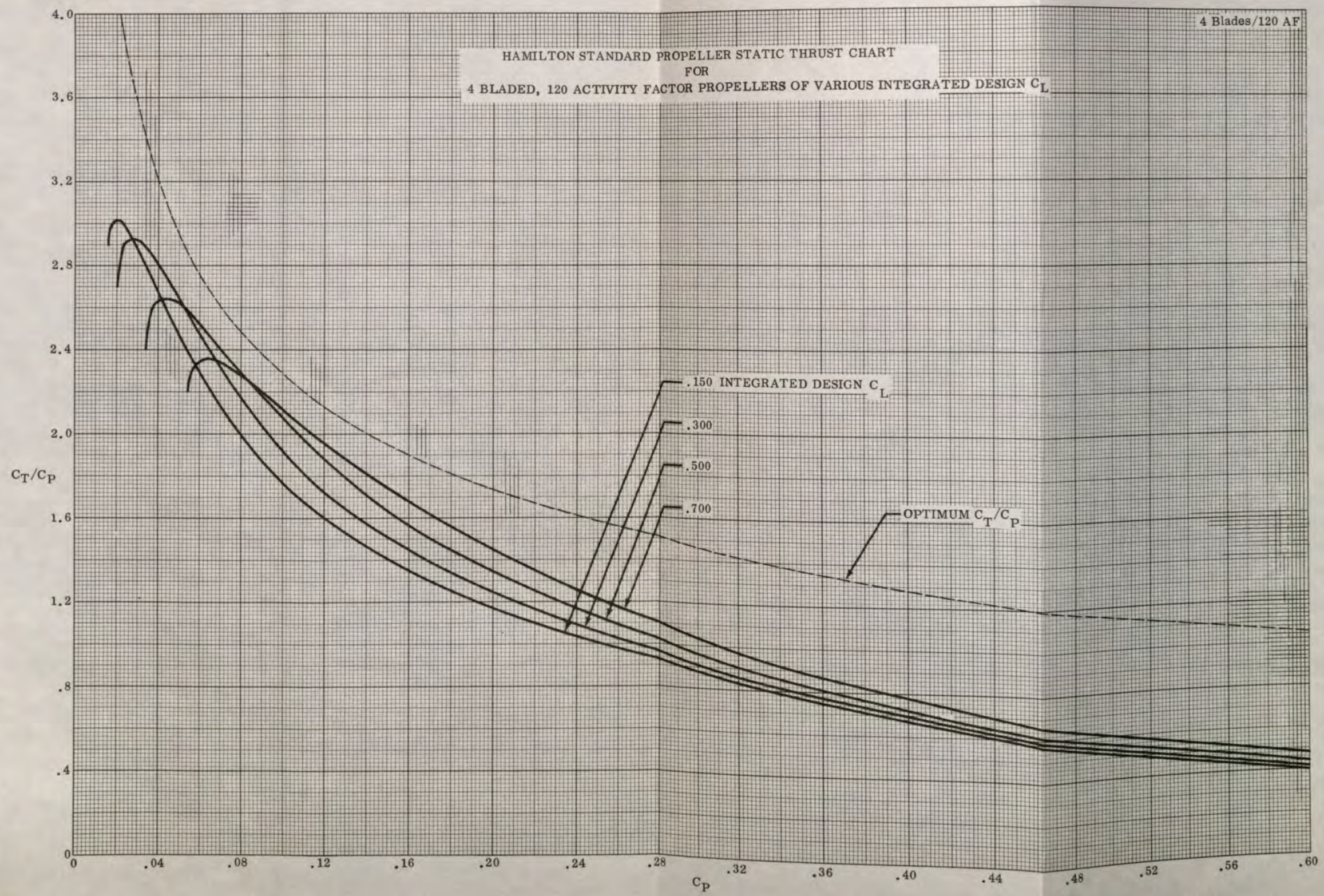
4 Blades/120 AF
HAMILTON STANDARD PROPELLER STATIC THRUST CHART
FOR
4 BLADED, 120 ACTIVITY FACTOR PROPELLERS OF VARIOUS INTEGRATED DESIGN C_L
.150 INTEGRATED DESIGN C_L
.300
.500
.700
OPTIMUM C_T/C_P
C_T/C_P
C_P
4.0
3.6
3.2
2.8
2.4
2.0
1.6
1.2
.8
.4
0
.04
.08
.12
.16
.20
.24
.28
.32
.36
.40
.44
.48
.52
.56
.60

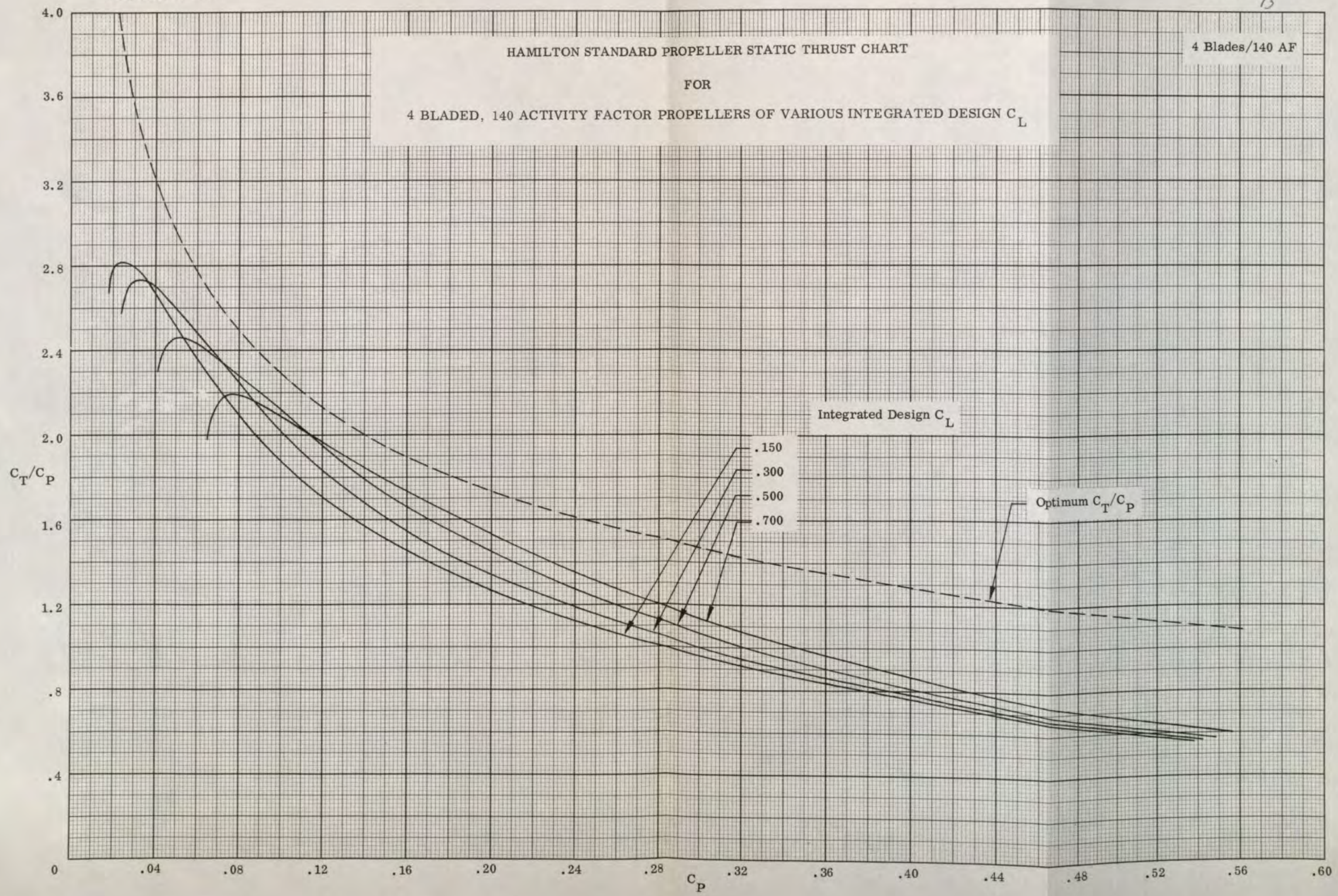
HAMILTON STANDARD PROPELLER STATIC THRUST CHART
FOR
4 BLADED, 140 ACTIVITY FACTOR PROPELLERS OF VARIOUS INTEGRATED DESIGN C_L
4 Blades/140 AF
Integrated Design C_L
.150
.300
.500
.700
Optimum C_T/C_P
C_T/C_P
C_P
4.0
3.6
3.2
2.8
2.4
2.0
1.6
1.2
.8
.4
0
.04
.08
.12
.16
.20
.24
.28
.32
.36
.40
.44
.48
.52
.56
.60

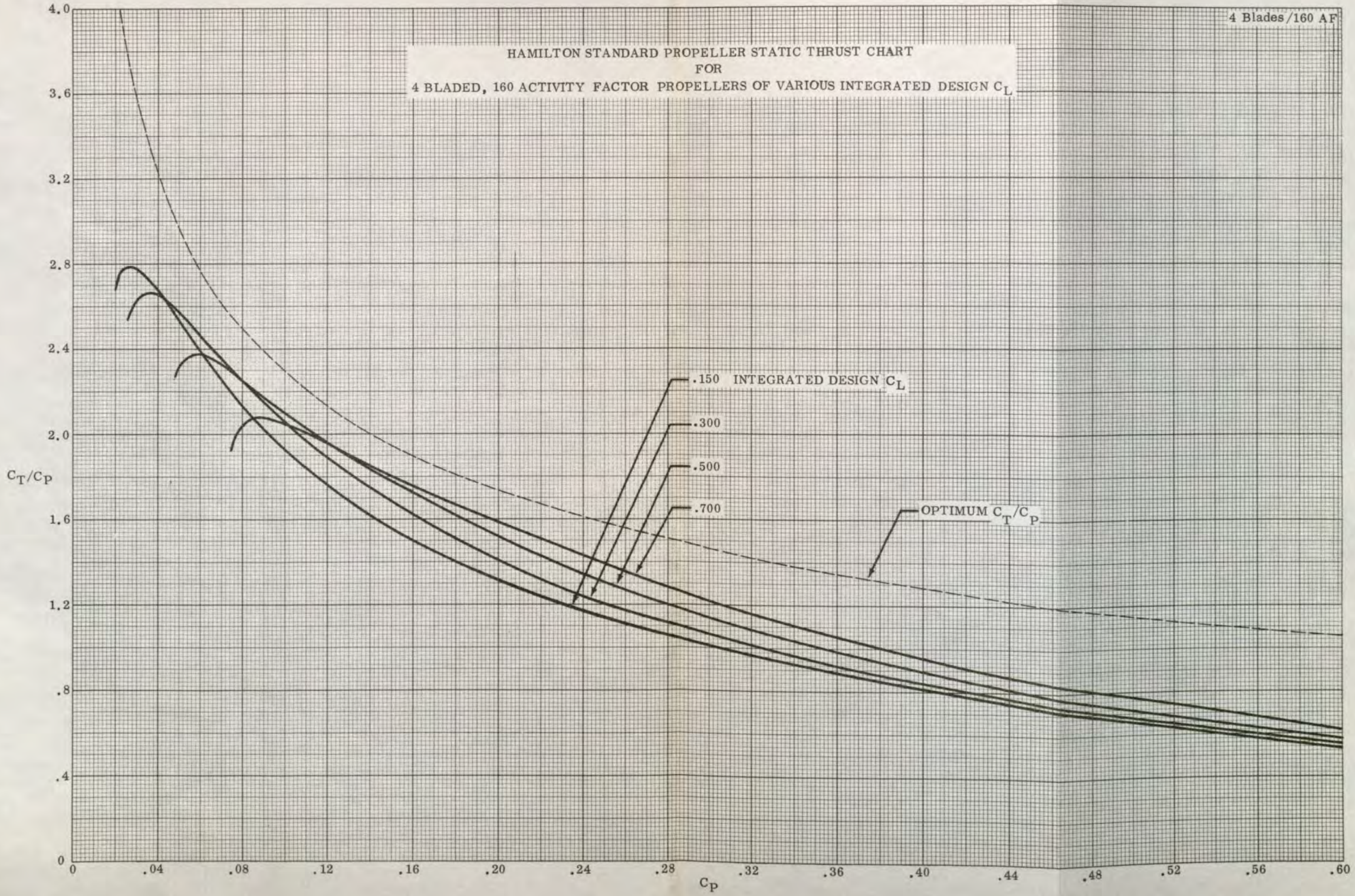
4 Blades/160 AF
HAMILTON STANDARD PROPELLER STATIC THRUST CHART
FOR
4 BLADED, 160 ACTIVITY FACTOR PROPELLERS OF VARIOUS INTEGRATED DESIGN C_L
.150 INTEGRATED DESIGN C_L
.300
.500
.700
OPTIMUM C_T/C_P
C_T/C_P
C_P
4.0
3.6
3.2
2.8
2.4
2.0
1.6
1.2
.8
.4
0
.04
.08
.12
.16
.20
.24
.28
.32
.36
.40
.44
.48
.52
.56
.60

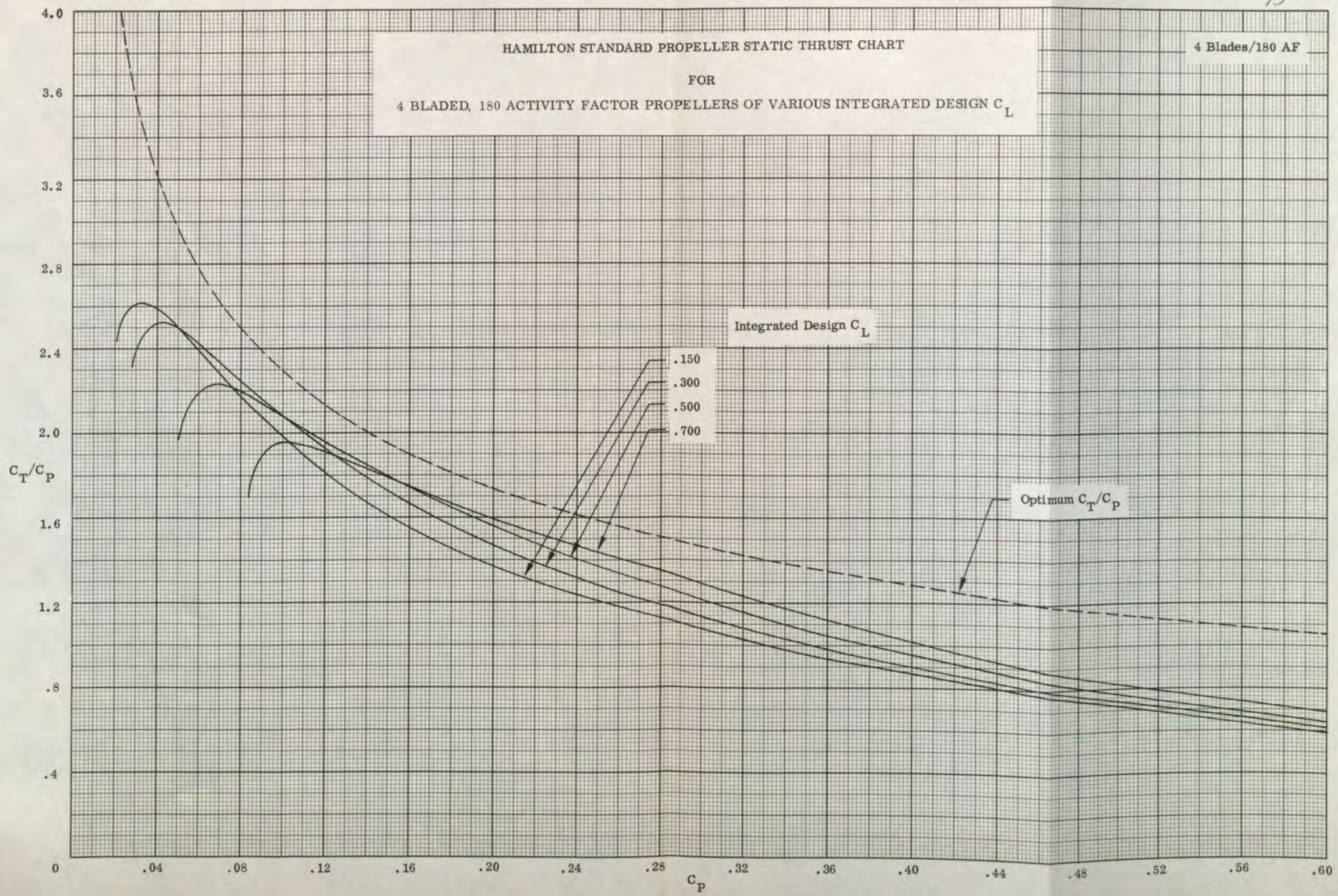
HAMILTON STANDARD PROPELLER STATIC THRUST CHART
FOR
4 BLADED, 180 ACTIVITY FACTOR PROPELLERS OF VARIOUS INTEGRATED DESIGN C_L
4 Blades/180 AF
Integrated Design C_L
.150
.300
.500
.700
Optimum C_T/C_P
C_T/C_P
C_P
4.0
3.6
3.2
2.8
2.4
2.0
1.6
1.2
.8
.4
0
.04
.08
.12
.16
.20
.24
.28
.32
.36
.40
.44
.48
.52
.56
.60

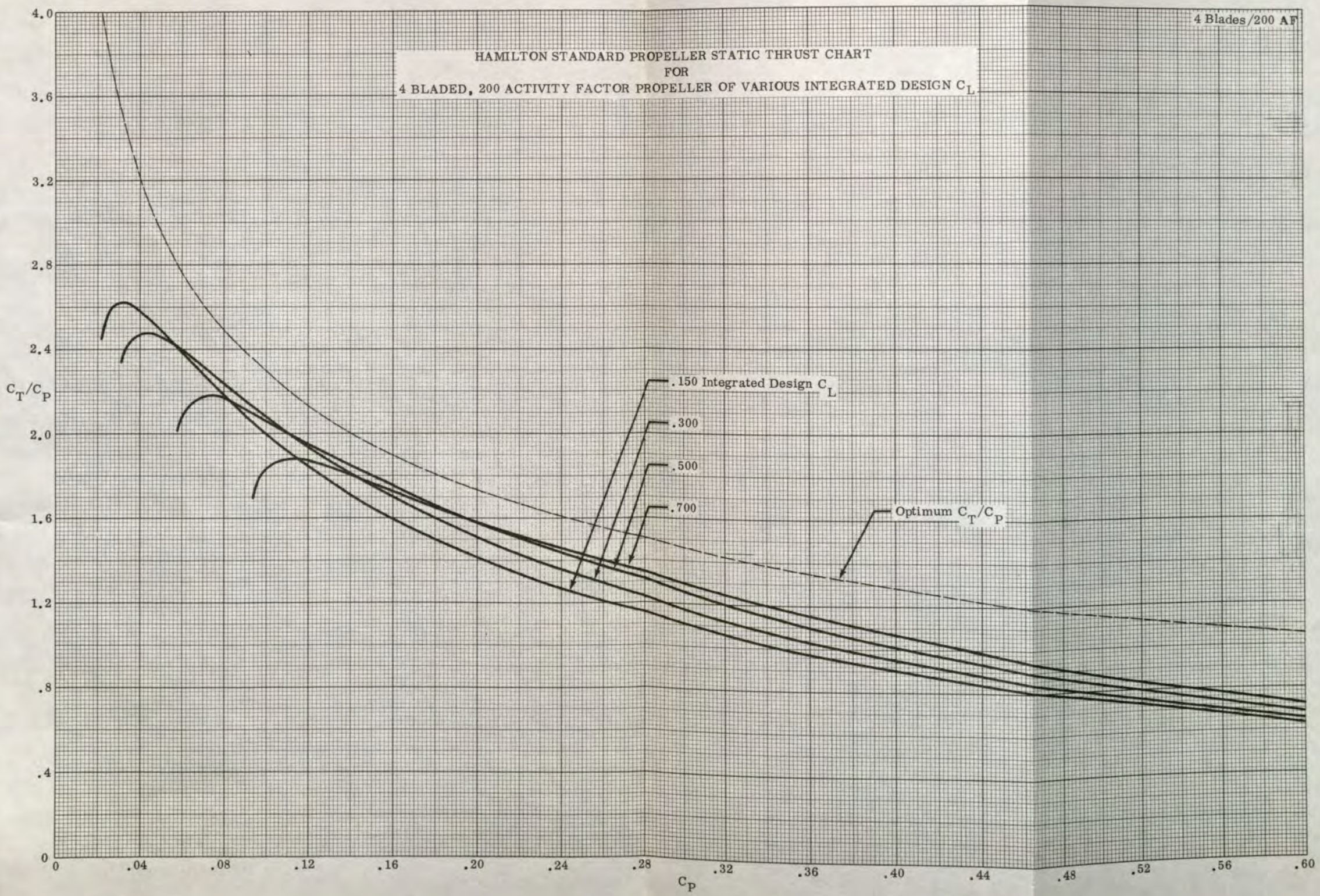
HAMILTON STANDARD PROPELLER STATIC THRUST CHART
FOR
4 BLADED, 200 ACTIVITY FACTOR PROPELLER OF VARIOUS INTEGRATED DESIGN C_L
4 Blades/200 AF
C_T/C_P
C_P
.150 Integrated Design C_L
.300
.500
.700
Optimum C_T/C_P
4.0
3.6
3.2
2.8
2.4
2.0
1.6
1.2
.8
.4
0
0
.04
.08
.12
.16
.20
.24
.28
.32
.36
.40
.44
.48
.52
.56
.60

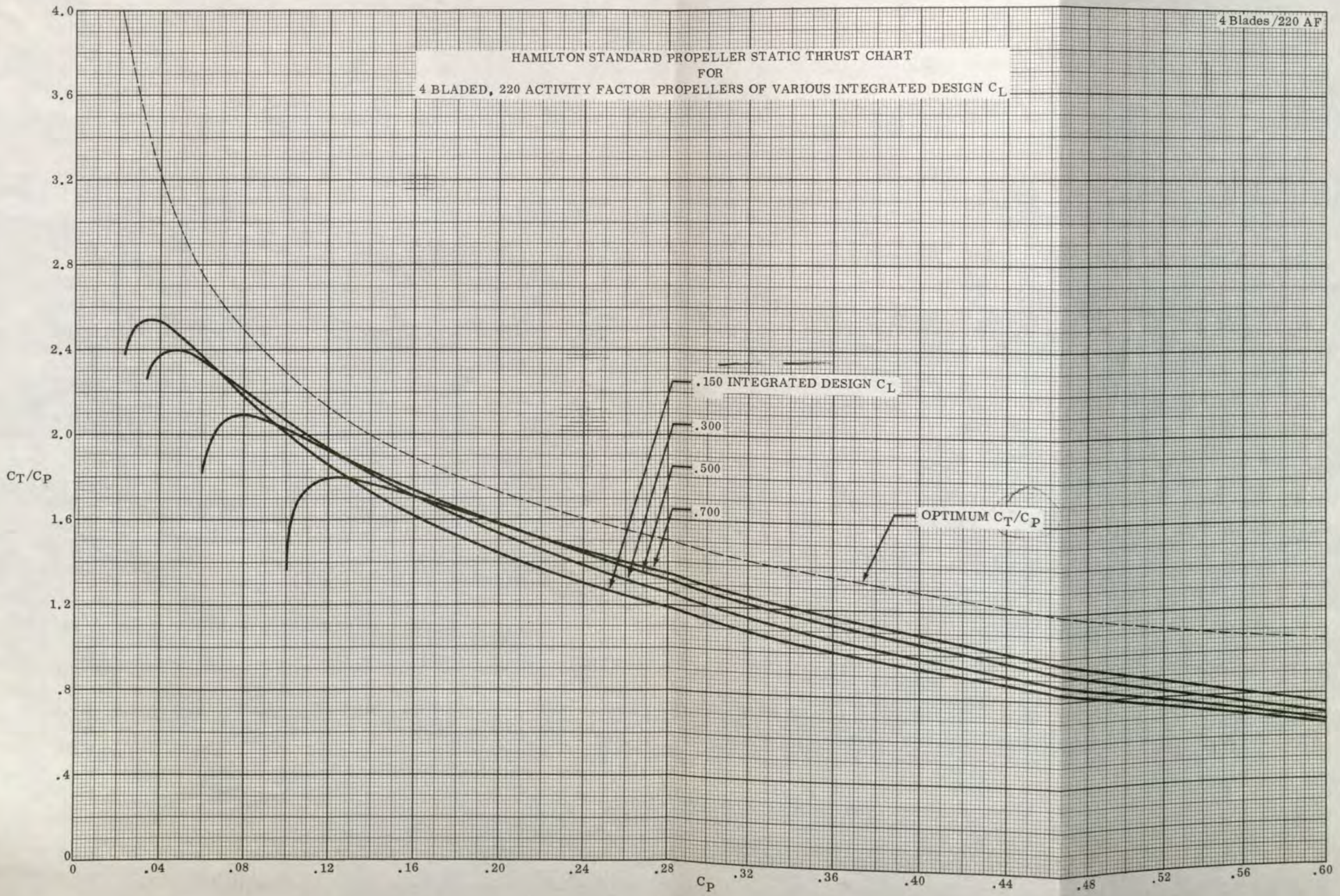
4 Blades /220 AF
HAMILTON STANDARD PROPELLER STATIC THRUST CHART
FOR
4 BLADED, 220 ACTIVITY FACTOR PROPELLERS OF VARIOUS INTEGRATED DESIGN C_L
.150 INTEGRATED DESIGN C_L
.300
.500
.700
OPTIMUM C_T/C_P
C_T/C_P
C_P
4.0
3.6
3.2
2.8
2.4
2.0
1.6
1.2
.8
.4
0
.04
.08
.12
.16
.20
.24
.28
.32
.36
.40
.44
.48
.52
.56
.60

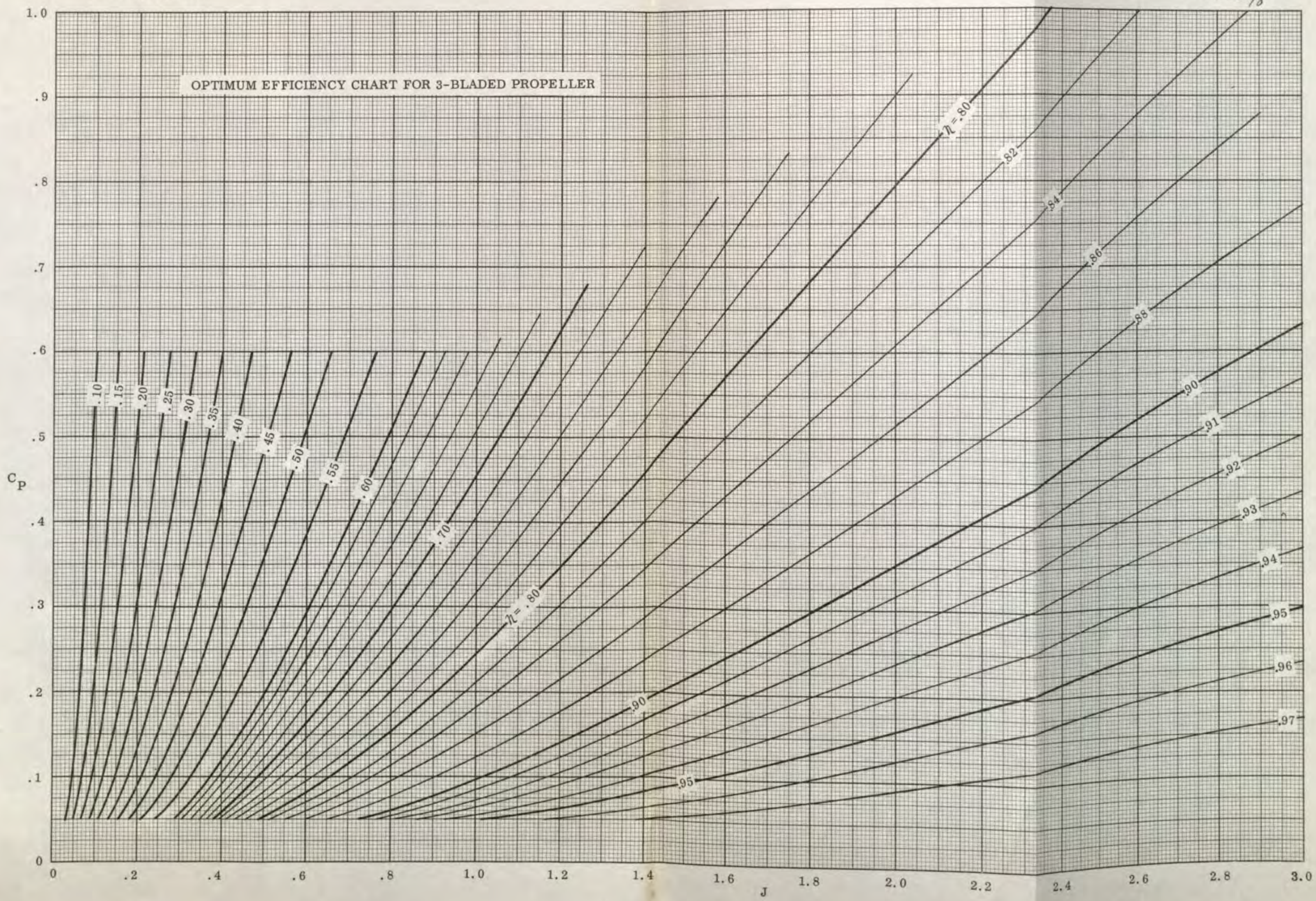
OPTIMUM EFFICIENCY CHART FOR 3-BLADED PROPELLER
C_P
J
0
.1
.2
.3
.4
.5
.6
.7
.8
.9
1.0
0
.2
.4
.6
.8
1.0
1.2
1.4
1.6
1.8
2.0
2.2
2.4
2.6
2.8
3.0
.10
.15
.20
.25
.30
.35
.40
.45
.50
.55
.60
.70
η = .80
.90
.95
η = .80
.82
.84
.86
.88
.90
.91
.92
.93
.94
.95
.96
.97

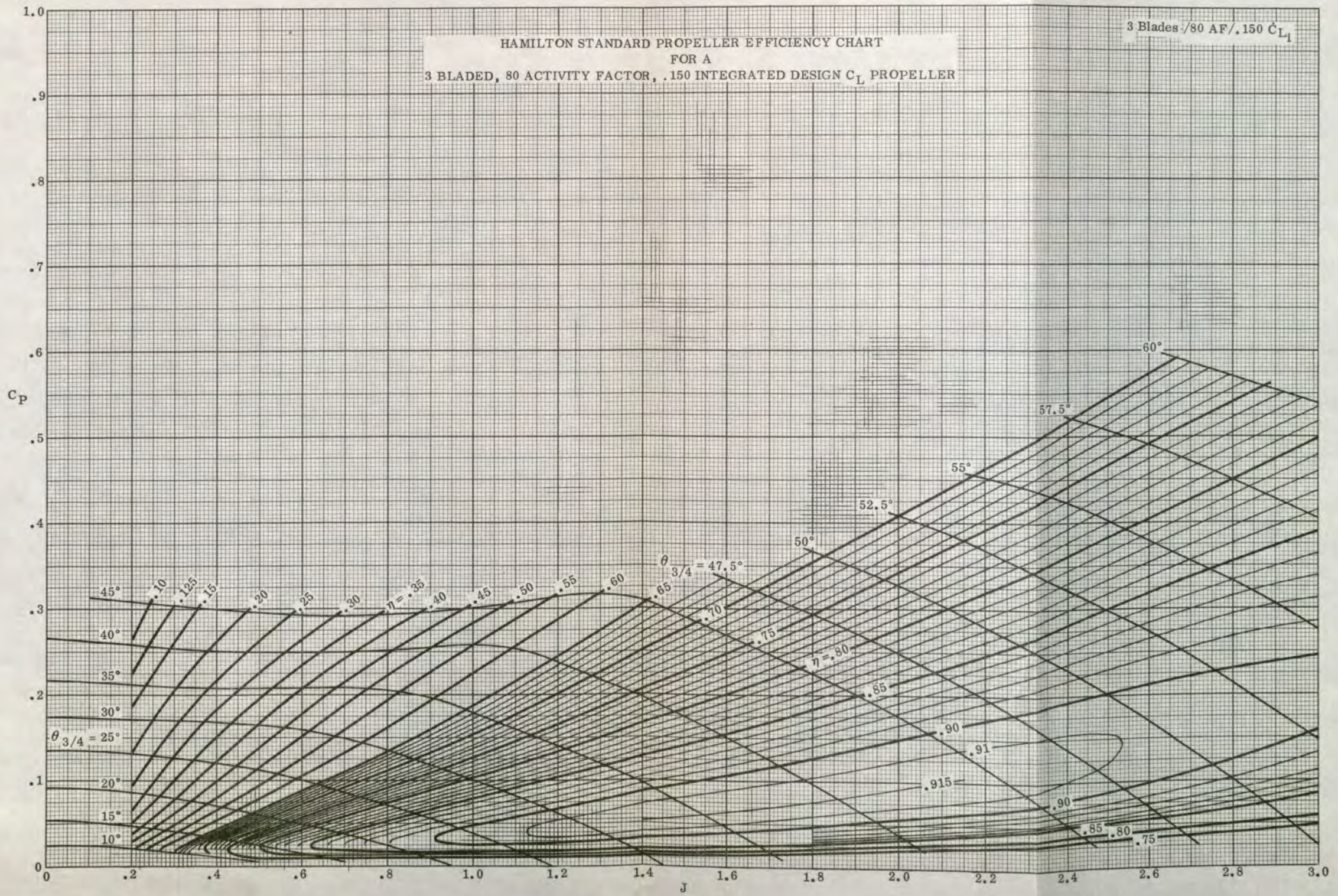
HAMILTON STANDARD PROPELLER EFFICIENCY CHART
FOR A
3 BLADED, 80 ACTIVITY FACTOR, .150 INTEGRATED DESIGN C_L PROPELLER
3 Blades /80 AF/.150 C_{L_i}
C_P
J
$\theta_{3/4}$ = 47.5°
$\theta_{3/4}$ = 25°
η = .35
η = .80
60°
57.5°
55°
52.5°
50°
45°
40°
35°
30°
20°
15°
10°
.10
.125
.15
.20
.25
.30
.40
.45
.50
.55
.60
.65
.70
.75
.85
.90
.91
.915
.90
.85
.80
.75

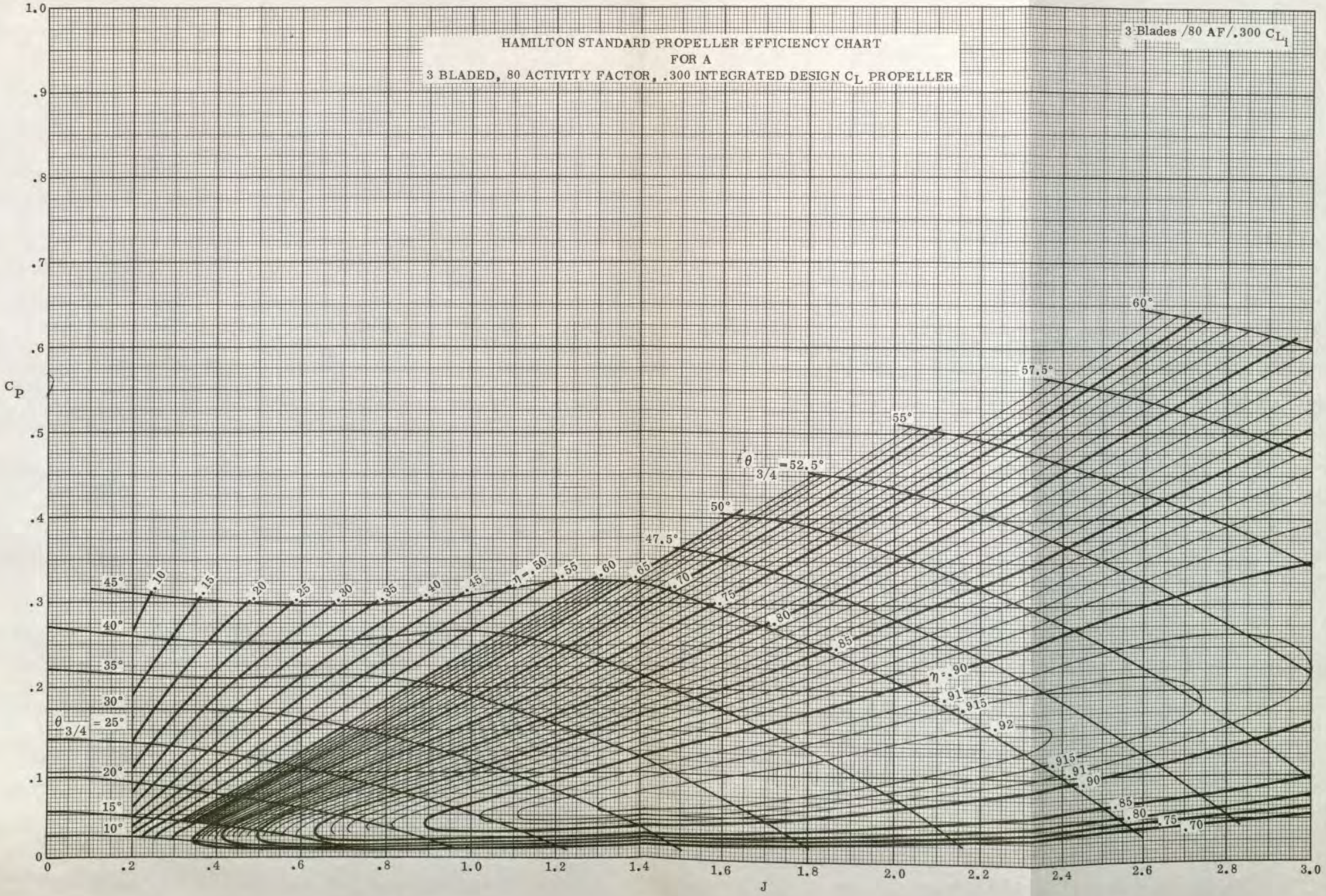
HAMILTON STANDARD PROPELLER EFFICIENCY CHART
FOR A
3 BLADED, 80 ACTIVITY FACTOR, .300 INTEGRATED DESIGN C_L PROPELLER
3 Blades /80 AF/.300 C_{L_i}
C_P
J
$\theta_{3/4}$ = 52.5°
$\theta_{3/4}$ = 25°
60°
57.5°
55°
50°
47.5°
45°
40°
35°
30°
20°
15°
10°
η = .50
η = .90
.10
.15
.20
.25
.30
.35
.40
.45
.55
.60
.65
.70
.75
.80
.85
.91
.915
.92
.90
.85
.80
.75
.70
0
.1
.2
.3
.4
.5
.6
.7
.8
.9
1.0
0
.2
.4
.6
.8
1.0
1.2
1.4
1.6
1.8
2.0
2.2
2.4
2.6
2.8
3.0

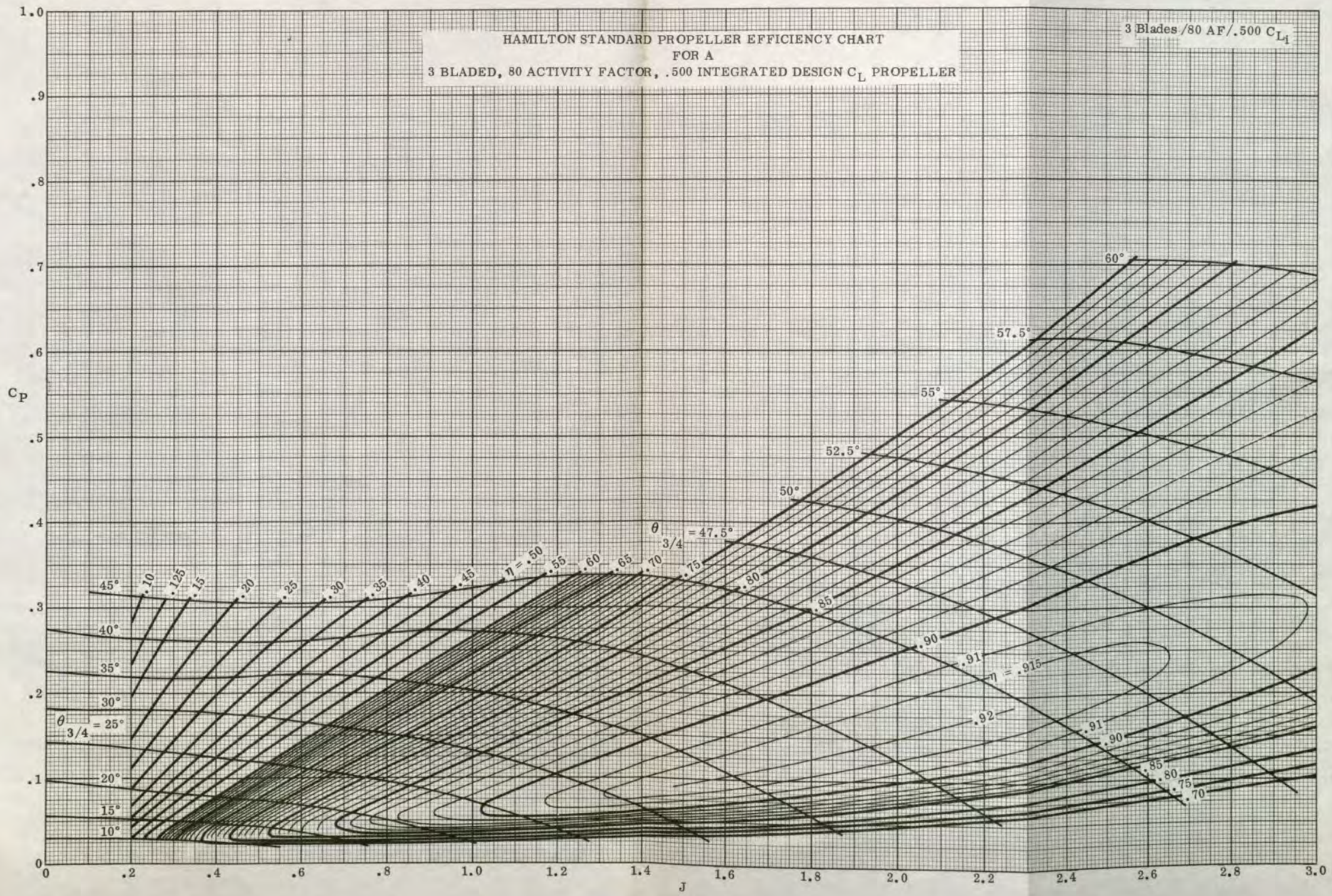
HAMILTON STANDARD PROPELLER EFFICIENCY CHART
FOR A
3 BLADED, 80 ACTIVITY FACTOR, .500 INTEGRATED DESIGN C_L PROPELLER
3 Blades /80 AF/.500 C_{L_i}
C_P
J
$\theta_{3/4}$ = 47.5°
$\theta_{3/4}$ = 25°
η = .50
η = .915
60°
57.5°
55°
52.5°
50°
45°
40°
35°
30°
20°
15°
10°
.10
.125
.15
.20
.25
.30
.35
.40
.45
.55
.60
.65
.70
.75
.80
.85
.90
.91
.92
.70
.75
.80
.85
.90
.91
0
.1
.2
.3
.4
.5
.6
.7
.8
.9
1.0
.2
.4
.6
.8
1.0
1.2
1.4
1.6
1.8
2.0
2.2
2.4
2.6
2.8
3.0

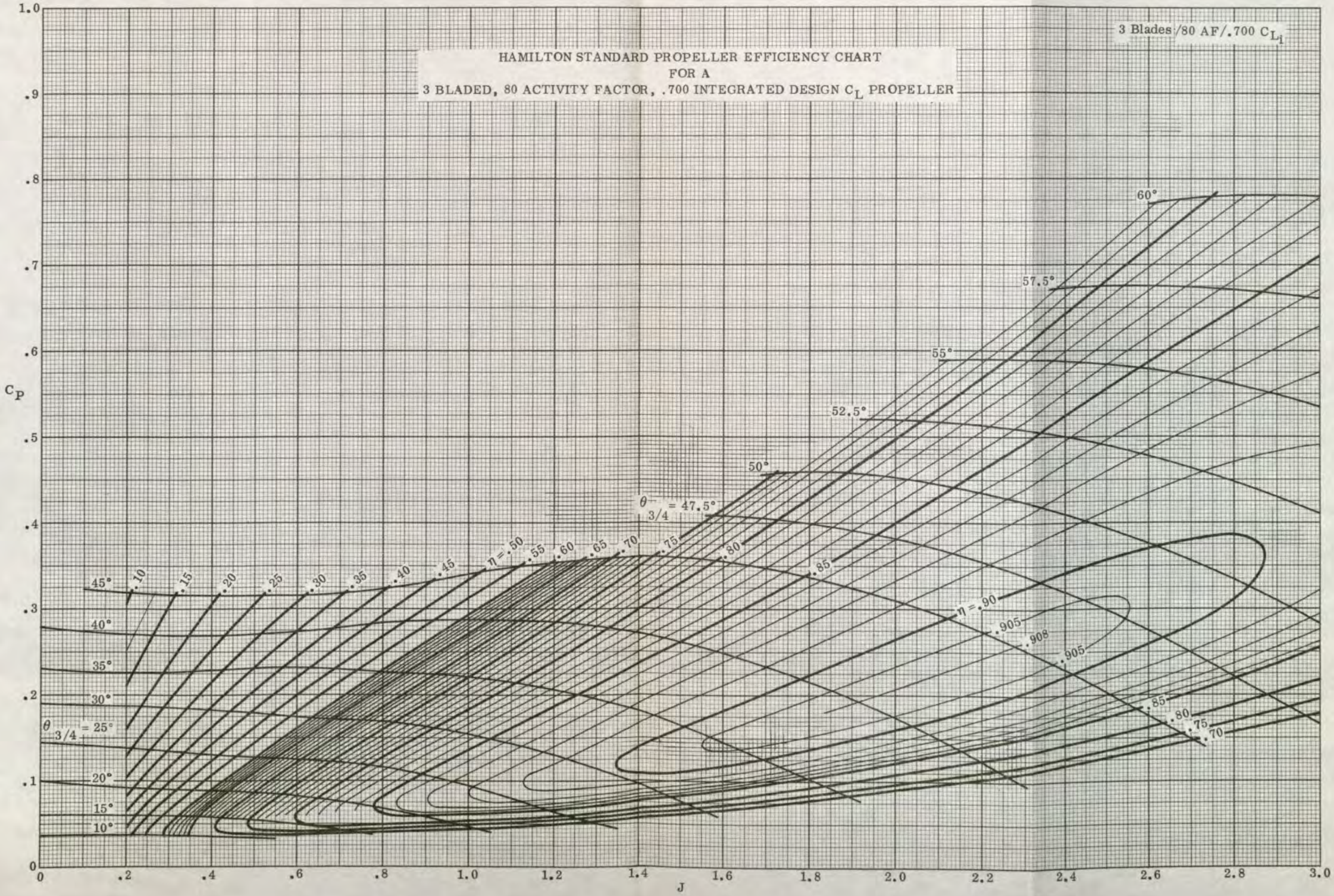
HAMILTON STANDARD PROPELLER EFFICIENCY CHART
FOR A
3 BLADED, 80 ACTIVITY FACTOR, .700 INTEGRATED DESIGN C_L PROPELLER
3 Blades/80 AF/.700 C_{L_i}
C_P
J
$\theta_{3/4}$ = 25°
$\theta_{3/4}$ = 47.5°
η = .50
η = .90
.905
.908
.905
.85
.80
.75
.70
.85
.80
.75
.70
.65
.60
.55
.50
.45
.40
.35
.30
.25
.20
.15
.10
45°
40°
35°
30°
20°
15°
10°
50°
52.5°
55°
57.5°
60°

HAMILTON STANDARD PROPELLER EFFICIENCY CHART
FOR A
3 BLADED, 100 ACTIVITY FACTOR, .150 INTEGRATED DESIGN C_L PROPELLER

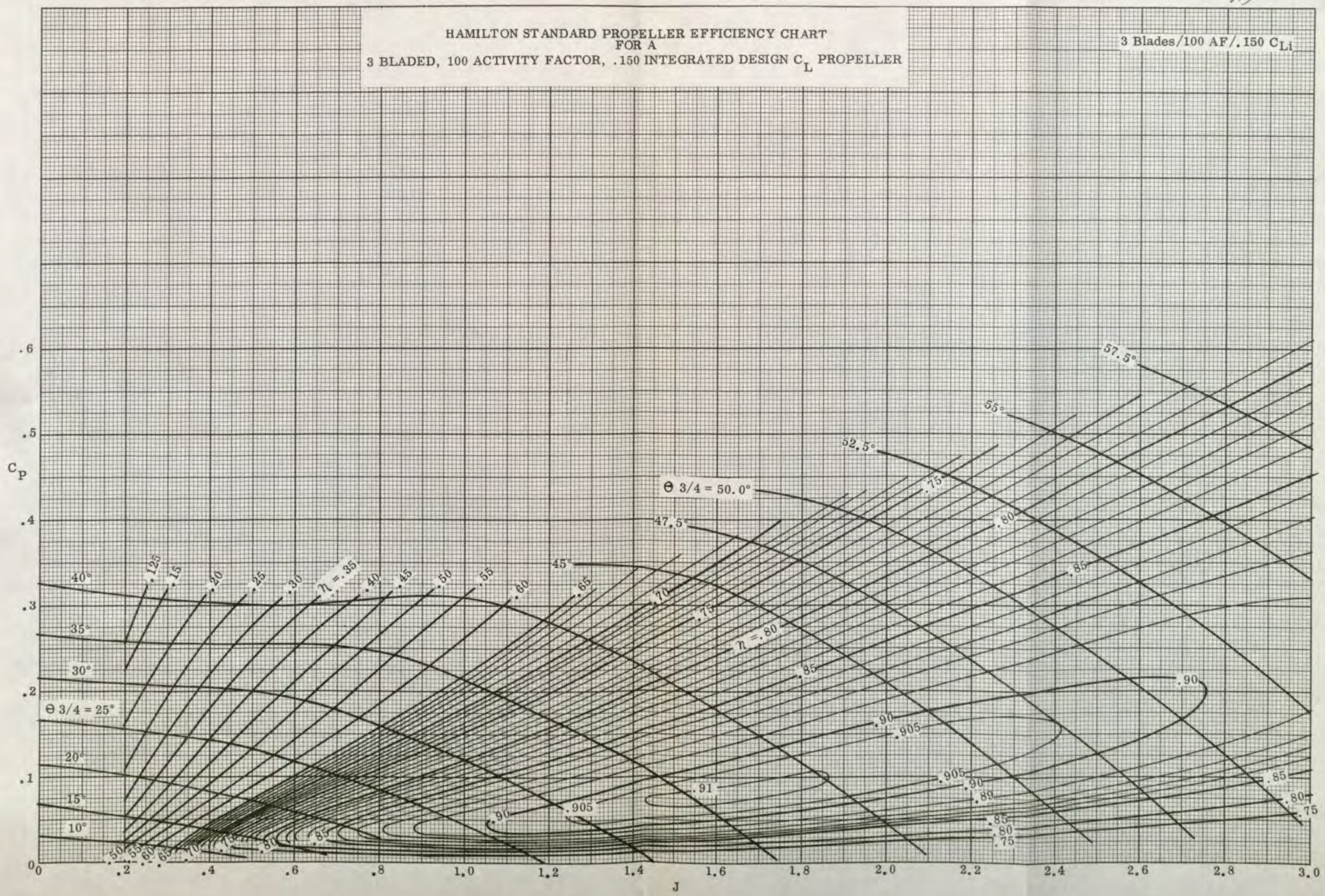

February 1, 1961

FIGURE 124

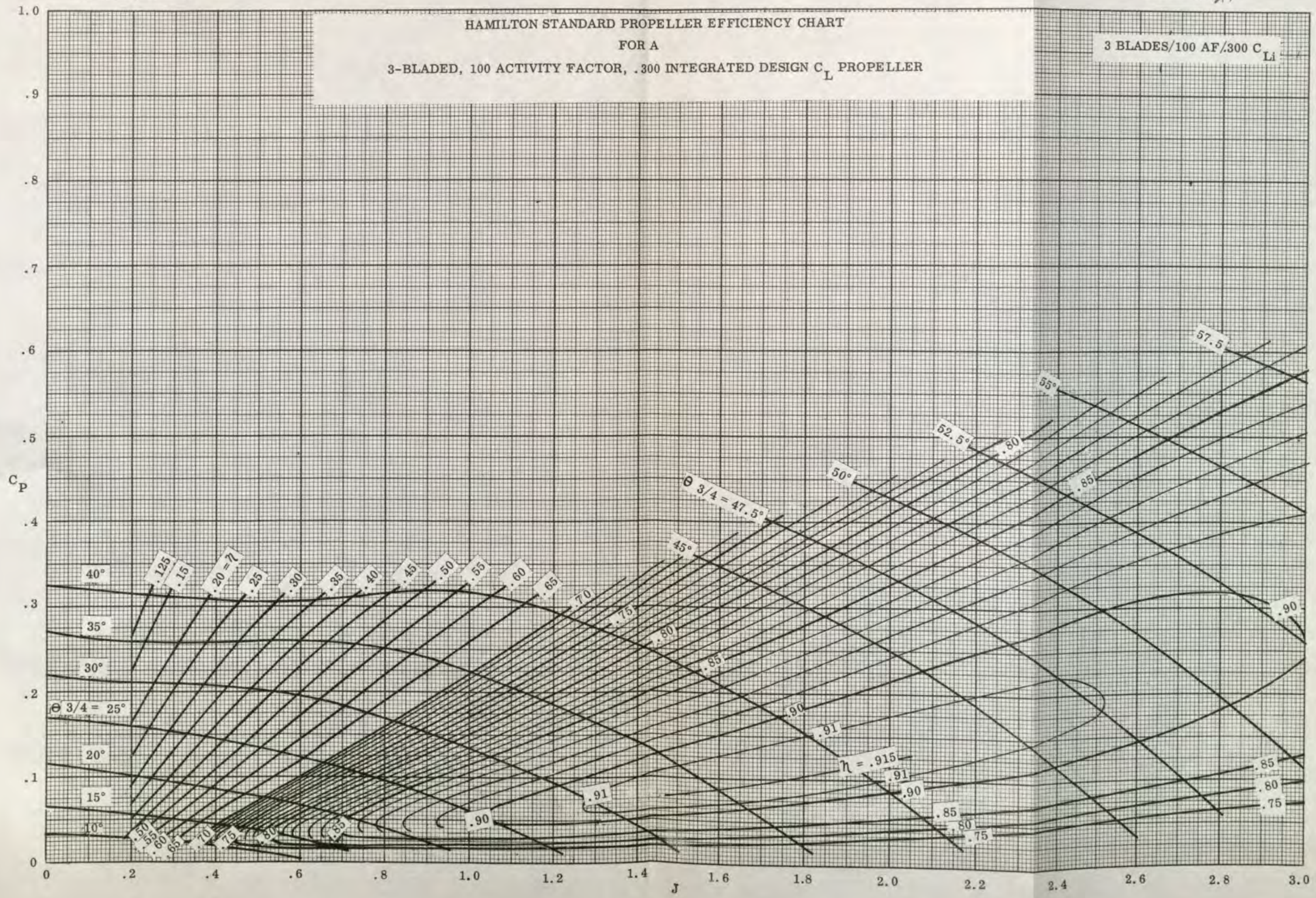

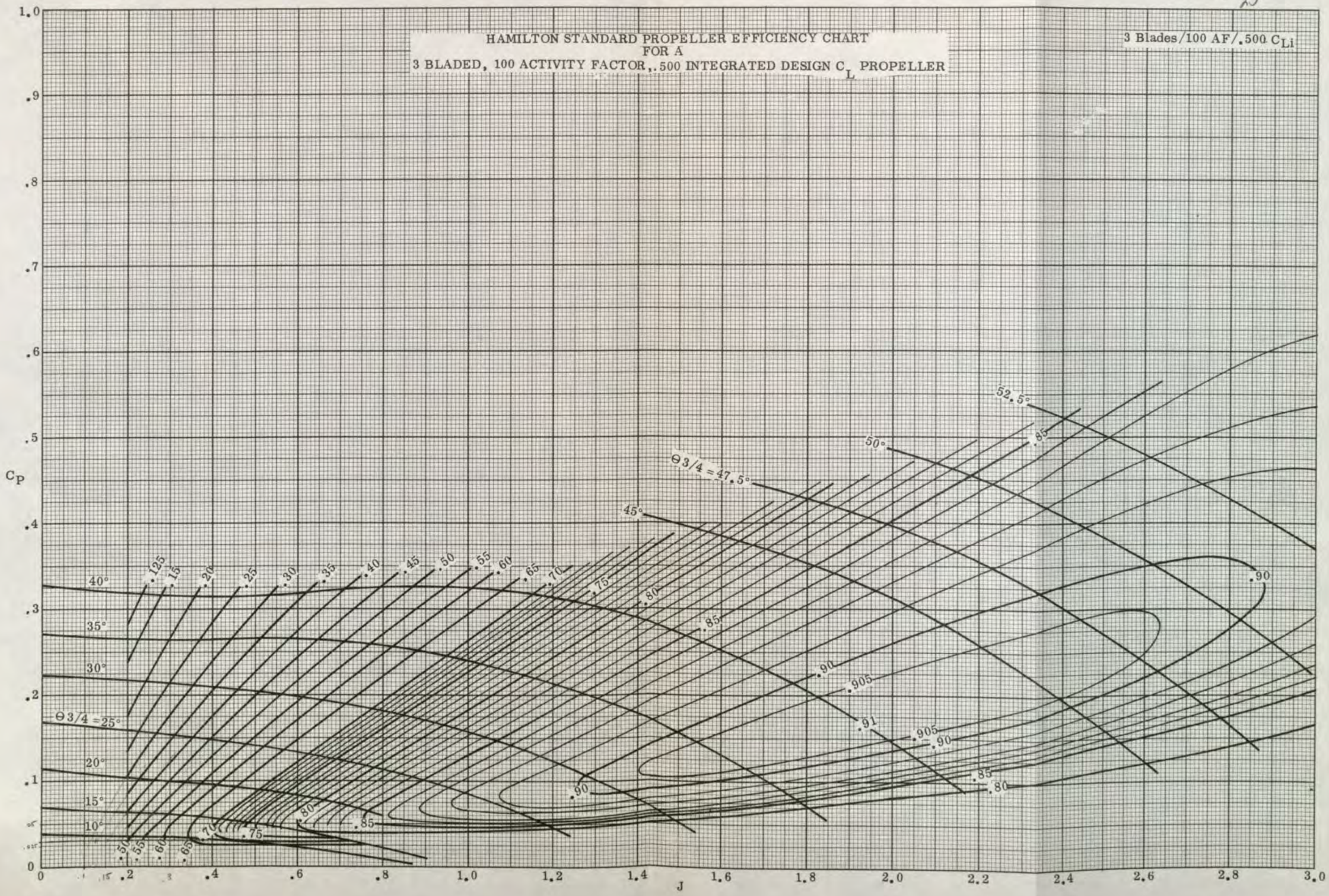
HAMILTON STANDARD PROPELLER EFFICIENCY CHART
FOR A
3 BLADED, 100 ACTIVITY FACTOR, .500 INTEGRATED DESIGN C_L PROPELLER
3 Blades/100 AF/.500 C_{Li}
C_P
J
$\Theta 3/4 = 47.5°$
$\Theta 3/4 = 25°$
40°
35°
30°
20°
15°
10°
45°
50°
52.5°
.125
.15
.20
.25
.30
.35
.40
.45
.50
.55
.60
.65
.70
.75
.80
.85
.90
.905
.91

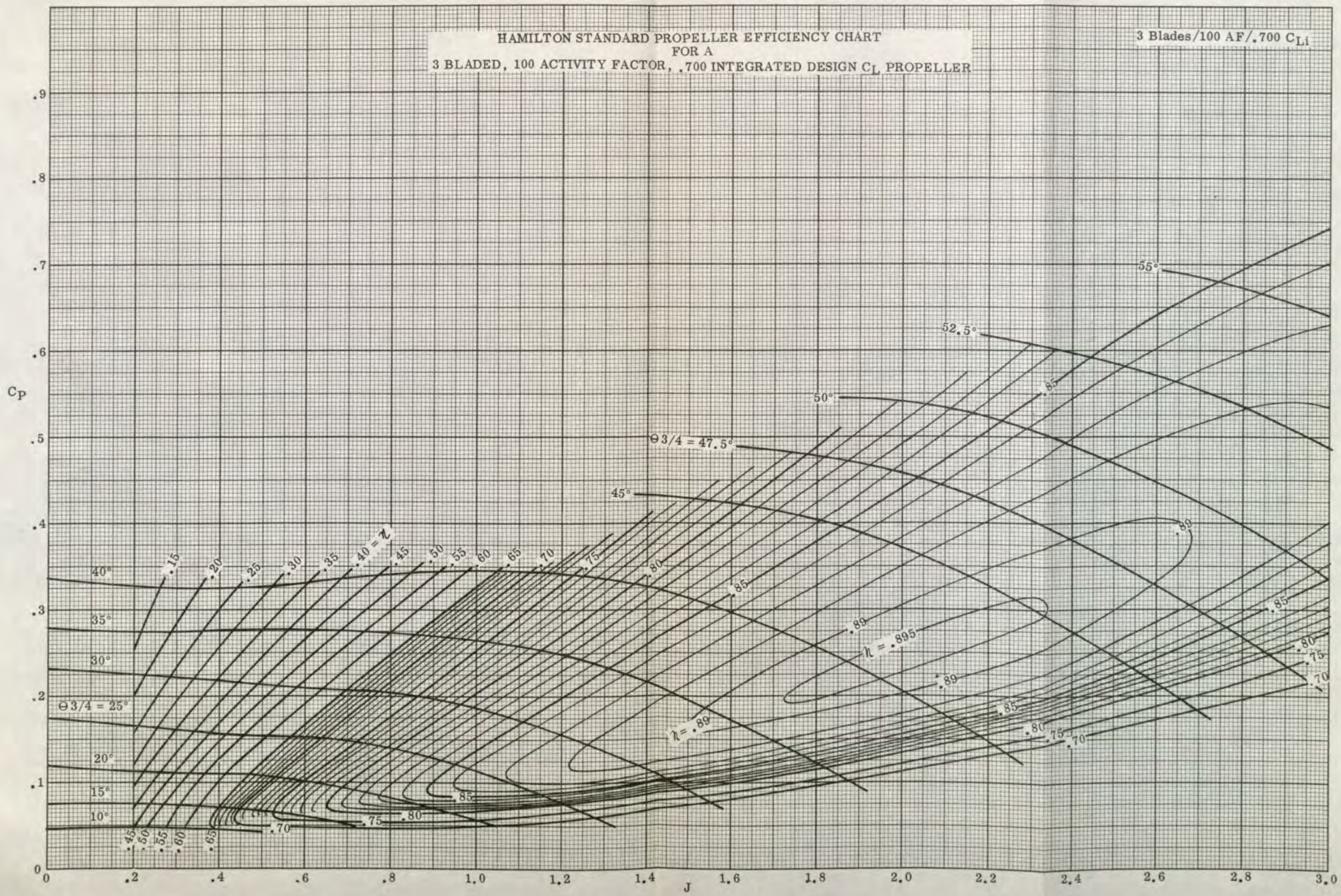
HAMILTON STANDARD PROPELLER EFFICIENCY CHART
FOR A
3 BLADED, 100 ACTIVITY FACTOR, .700 INTEGRATED DESIGN C_L PROPELLER
3 Blades/100 AF/.700 C_{Li}
C_P
J
Θ 3/4 = 25°
Θ 3/4 = 47.5°
η = .89
η = .895
η = .40

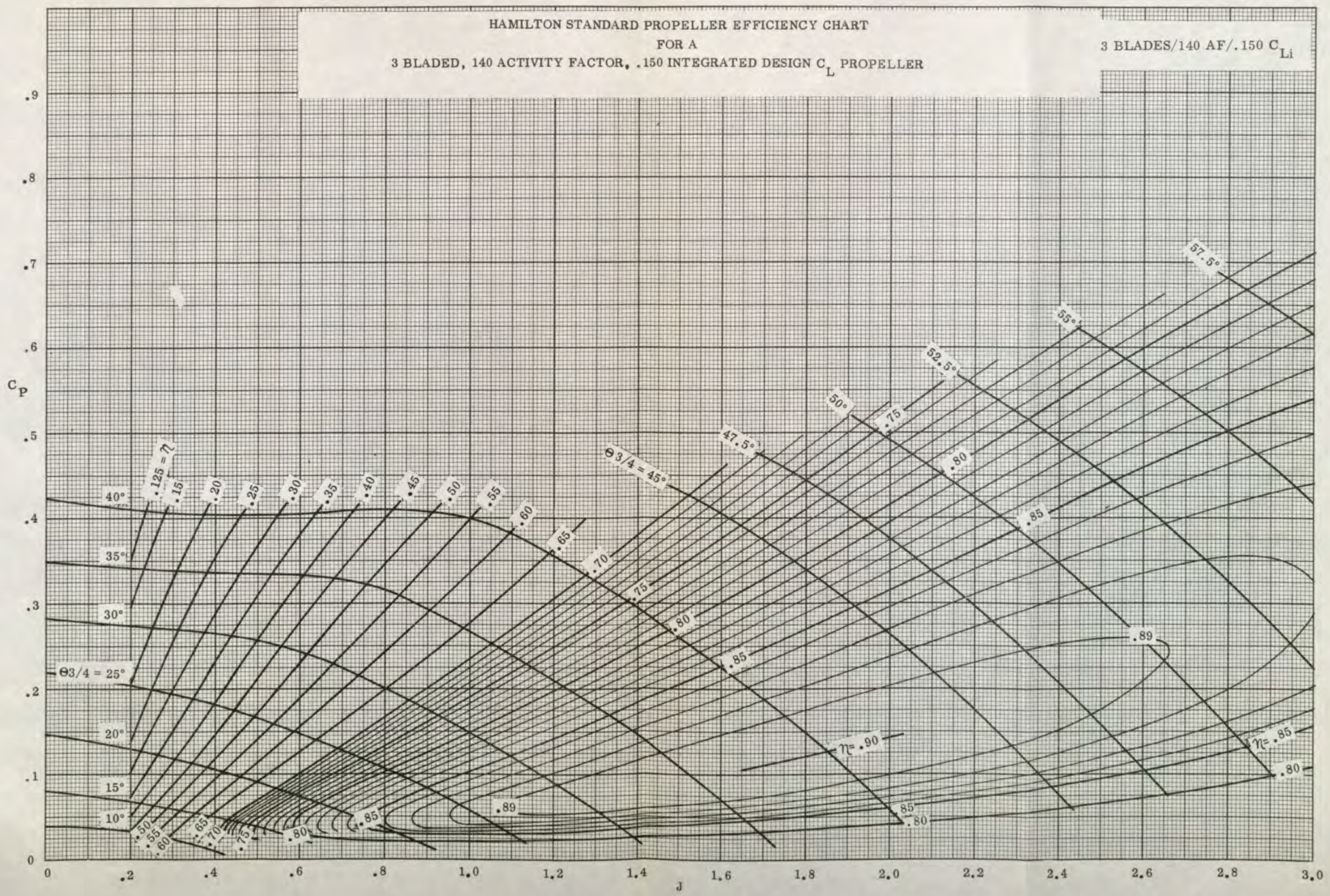
HAMILTON STANDARD PROPELLER EFFICIENCY CHART
FOR A
3 BLADED, 140 ACTIVITY FACTOR, .150 INTEGRATED DESIGN C_L PROPELLER
3 BLADES/140 AF/.150 C_{Li}
C_P
J
$\Theta 3/4 = 25°$
$\Theta 3/4 = 45°$
η = .125
η = .90
η = .85
η = .80
.89
40°
35°
30°
20°
15°
10°
57.5°
55°
52.5°
50°
47.5°

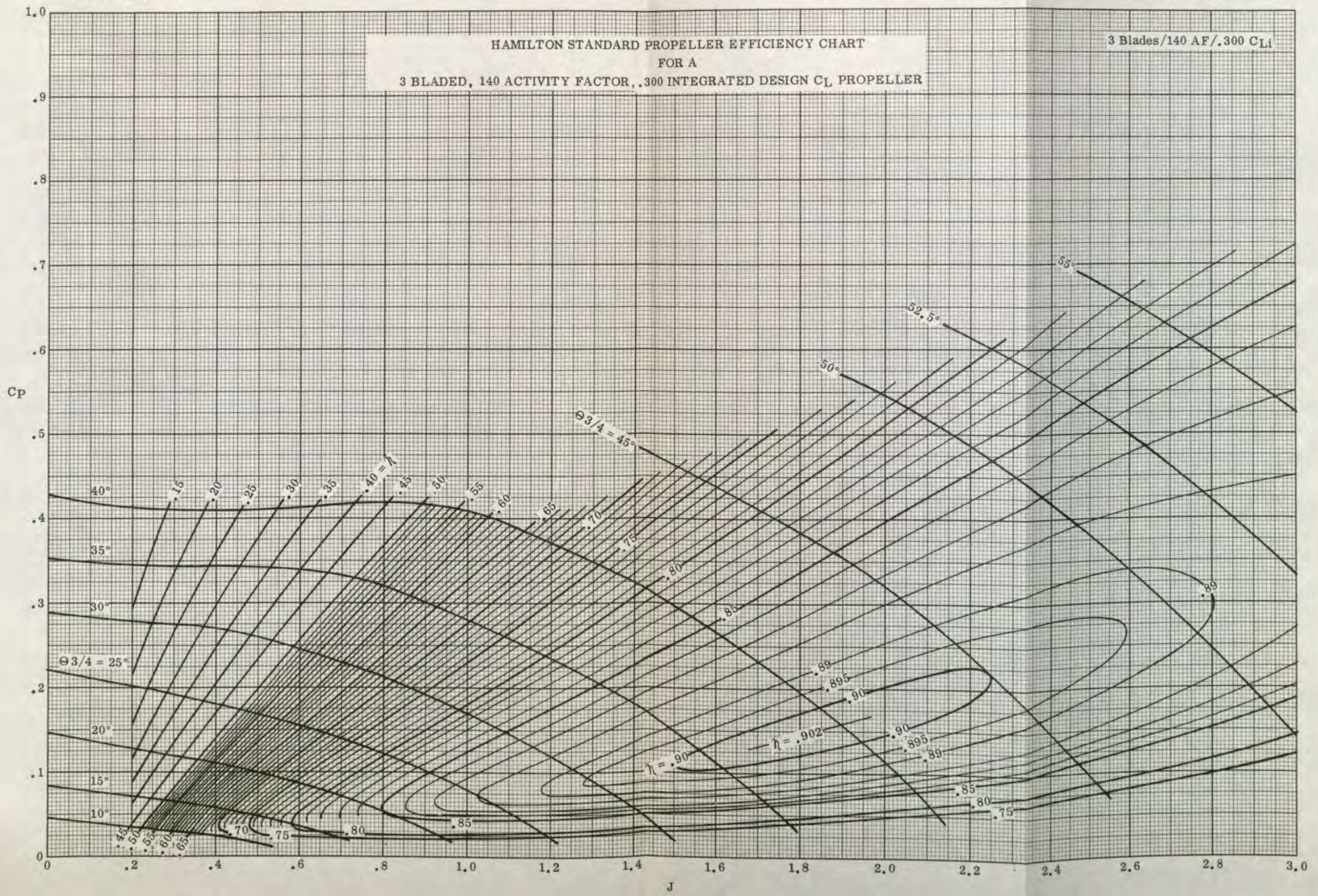
HAMILTON STANDARD PROPELLER EFFICIENCY CHART
FOR A
3 BLADED, 140 ACTIVITY FACTOR, .300 INTEGRATED DESIGN C_L PROPELLER
3 Blades/140 AF/.300 C_{Li}
Cp
J
θ3/4 = 25°
θ3/4 = 45°
40° = λ
λ = .902
λ = .90

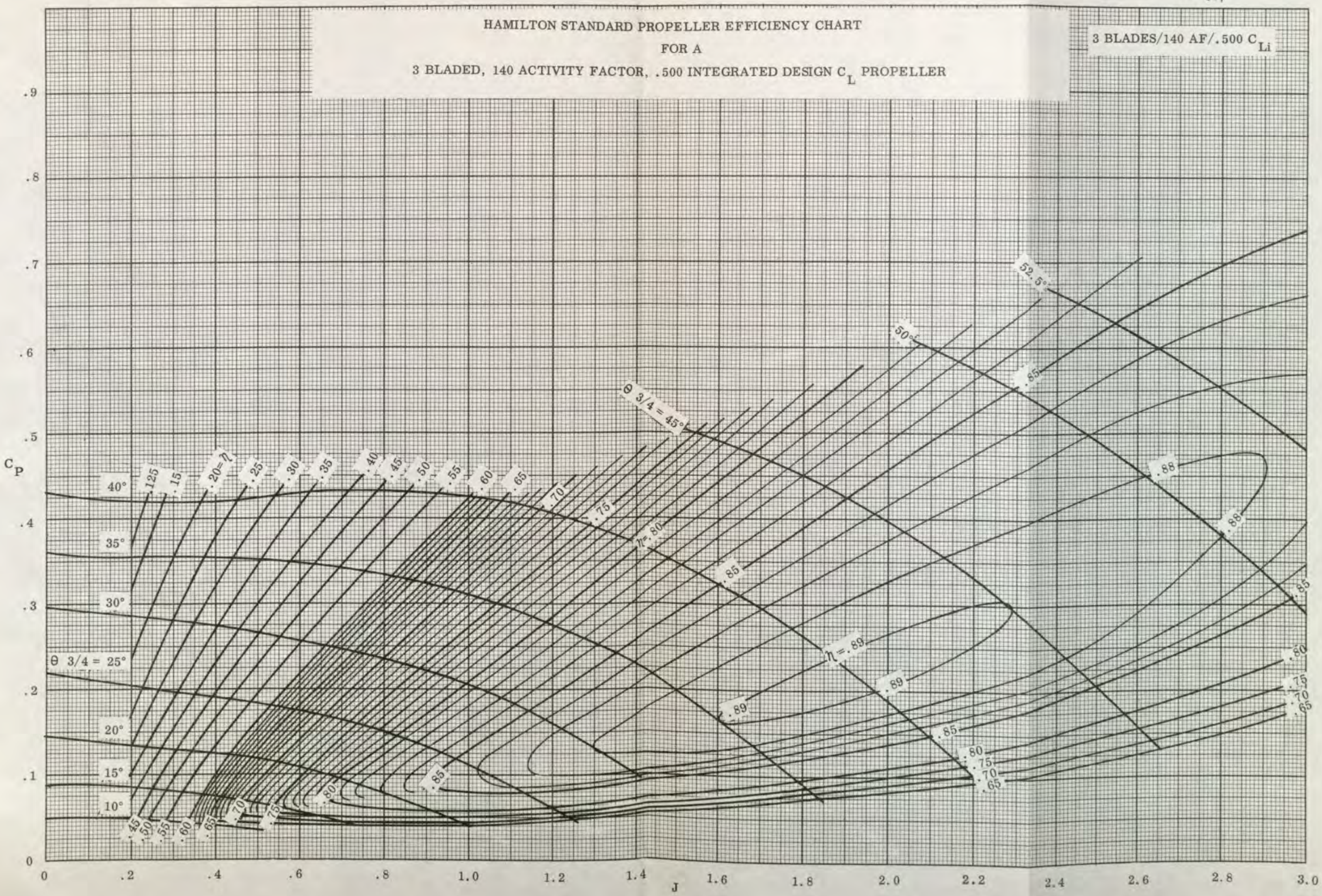
HAMILTON STANDARD PROPELLER EFFICIENCY CHART
FOR A
3 BLADED, 140 ACTIVITY FACTOR, .500 INTEGRATED DESIGN C_L PROPELLER
3 BLADES/140 AF/.500 C_{Li}
C_P
J
θ 3/4 = 25°
θ 3/4 = 45°
η = .80
η = .89
η = .20
η = .88
η = .85
η = .75
η = .70
η = .65
η = .60
η = .55
η = .50
η = .45
η = .40
η = .35
η = .30
η = .25
η = .15
η = .125
10°
15°
20°
30°
35°
40°
50°
52.5°

February 1, 1961

FIGURE 30

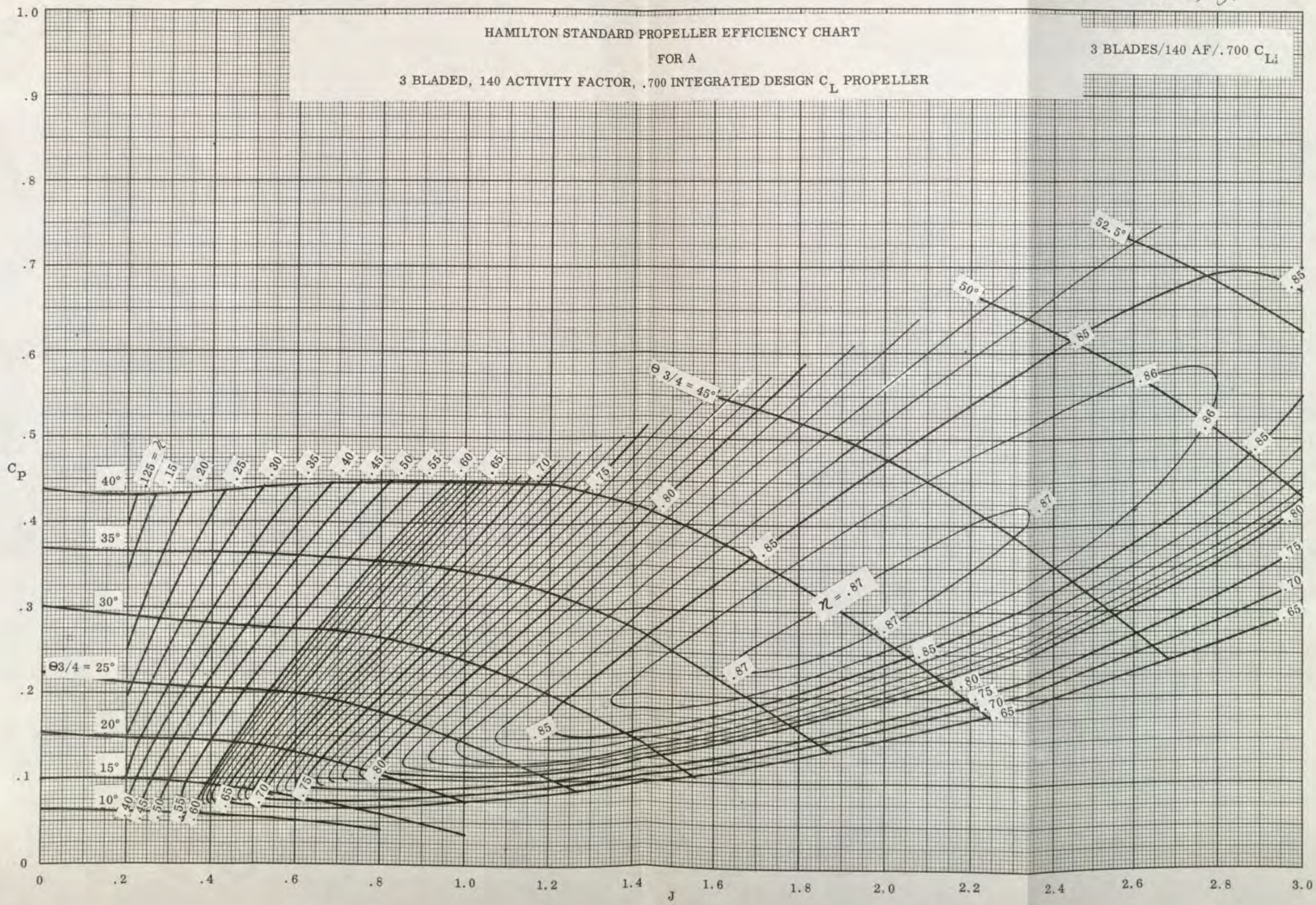

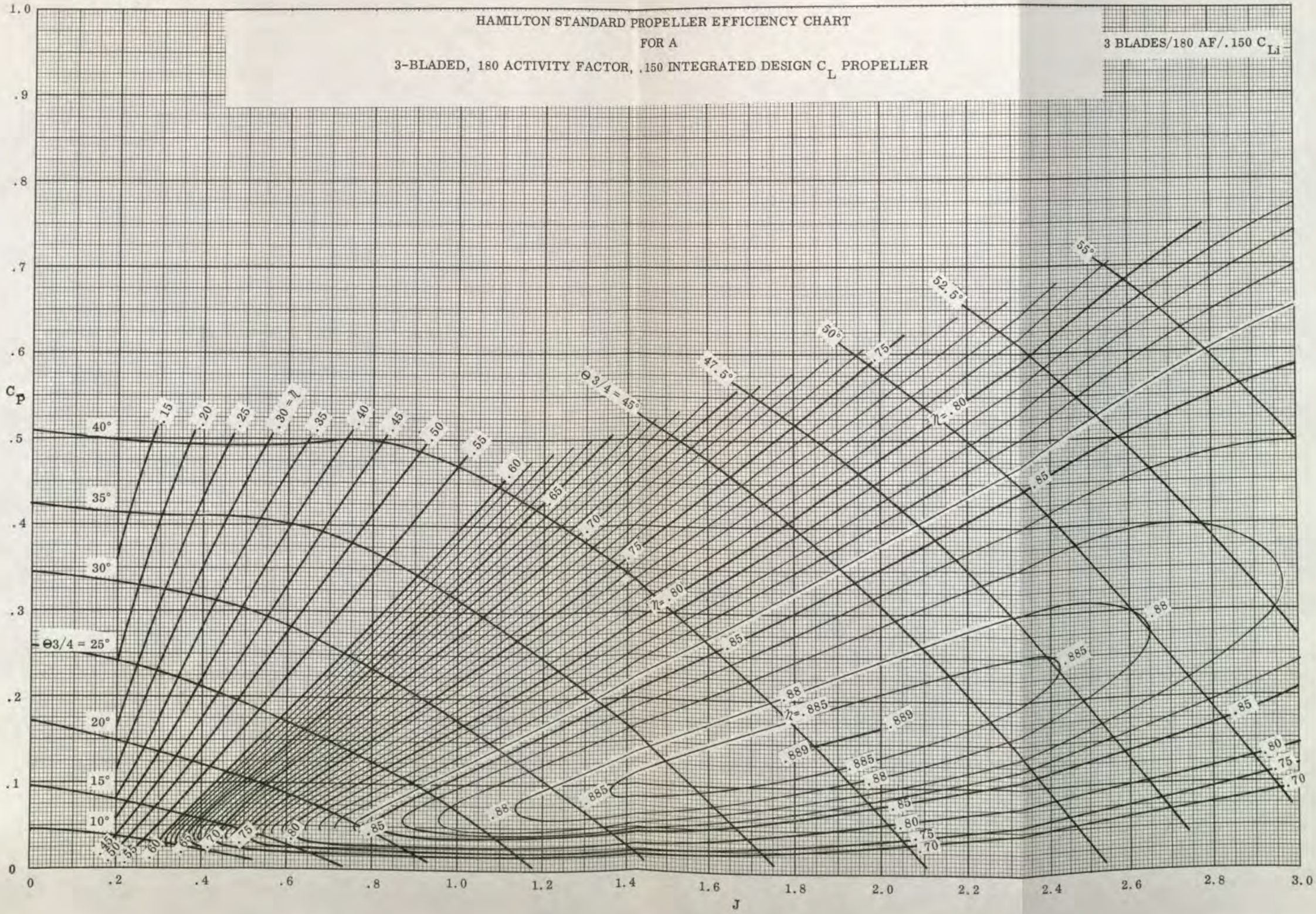
HAMILTON STANDARD PROPELLER EFFICIENCY CHART
FOR A
3-BLADED, 180 ACTIVITY FACTOR, .150 INTEGRATED DESIGN C_L PROPELLER
3 BLADES/180 AF/.150 C_{Li}
C_P
J
$\theta 3/4 = 25°$
$\theta 3/4 = 45°$
$\eta = .80$
$\eta = .885$

FIGURE 19 32

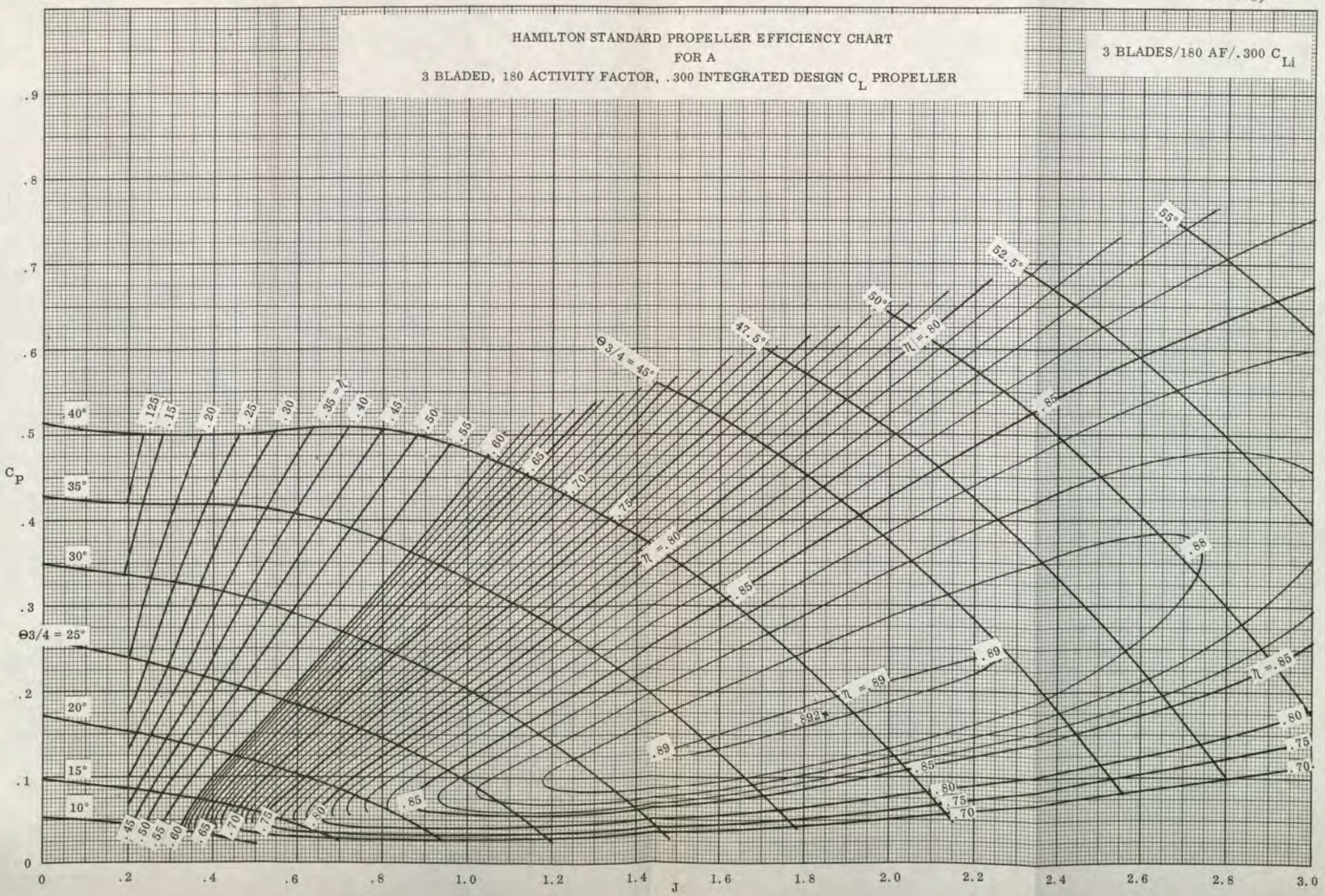
HAMILTON STANDARD PROPELLER EFFICIENCY CHART
FOR A
3 BLADED, 180 ACTIVITY FACTOR, .300 INTEGRATED DESIGN C_L PROPELLER
3 BLADES/180 AF/.300 C_{Li}
C_P
J
$\Theta 3/4 = 25°$
$\Theta 3/4 = 45°$
10°
15°
20°
30°
35°
40°
47.5°
50°
52.5°
55°
$\eta = .35$
$\eta = .80$
$\eta = .85$
$\eta = .89$
.892
.88
.89
.85
.80
.75
.70
.65
.60
.55
.50
.45
.40
.35
.30
.25
.20
.15
.125
0
.1
.2
.3
.4
.5
.6
.7
.8
.9
1.0
1.2
1.4
1.6
1.8
2.0
2.2
2.4
2.6
2.8
3.0

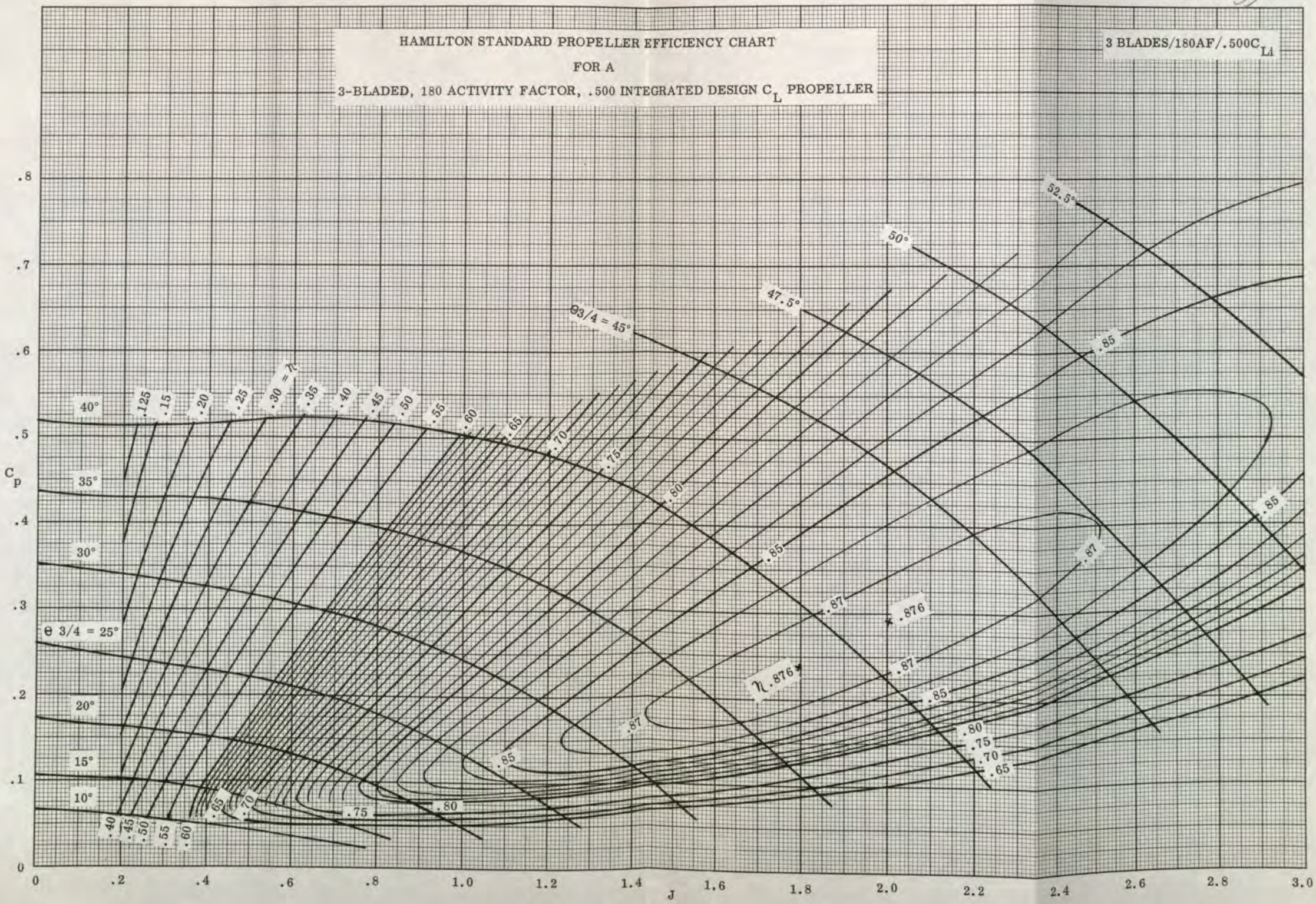
HAMILTON STANDARD PROPELLER EFFICIENCY CHART
FOR A
3-BLADED, 180 ACTIVITY FACTOR, .500 INTEGRATED DESIGN C_L PROPELLER
3 BLADES/180AF/.500C_{Li}
C_p
J
θ 3/4 = 25°
θ 3/4 = 45°
η .876
.876
52.5°
50°
47.5°
40°
35°
30°
20°
15°
10°

FIGURE 21 34

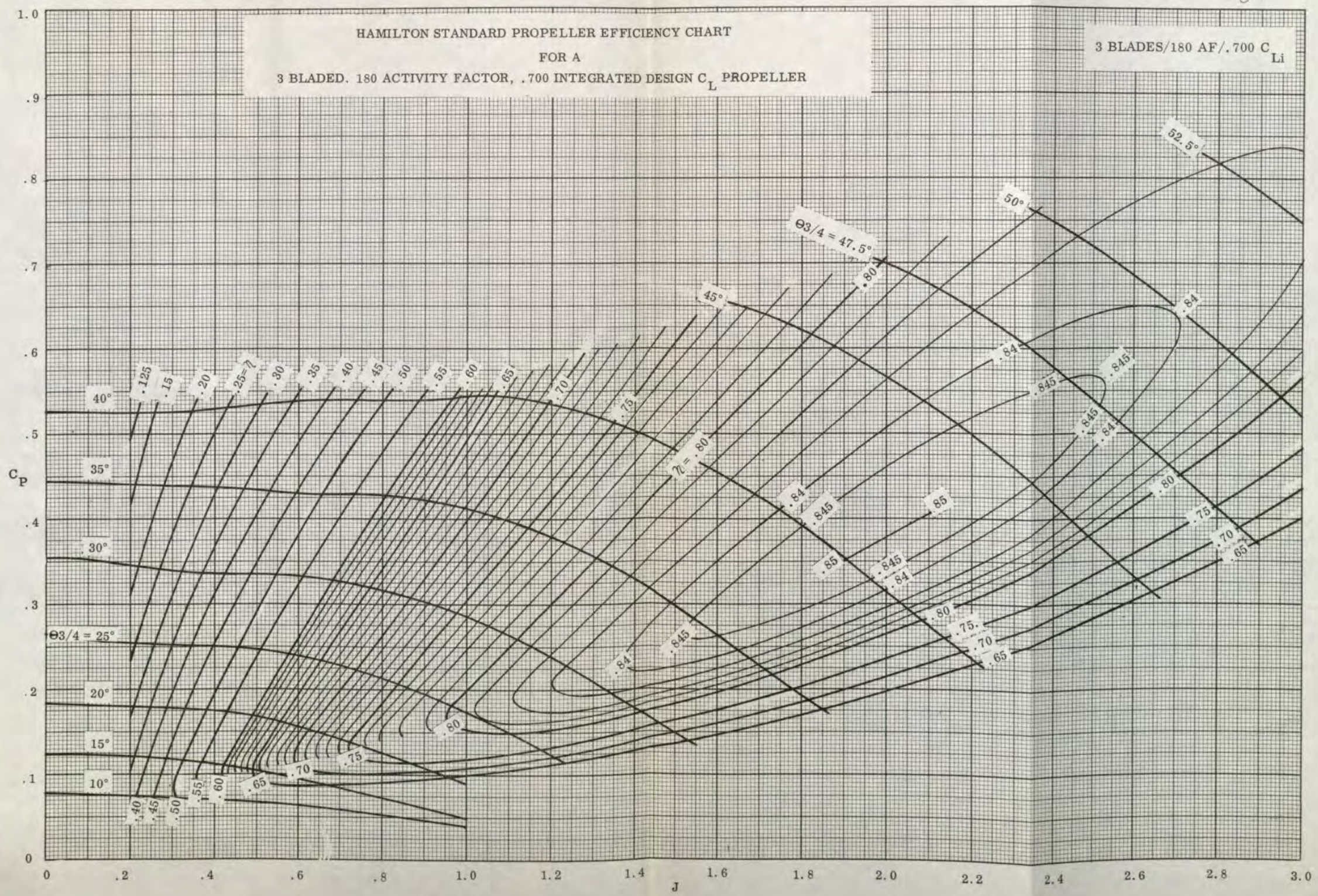
HAMILTON STANDARD PROPELLER EFFICIENCY CHART
FOR A
3 BLADED. 180 ACTIVITY FACTOR, .700 INTEGRATED DESIGN C_L PROPELLER
3 BLADES/180 AF/.700 C_{Li}
C_P
J
$\Theta 3/4 = 25°$
$\Theta 3/4 = 47.5°$
$\eta = .80$
10°
15°
20°
30°
35°
40°
45°
50°
52.5°
.125
.15
.20
.25=η
.30
.35
.40
.45
.50
.55
.60
.65
.70
.75
.80
.84
.845
.85

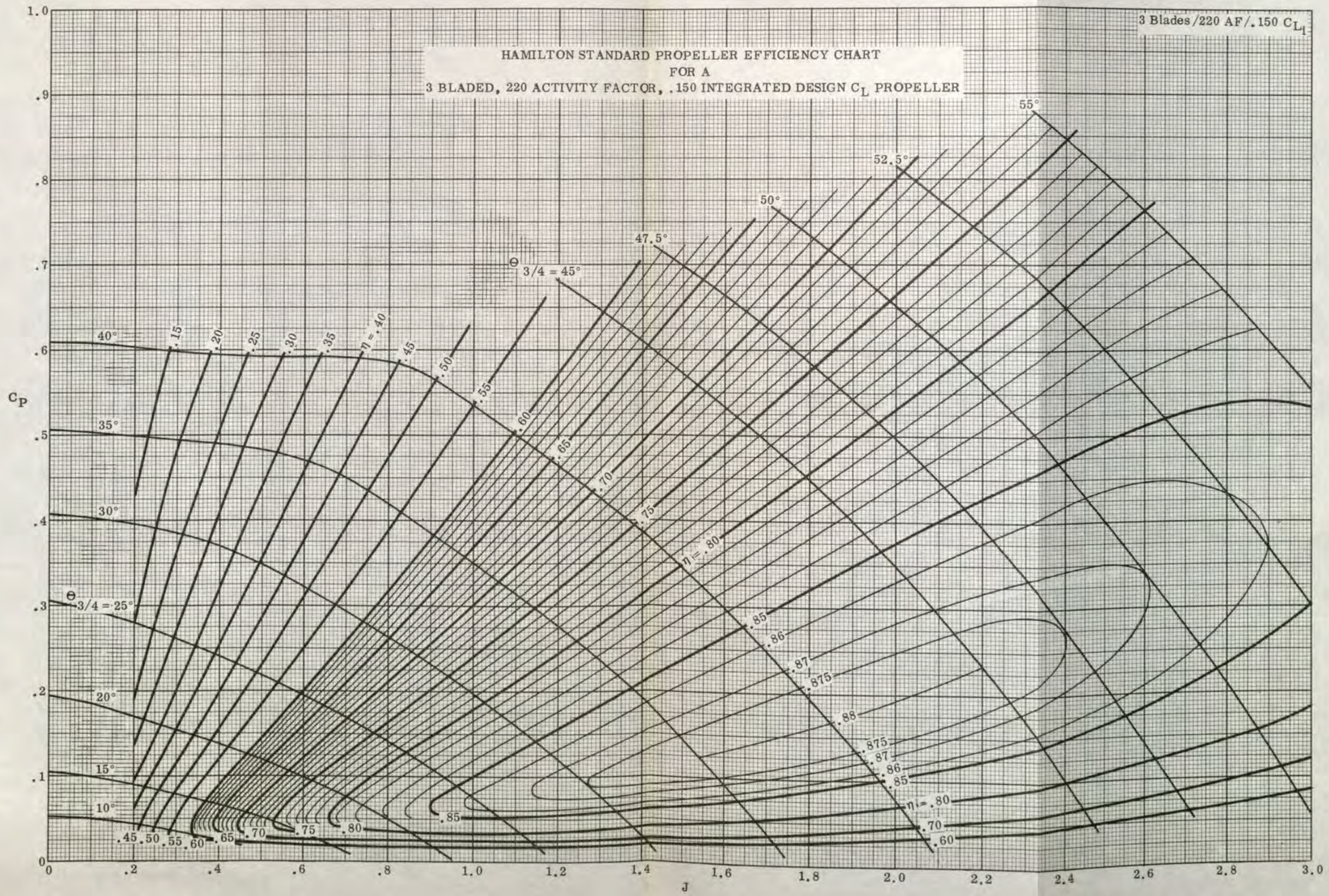
HAMILTON STANDARD PROPELLER EFFICIENCY CHART
FOR A
3 BLADED, 220 ACTIVITY FACTOR, .150 INTEGRATED DESIGN C_L PROPELLER
3 Blades/220 AF/.150 C_{L_i}
C_P
J
$\Theta_{3/4}$ = 45°
$\Theta_{3/4}$ = 25°
40°
35°
30°
20°
15°
10°
55°
52.5°
50°
47.5°
η = .40
η = .80
η = .80
.15
.20
.25
.30
.35
.45
.50
.55
.60
.65
.70
.75
.80
.85
.86
.87
.875
.88
.875
.87
.86
.85
.80
.70
.60
.45
.50
.55
.60
.65
.70
.75
.80
.85
0
.1
.2
.3
.4
.5
.6
.7
.8
.9
1.0
0
.2
.4
.6
.8
1.0
1.2
1.4
1.6
1.8
2.0
2.2
2.4
2.6
2.8
3.0

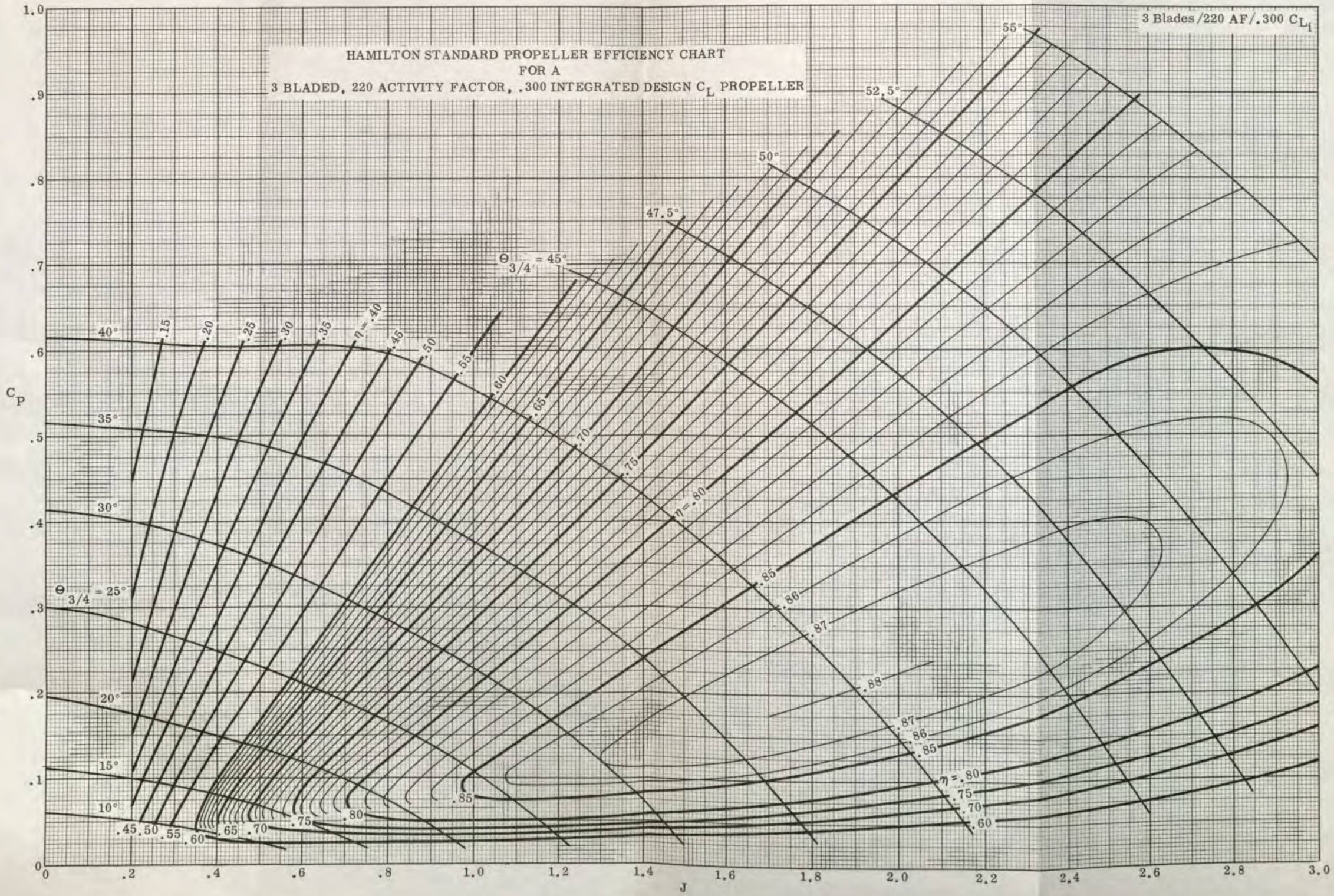
HAMILTON STANDARD PROPELLER EFFICIENCY CHART
FOR A
3 BLADED, 220 ACTIVITY FACTOR, .300 INTEGRATED DESIGN C_L PROPELLER
3 Blades /220 AF/.300 C_{L_i}
C_P
J
$\Theta_{3/4} = 45°$
$\Theta_{3/4} = 25°$
$\eta = .40$
$\eta = .80$
55°
52.5°
50°
47.5°
40°
35°
30°
20°
15°
10°
.15
.20
.25
.30
.35
.45
.50
.55
.60
.65
.70
.75
.80
.85
.86
.87
.88

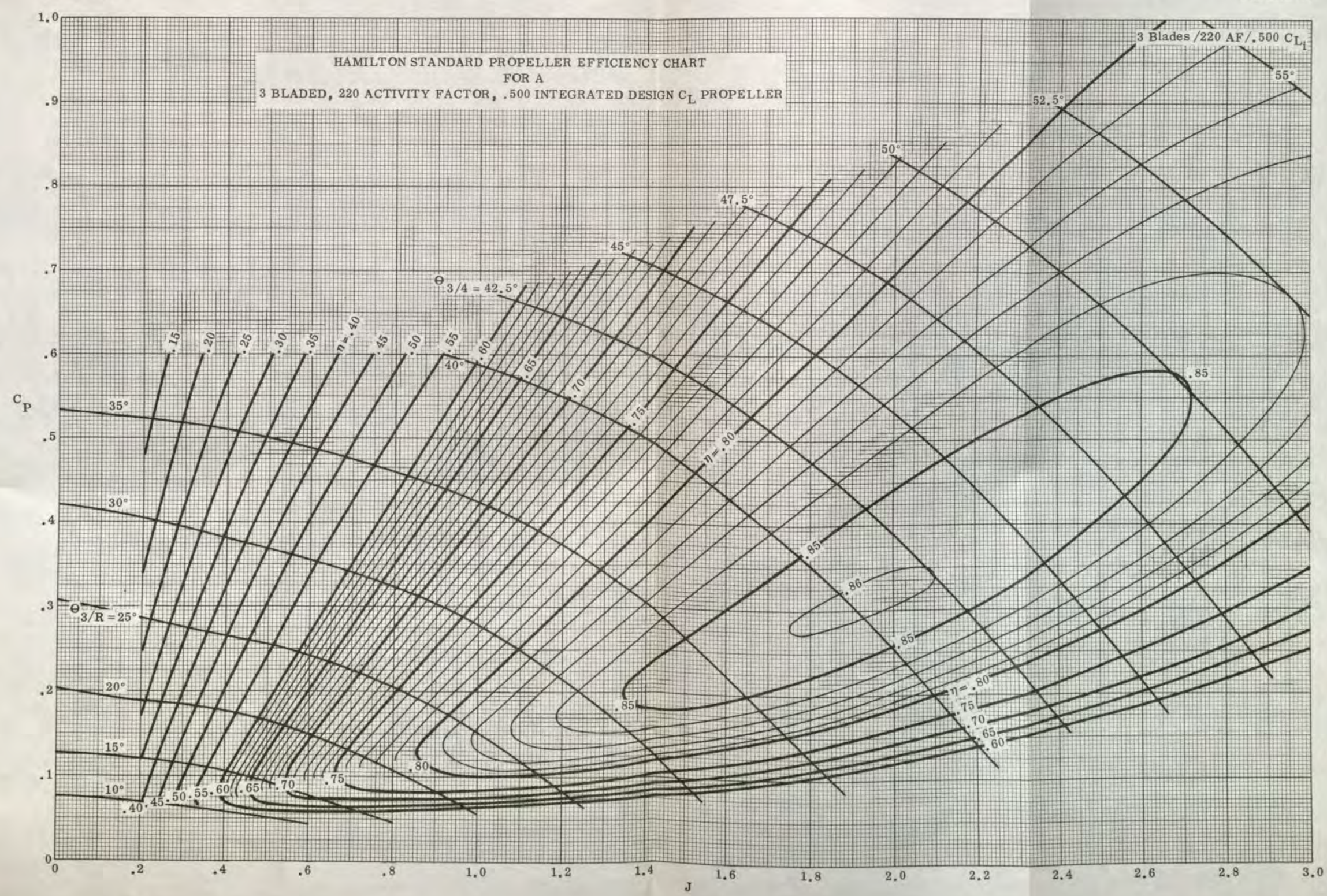
HAMILTON STANDARD PROPELLER EFFICIENCY CHART
FOR A
3 BLADED, 220 ACTIVITY FACTOR, .500 INTEGRATED DESIGN C_L PROPELLER
3 Blades /220 AF/.500 C_{L_i}
C_P
J
Θ 3/4 = 42.5°
Θ 3/R = 25°
35°
30°
20°
15°
10°
40°
45°
47.5°
50°
52.5°
55°
η = .40
η = .80
.15
.20
.25
.30
.35
.45
.50
.55
.60
.65
.70
.75
.85
.86

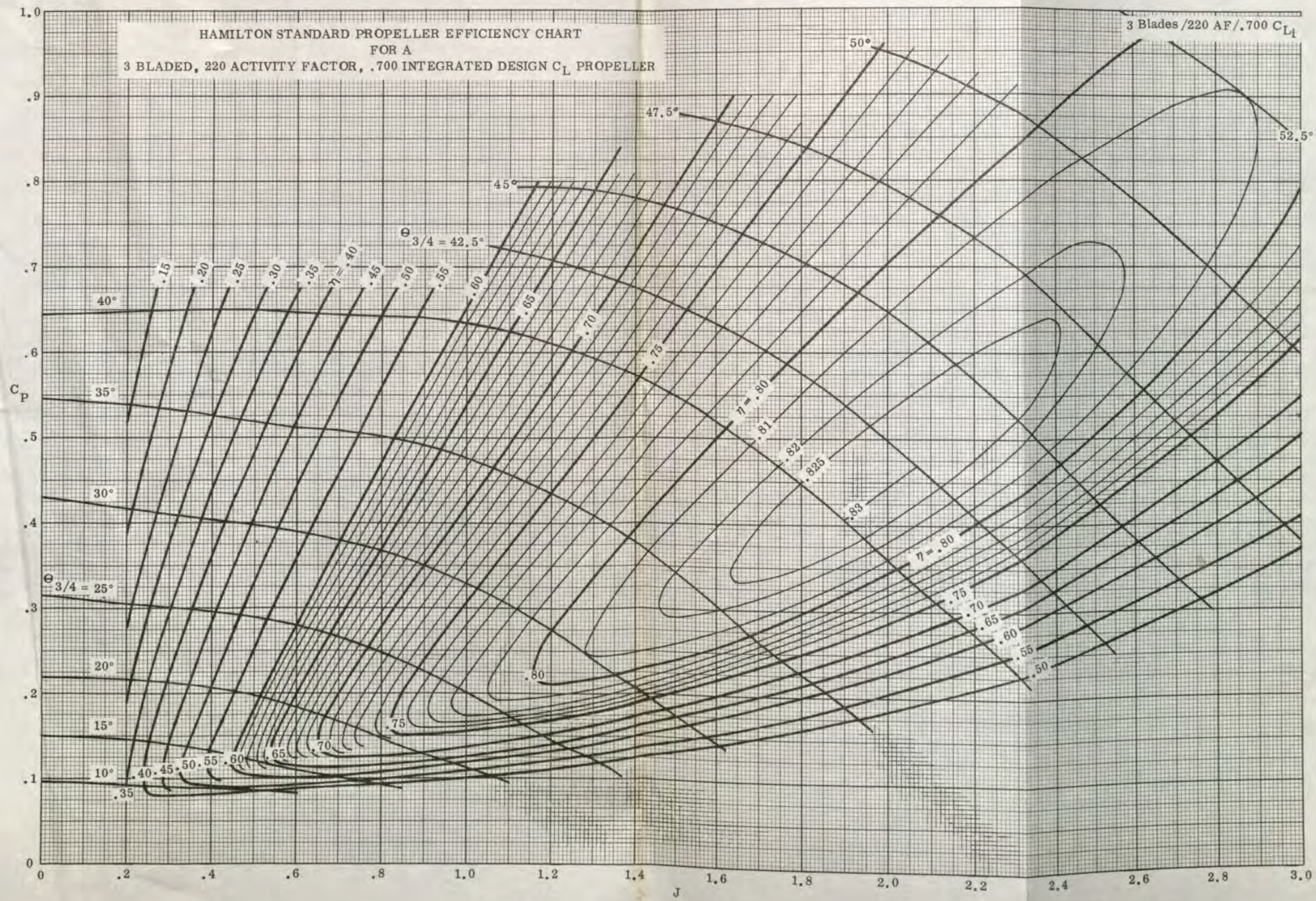
HAMILTON STANDARD PROPELLER EFFICIENCY CHART
FOR A
3 BLADED, 220 ACTIVITY FACTOR, .700 INTEGRATED DESIGN C_L PROPELLER
3 Blades /220 AF/.700 C_{L_i}
C_P
J
$\Theta_{3/4}$ = 42.5°
$\Theta_{3/4}$ = 25°
50°
47.5°
45°
52.5°
40°
35°
30°
20°
15°
10°
η = .40
η = .80
η = .81
η = .82
η = .825
η = .83
.15
.20
.25
.30
.35
.45
.50
.55
.60
.65
.70
.75
.80
.35
.40
.45
.50
.55
.60
.65
.70
.75
.80
.75
.70
.65
.60
.55
.50
0
.1
.2
.3
.4
.5
.6
.7
.8
.9
1.0
0
.2
.4
.6
.8
1.0
1.2
1.4
1.6
1.8
2.0
2.2
2.4
2.6
2.8
3.0

4 BLADE - FLIGHT

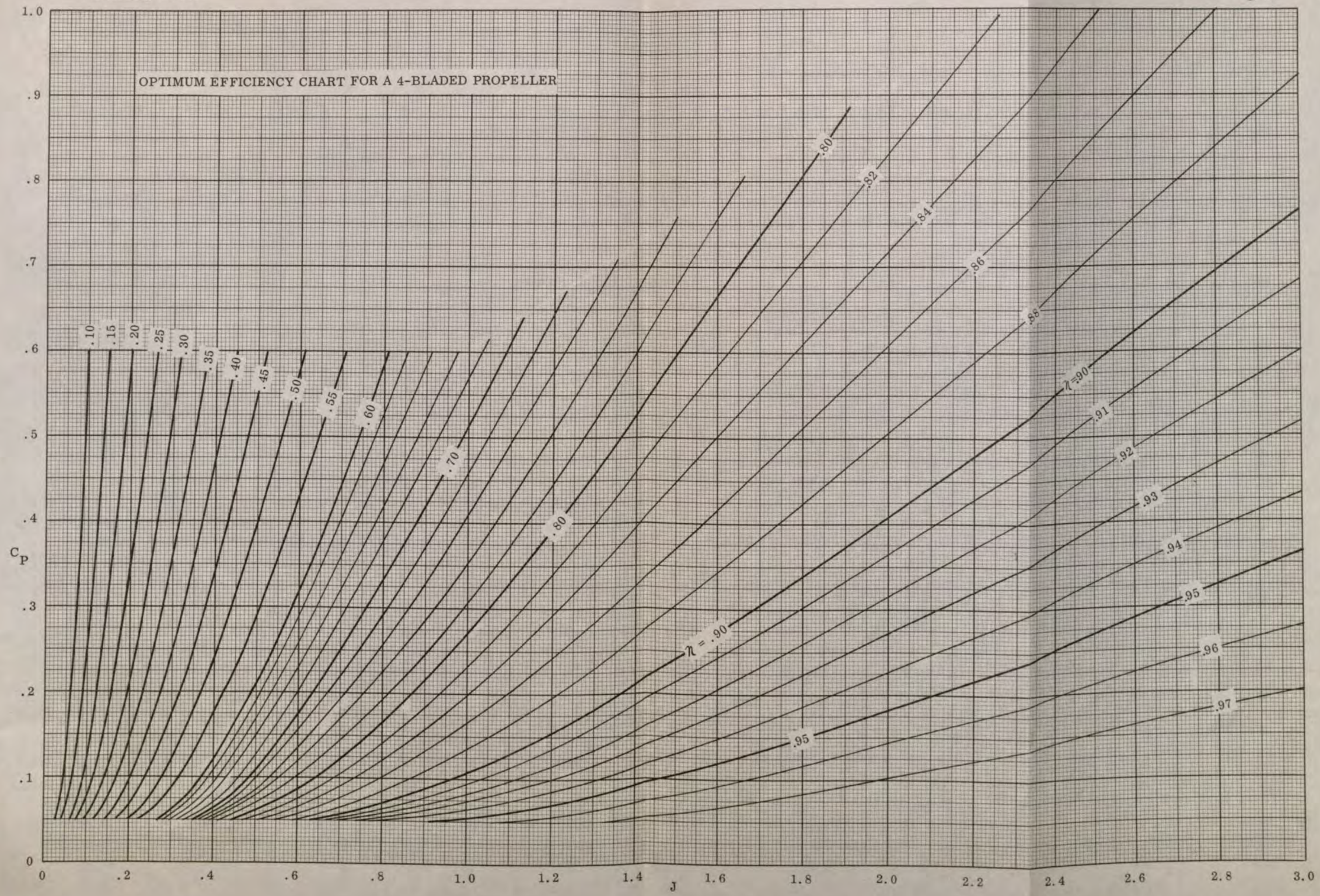
OPTIMUM EFFICIENCY CHART FOR A 4-BLADED PROPELLER
C_P
J
.10
.15
.20
.25
.30
.35
.40
.45
.50
.55
.60
.70
.80
η = .90
.95
.80
.82
.84
.86
.88
η=.90
.91
.92
.93
.94
.95
.96
.97
0
.1
.2
.3
.4
.5
.6
.7
.8
.9
1.0
0
.2
.4
.6
.8
1.0
1.2
1.4
1.6
1.8
2.0
2.2
2.4
2.6
2.8
3.0

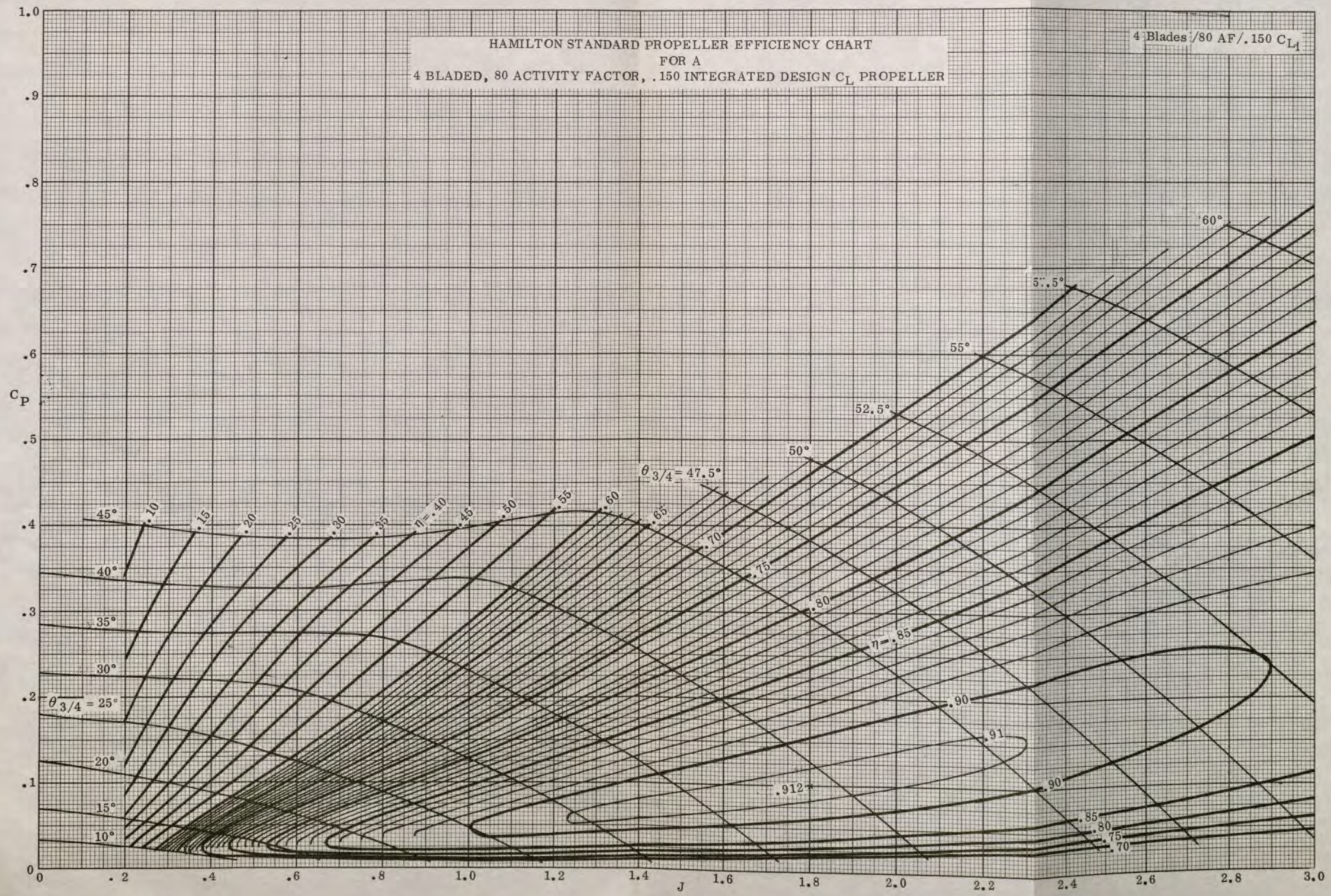
HAMILTON STANDARD PROPELLER EFFICIENCY CHART
FOR A
4 BLADED, 80 ACTIVITY FACTOR, .150 INTEGRATED DESIGN C_L PROPELLER
4 Blades /80 AF/.150 C_{L_1}
C_P
J
$\theta_{3/4}$ = 47.5°
$\theta_{3/4}$ = 25°
60°
57.5°
55°
52.5°
50°
45°
40°
35°
30°
20°
15°
10°
η = .40
η = .85
.10
.15
.20
.25
.30
.35
.45
.50
.55
.60
.65
.70
.75
.80
.90
.91
.912
.85
.80
.75
.70
0
.1
.2
.3
.4
.5
.6
.7
.8
.9
1.0
.2
.4
.6
.8
1.0
1.2
1.4
1.6
1.8
2.0
2.2
2.4
2.6
2.8
3.0

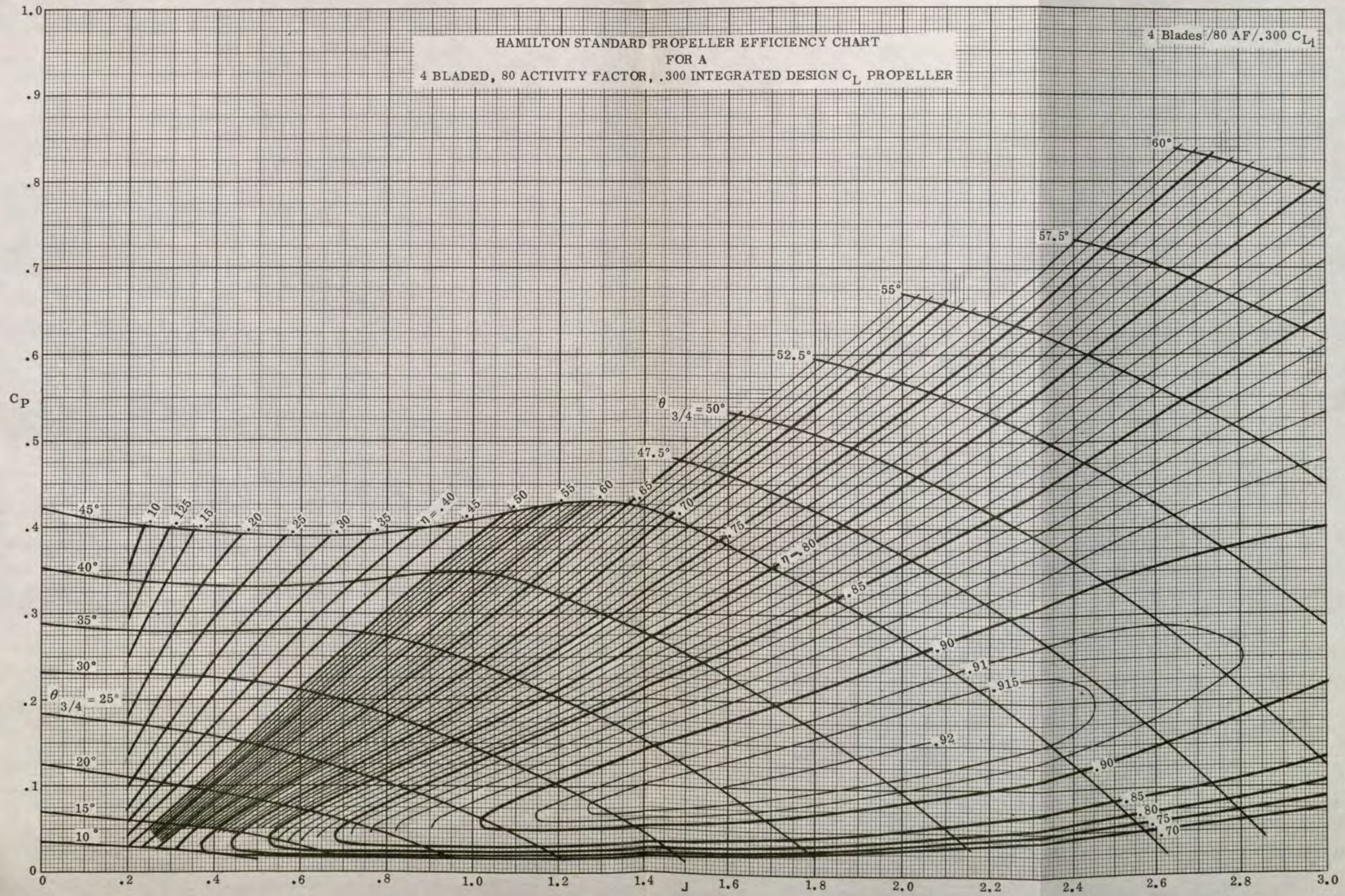
HAMILTON STANDARD PROPELLER EFFICIENCY CHART
FOR A
4 BLADED, 80 ACTIVITY FACTOR, .300 INTEGRATED DESIGN C_L PROPELLER
4 Blades /80 AF/.300 C_{L_i}
C_P
J
$\theta_{3/4} = 50°$
$\theta_{3/4} = 25°$
$\eta = .40$
$\eta = .80$
60°
57.5°
55°
52.5°
47.5°
45°
40°
35°
30°
20°
15°
10°
.10
.125
.15
.20
.25
.30
.35
.45
.50
.55
.60
.65
.70
.75
.85
.90
.91
.915
.92
.90
.85
.80
.75
.70

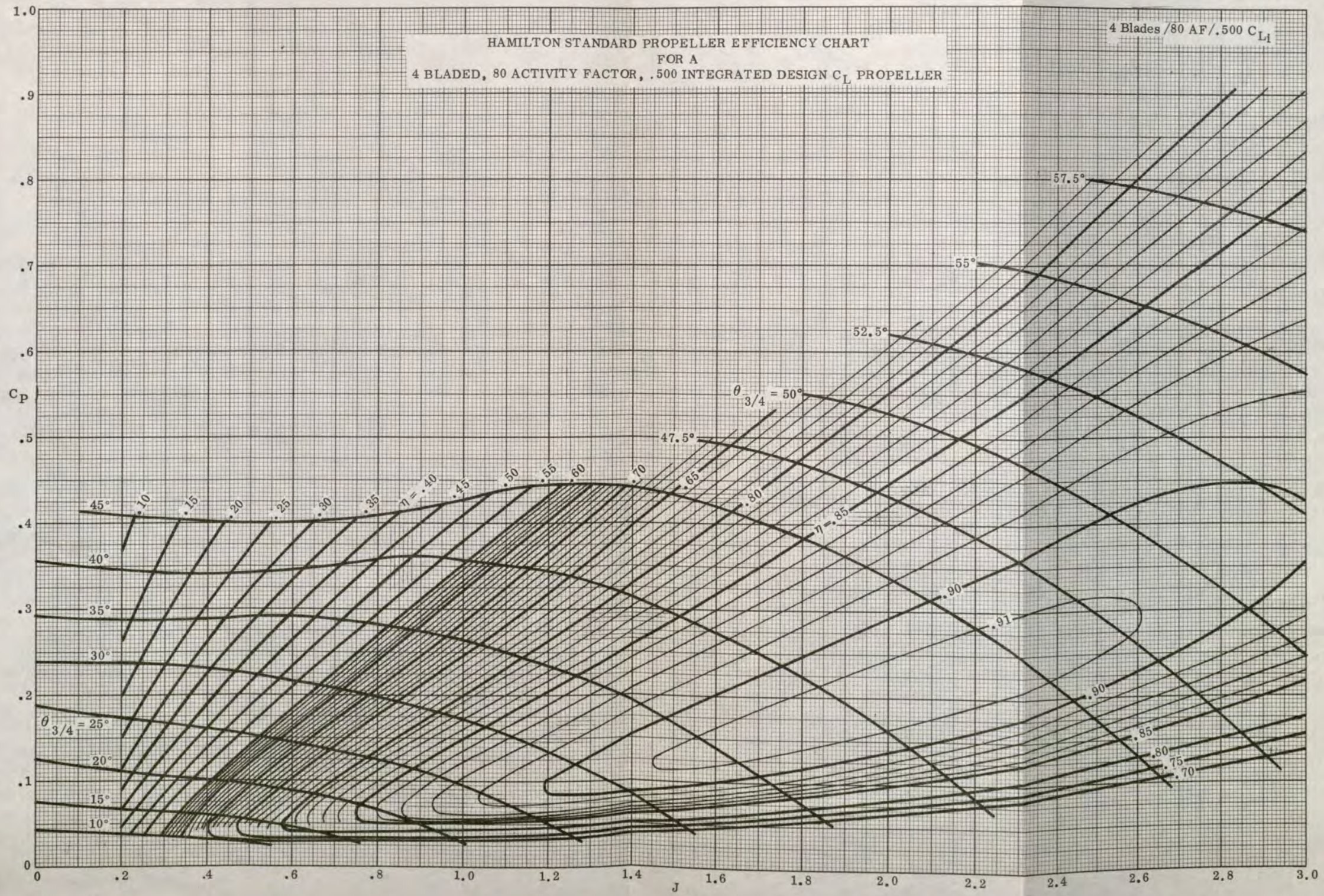
HAMILTON STANDARD PROPELLER EFFICIENCY CHART
FOR A
4 BLADED, 80 ACTIVITY FACTOR, .500 INTEGRATED DESIGN C_L PROPELLER
4 Blades /80 AF/.500 C_{L_i}
C_P
J
$\theta_{3/4}$ = 50°
$\theta_{3/4}$ = 25°
57.5°
55°
52.5°
47.5°
45°
40°
35°
30°
20°
15°
10°
η = .40
η = .85
.10
.15
.20
.25
.30
.35
.45
.50
.55
.60
.65
.70
.80
.90
.91
.85
.75

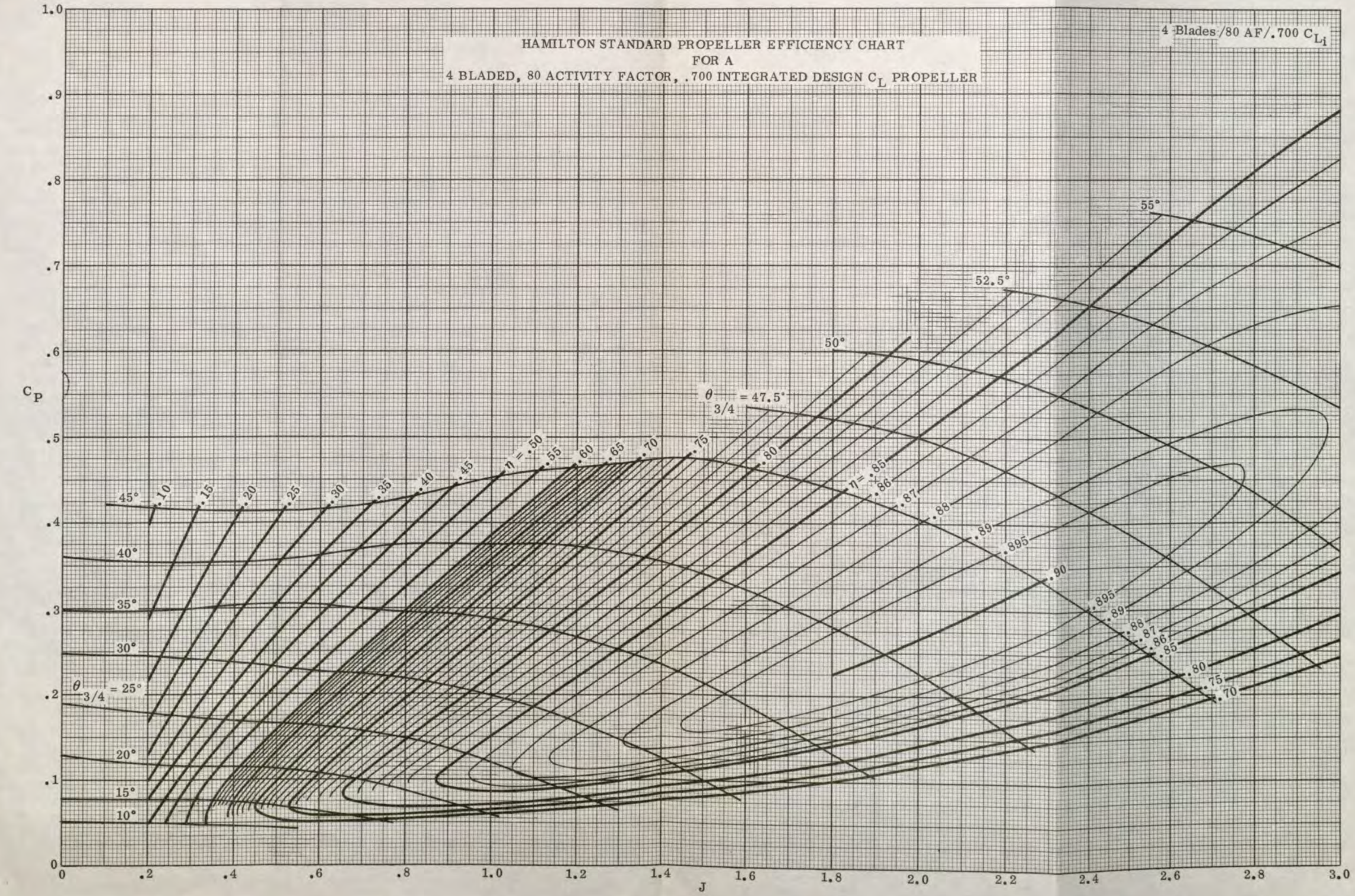
HAMILTON STANDARD PROPELLER EFFICIENCY CHART
FOR A
4 BLADED, 80 ACTIVITY FACTOR, .700 INTEGRATED DESIGN C_L PROPELLER
4 Blades /80 AF/.700 C_{L_i}
C_P
J
$\theta_{3/4}$ = 47.5°
$\theta_{3/4}$ = 25°
55°
52.5°
50°
45°
40°
35°
30°
20°
15°
10°
η = .50
η = .85
.10
.15
.20
.25
.30
.35
.40
.45
.55
.60
.65
.70
.75
.80
.86
.87
.88
.89
.895
.90
.895
.89
.88
.87
.86
.85
.80
.75
.70
0
.1
.2
.3
.4
.5
.6
.7
.8
.9
1.0
0
.2
.4
.6
.8
1.0
1.2
1.4
1.6
1.8
2.0
2.2
2.4
2.6
2.8
3.0

FIGURE 22 44

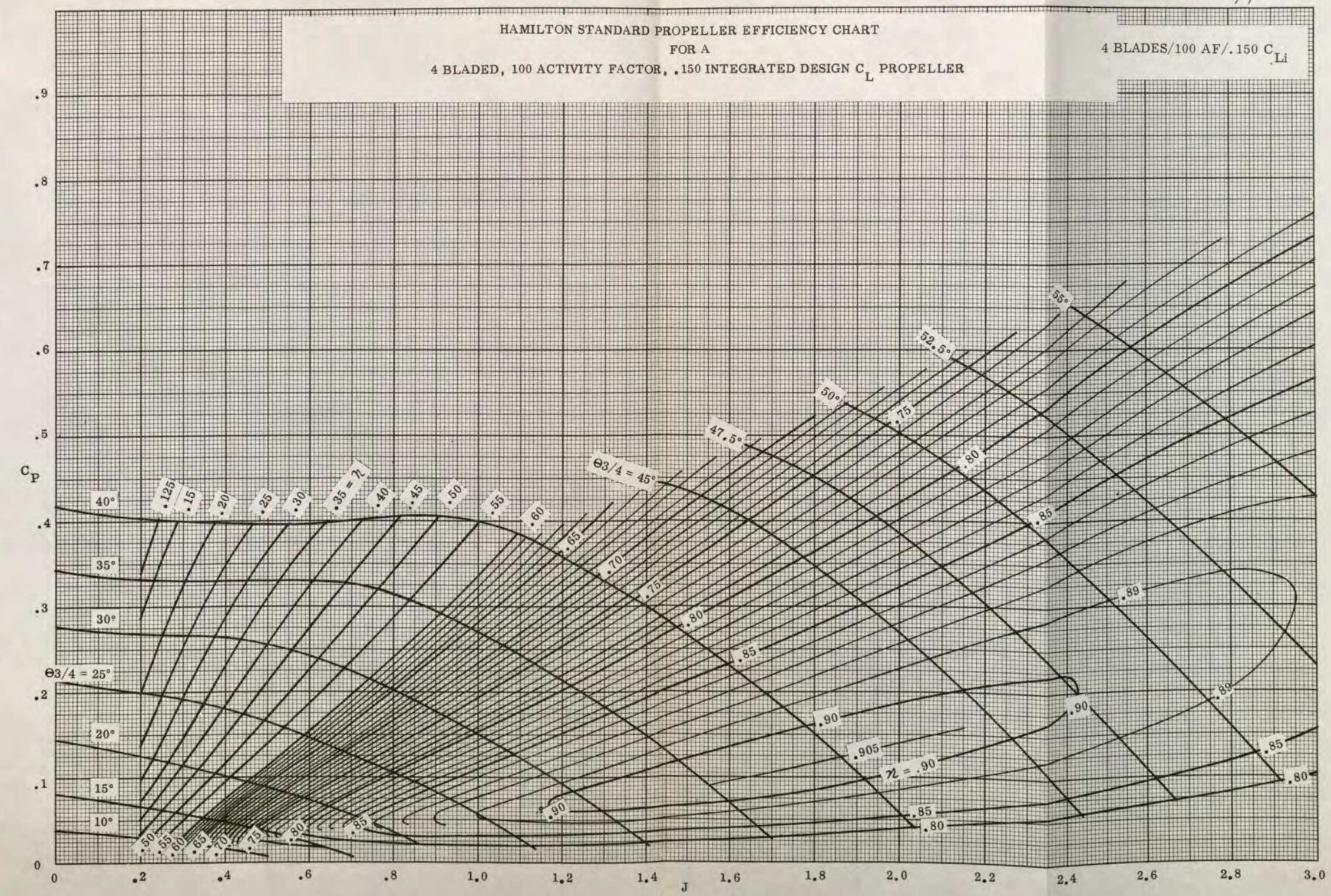
HAMILTON STANDARD PROPELLER EFFICIENCY CHART
FOR A
4 BLADED, 100 ACTIVITY FACTOR, .150 INTEGRATED DESIGN C_L PROPELLER
4 BLADES/100 AF/.150 C_{Li}
C_P
J
$\theta 3/4 = 25°$
$\theta 3/4 = 45°$
$\eta = .90$
.125
.15
.20
.25
.30
.35 = η
.40
.45
.50
.55
.60
.65
.70
.75
.80
.85
.89
.90
.905
10°
15°
20°
30°
35°
40°
47.5°
50°
52.5°
55°

FIGURE 23 45

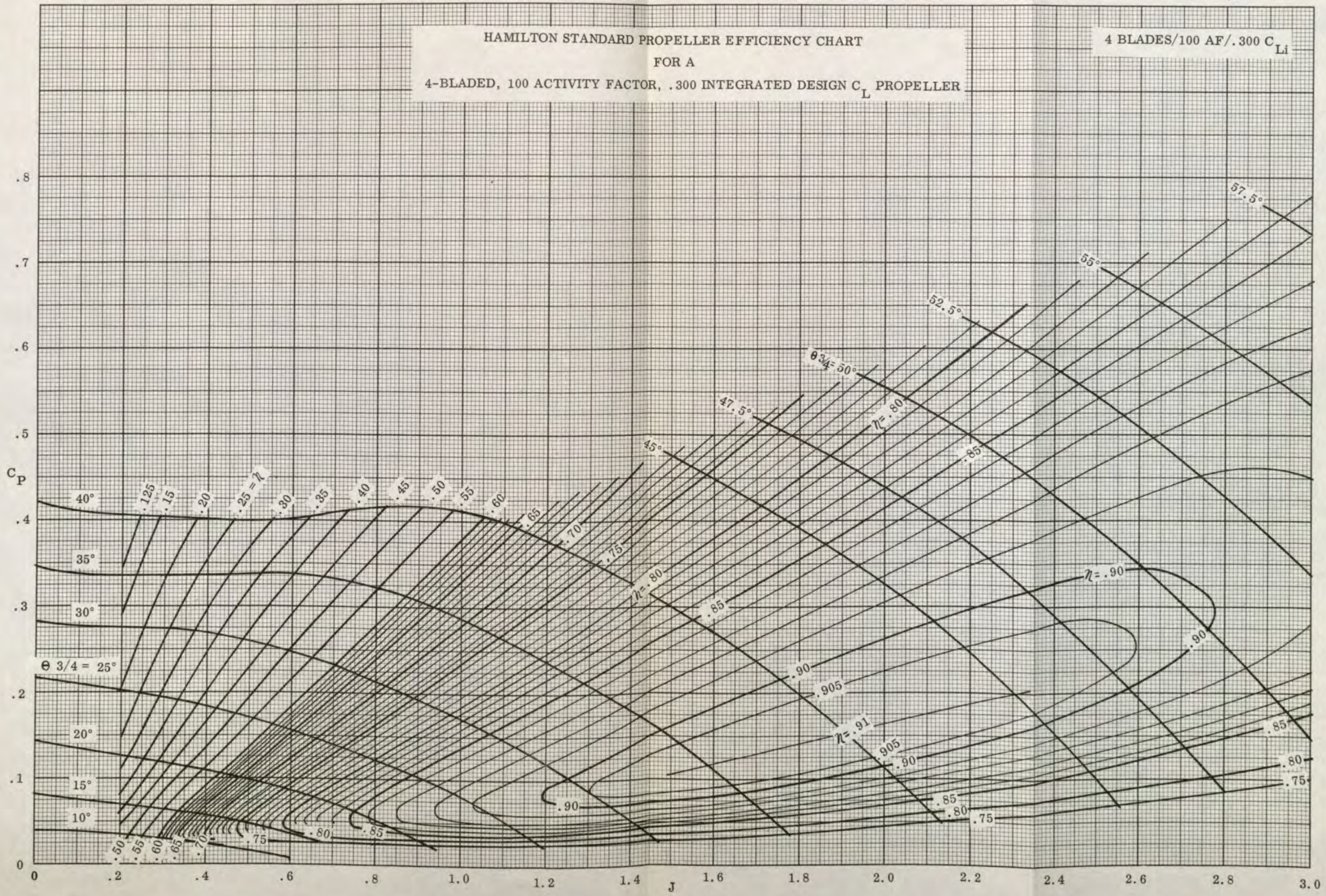
HAMILTON STANDARD PROPELLER EFFICIENCY CHART
FOR A
4-BLADED, 100 ACTIVITY FACTOR, .300 INTEGRATED DESIGN C_L PROPELLER
4 BLADES/100 AF/.300 C_{Li}
C_P
J
θ 3/4 = 25°
θ 3/4 = 50°
η = .91
η = .905
η = .90
η = .85
η = .80
η = .75
η = .70
η = .65
η = .60
η = .55
η = .50
η = .45
η = .40
η = .35
η = .30
η = .25
η = .20
η = .15
η = .125
40°
35°
30°
20°
15°
10°
45°
47.5°
52.5°
55°
57.5°

FIGURE 24~~4~~6

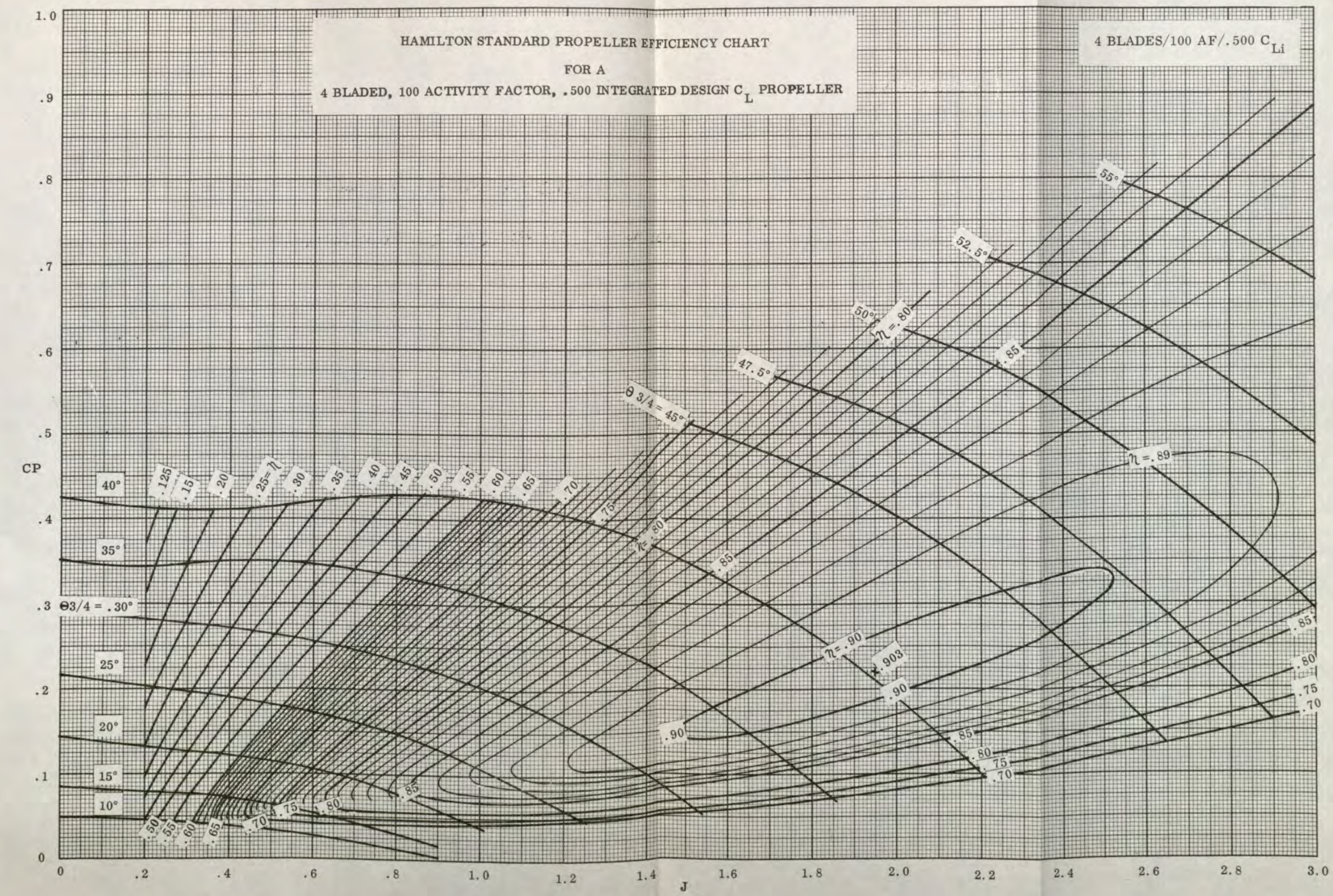
HAMILTON STANDARD PROPELLER EFFICIENCY CHART
FOR A
4 BLADED, 100 ACTIVITY FACTOR, .500 INTEGRATED DESIGN C_L PROPELLER
4 BLADES/100 AF/.500 C_{Li}
CP
J
θ 3/4 = 45°
θ3/4 = .30°
40°
35°
25°
20°
15°
10°
55°
52.5°
50°
47.5°
η = .89
η = .90
η = .80
η = .903
.125
.15
.20
.25 = η
.30
.35
.40
.45
.50
.55
.60
.65
.70
.75
.80
.85
.90
.903

FIGURE 25 47

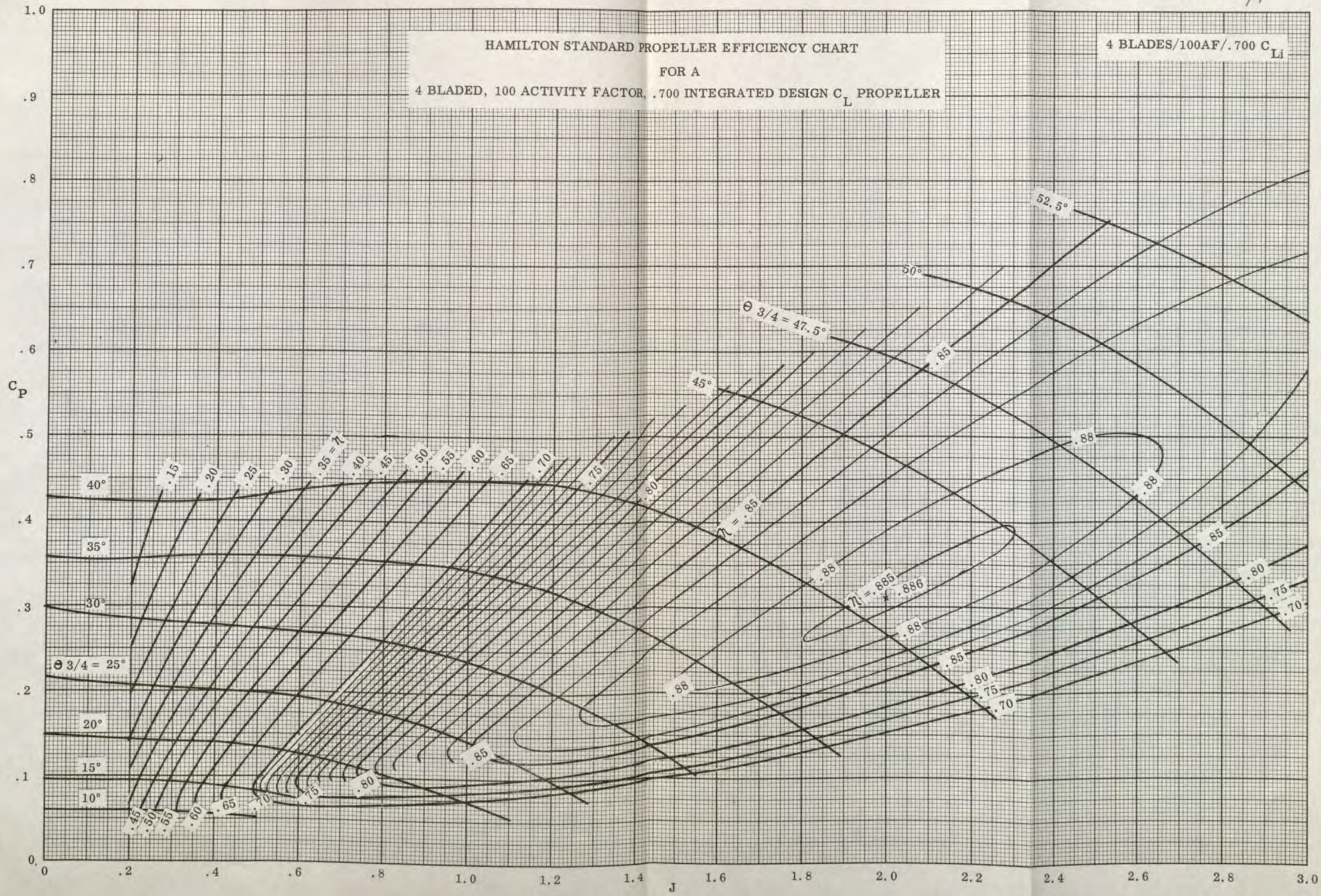
HAMILTON STANDARD PROPELLER EFFICIENCY CHART
FOR A
4 BLADED, 100 ACTIVITY FACTOR, .700 INTEGRATED DESIGN C_L PROPELLER
4 BLADES/100AF/.700 C_{Li}
C_P
J
θ 3/4 = 25°
θ 3/4 = 47.5°
η = .885
η = .886

FIGURE 26 48

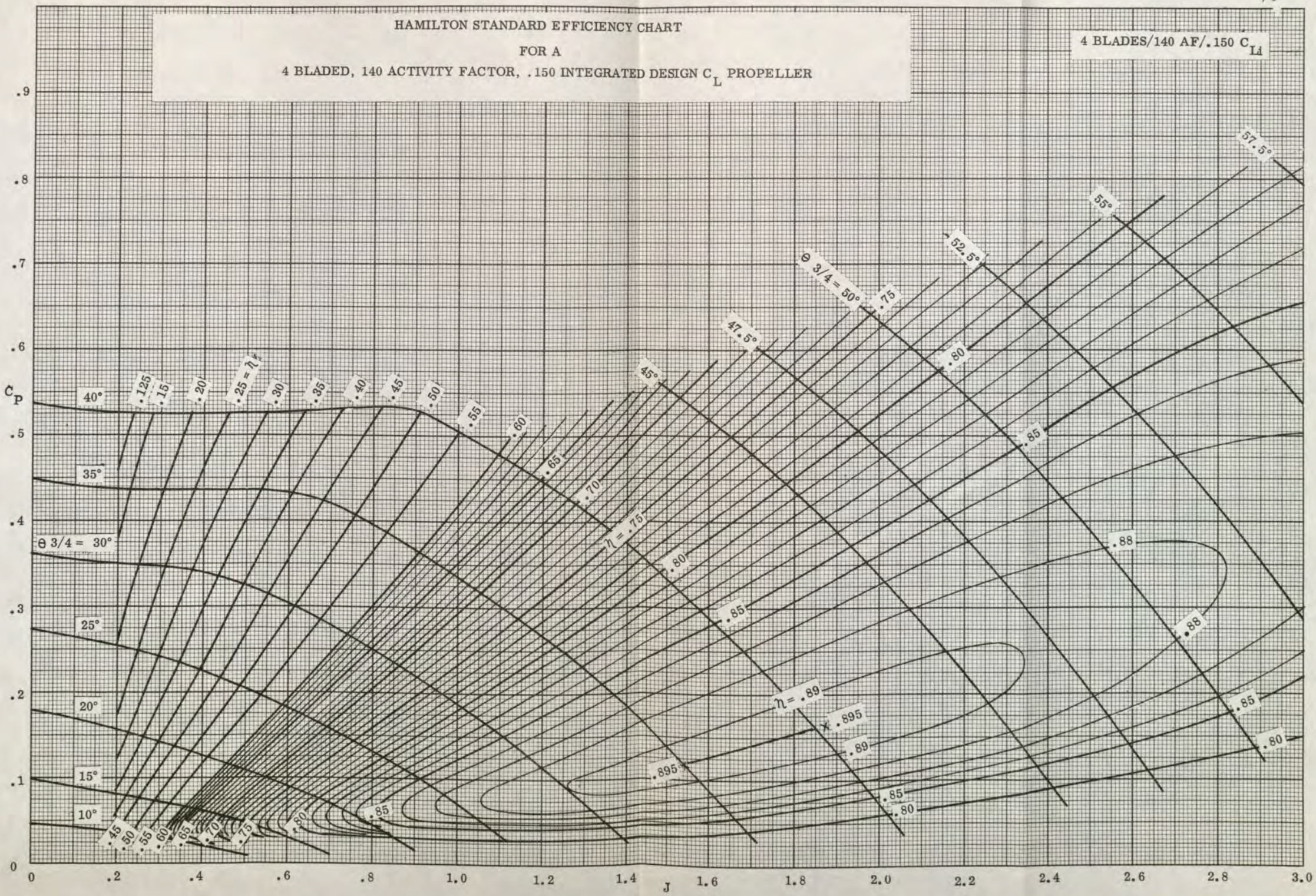
HAMILTON STANDARD EFFICIENCY CHART
FOR A
4 BLADED, 140 ACTIVITY FACTOR, .150 INTEGRATED DESIGN C_L PROPELLER
4 BLADES/140 AF/.150 C_{Li}
C_P
J
θ 3/4 = 30°
θ 3/4 = 50°
η = .75
η = .89
.895
.88
.85
.80
.75
.70
.65
.60
.55
.50
.45
.40
.35
.30
.25 = η
.20
.15
.125
40°
35°
25°
20°
15°
10°
45°
47.5°
52.5°
55°
57.5°
0
.2
.4
.6
.8
1.0
1.2
1.4
1.6
1.8
2.0
2.2
2.4
2.6
2.8
3.0

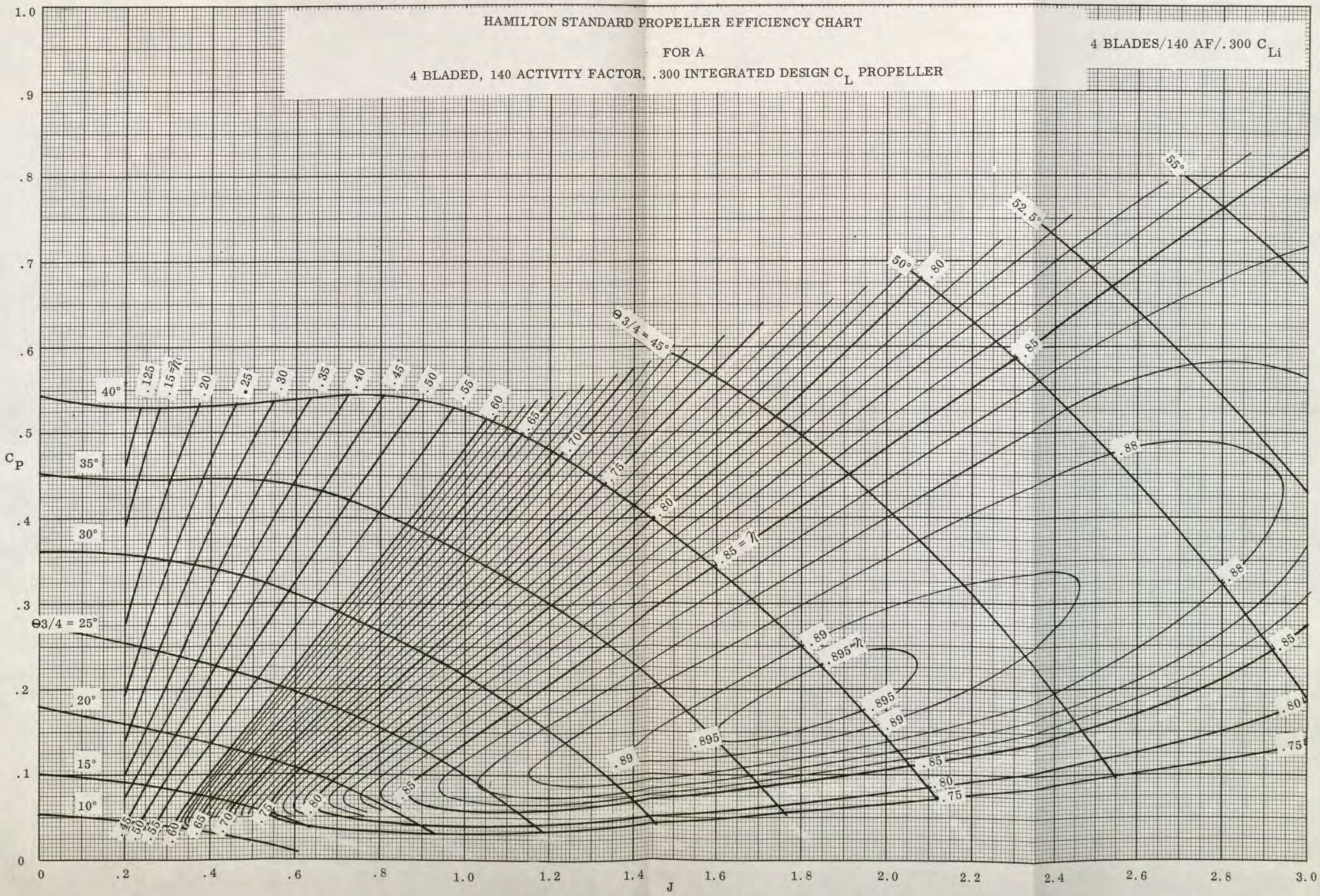
HAMILTON STANDARD PROPELLER EFFICIENCY CHART
FOR A
4 BLADED, 140 ACTIVITY FACTOR, .300 INTEGRATED DESIGN C_L PROPELLER
4 BLADES/140 AF/.300 C_{Li}
C_P
J
$\Theta 3/4 = 25°$
$\Theta 3/4 = 45°$
10°
15°
20°
25°
30°
35°
40°
50°
52.5°
55°
.125
.15 = η
.20
.25
.30
.35
.40
.45
.50
.55
.60
.65
.70
.75
.80
.85 = η
.88
.89
.895 = η
.895
.85
.80
.75

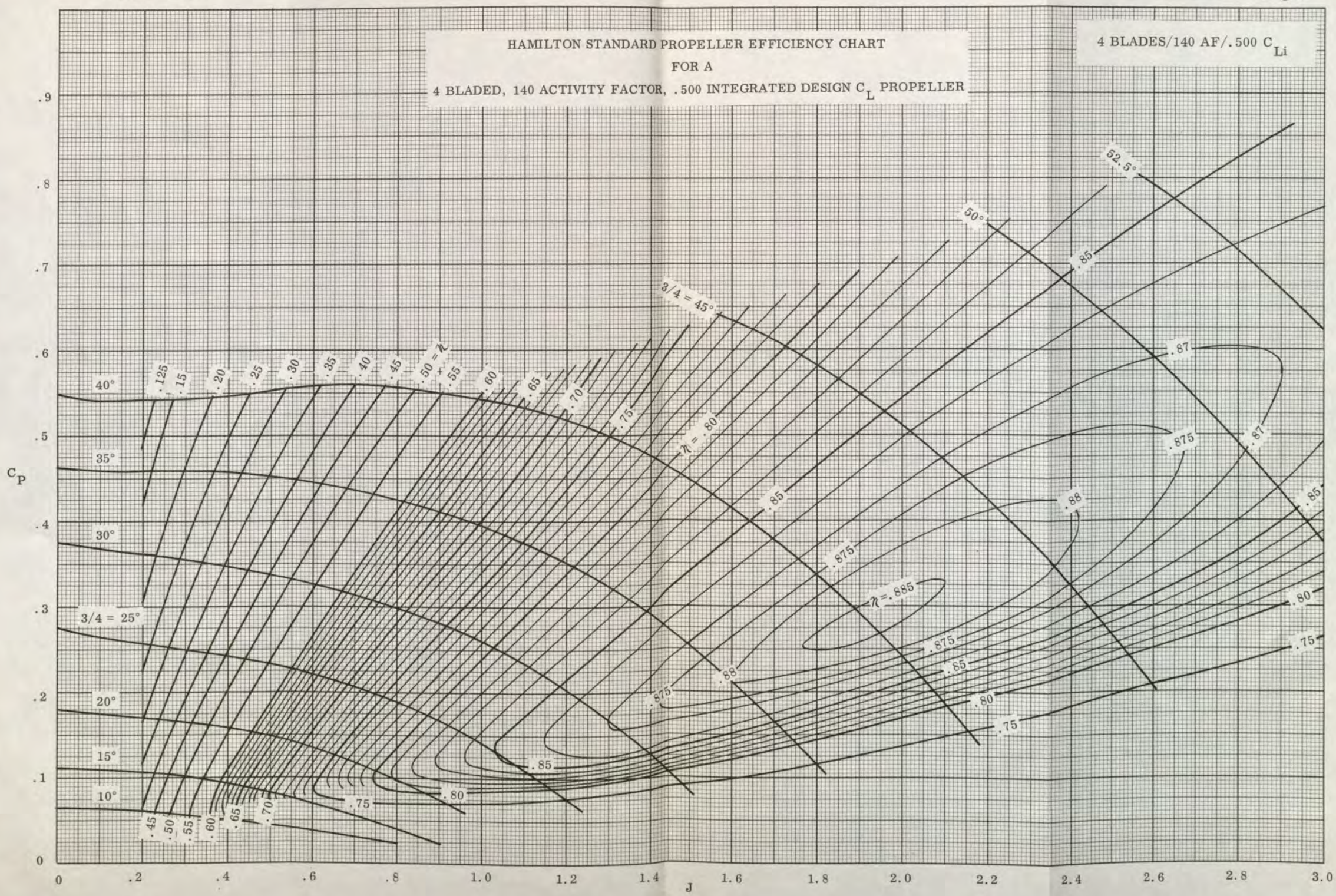
HAMILTON STANDARD PROPELLER EFFICIENCY CHART
FOR A
4 BLADED, 140 ACTIVITY FACTOR, .500 INTEGRATED DESIGN C_L PROPELLER
4 BLADES/140 AF/.500 C_{Li}
C_P
J
40°
35°
30°
3/4 = 25°
20°
15°
10°
3/4 = 45°
52.5°
50°
η = .50
η = .80
η = .885
.125
.15
.20
.25
.30
.35
.40
.45
.50
.55
.60
.65
.70
.75
.80
.85
.87
.875
.88

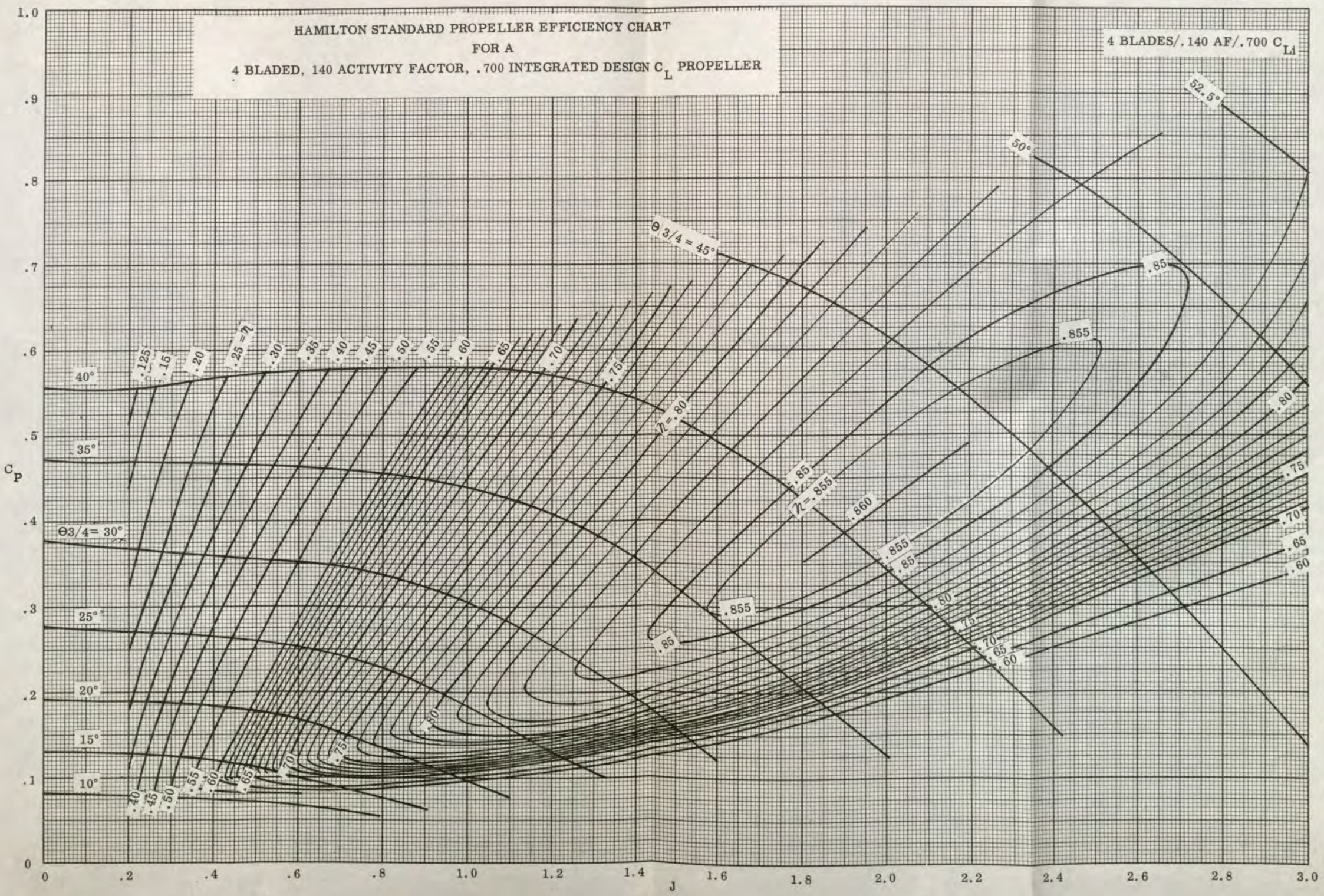
HAMILTON STANDARD PROPELLER EFFICIENCY CHART
FOR A
4 BLADED, 140 ACTIVITY FACTOR, .700 INTEGRATED DESIGN C_L PROPELLER
4 BLADES/.140 AF/.700 C_{Li}
C_P
J
θ 3/4 = 45°
θ3/4 = 30°
40°
35°
25°
20°
15°
10°
52.5°
50°
η = .80
η = .855
.85
.855
.860
.80
.75
.70
.65
.60
.125
.15
.20
.25 = η
.30
.35
.40
.45
.50
.55
.60
.65
.70
.75
.80
.85
.855

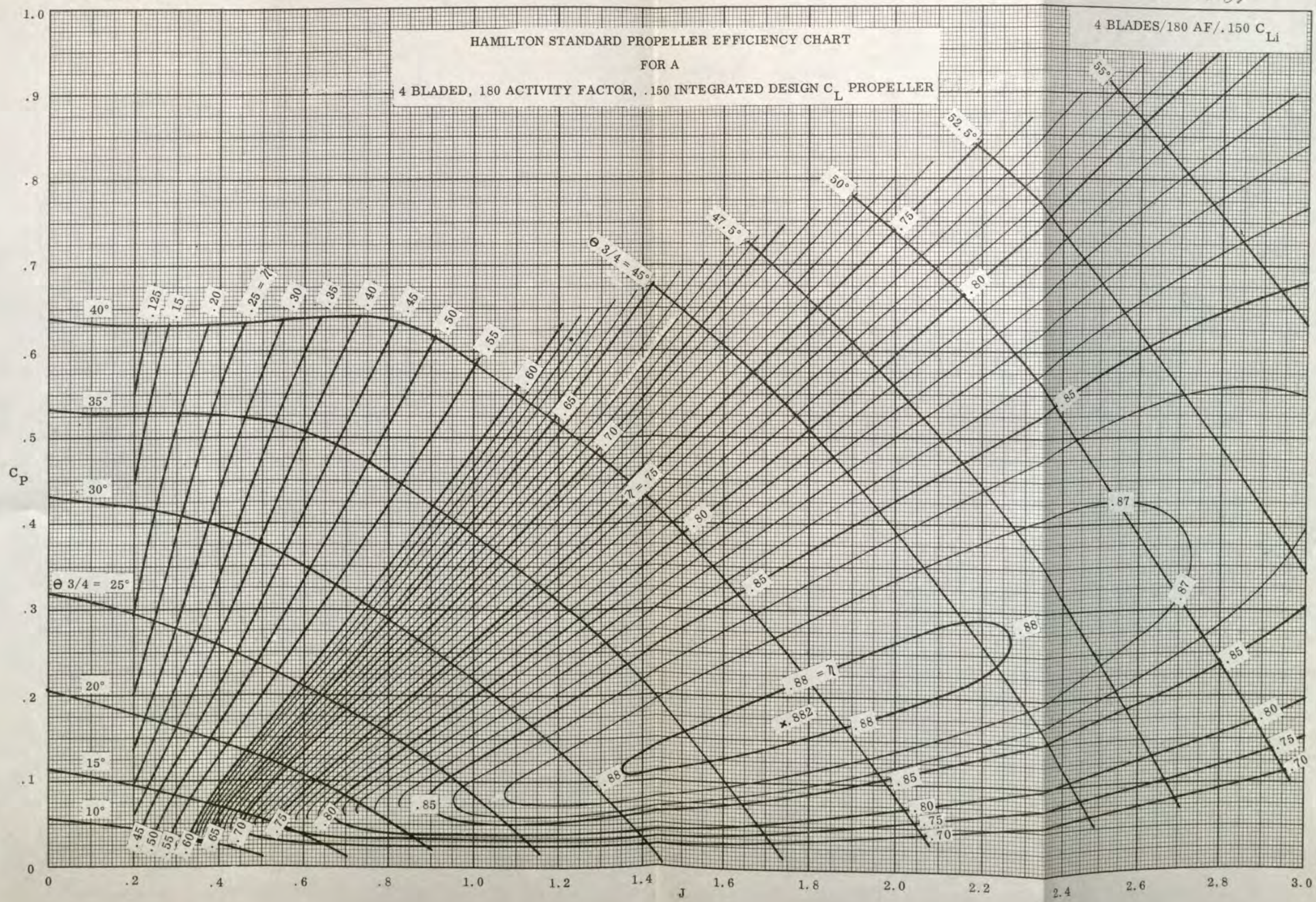
HAMILTON STANDARD PROPELLER EFFICIENCY CHART
FOR A
4 BLADED, 180 ACTIVITY FACTOR, .150 INTEGRATED DESIGN C_L PROPELLER
4 BLADES/180 AF/.150 C_{Li}
C_P
J
θ 3/4 = 25°
θ 3/4 = 45°
η = .75
η = .88
.882
40°
35°
30°
20°
15°
10°
55°
52.5°
50°
47.5°
.125
.15
.20
.25
.30
.35
.40
.45
.50
.55
.60
.65
.70
.75
.80
.85
.87
.88

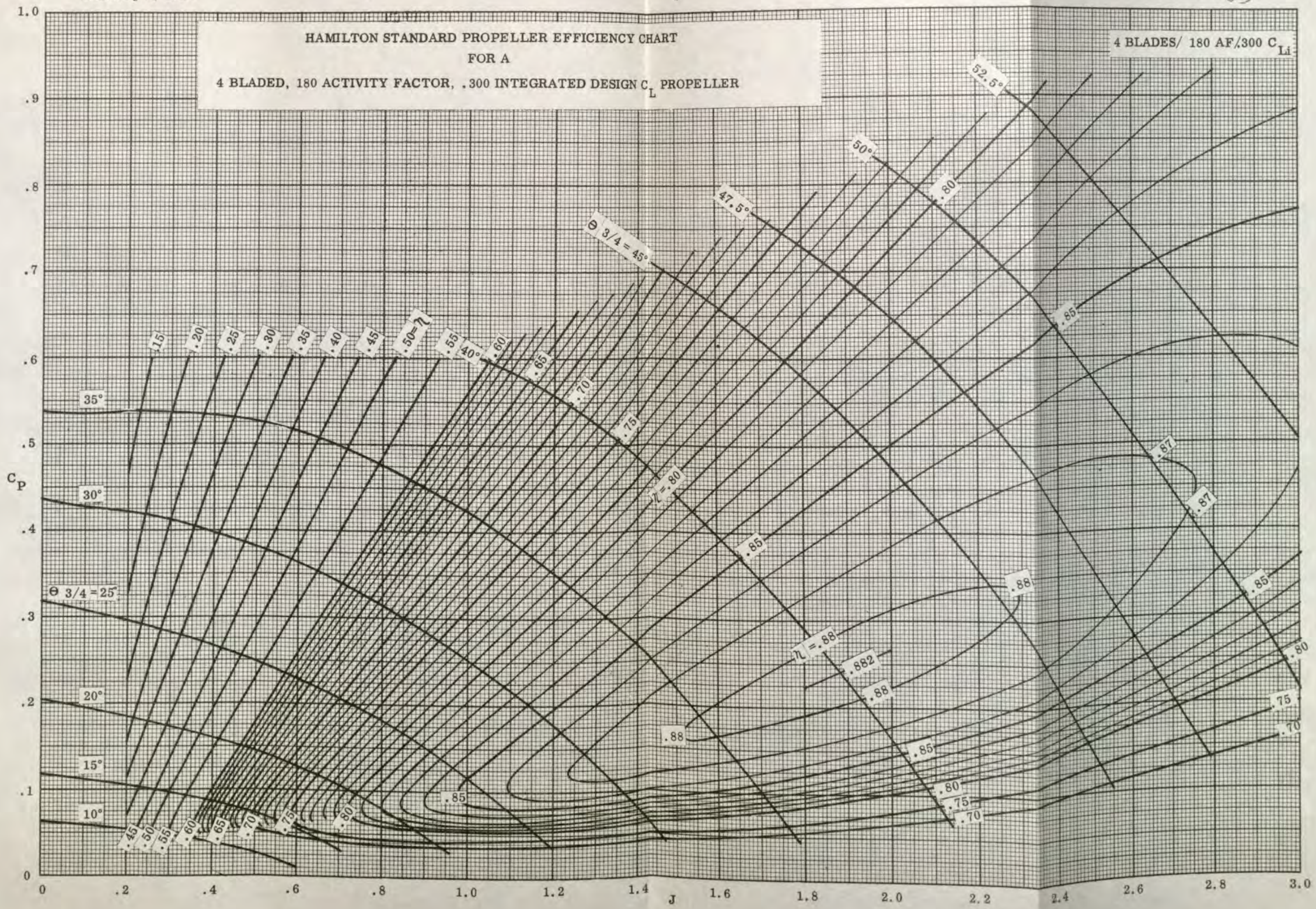
HAMILTON STANDARD PROPELLER EFFICIENCY CHART
FOR A
4 BLADED, 180 ACTIVITY FACTOR, .300 INTEGRATED DESIGN C_L PROPELLER
4 BLADES/ 180 AF/.300 C_{Li}
C_P
J
θ 3/4 = 45°
θ 3/4 = 25°
η = .80
η = .88
35°
30°
20°
15°
10°
40°
50°
52.5°
47.5°
.15
.20
.25
.30
.35
.40
.45
.50
.55
.60
.65
.70
.75
.80
.85
.87
.88
.882

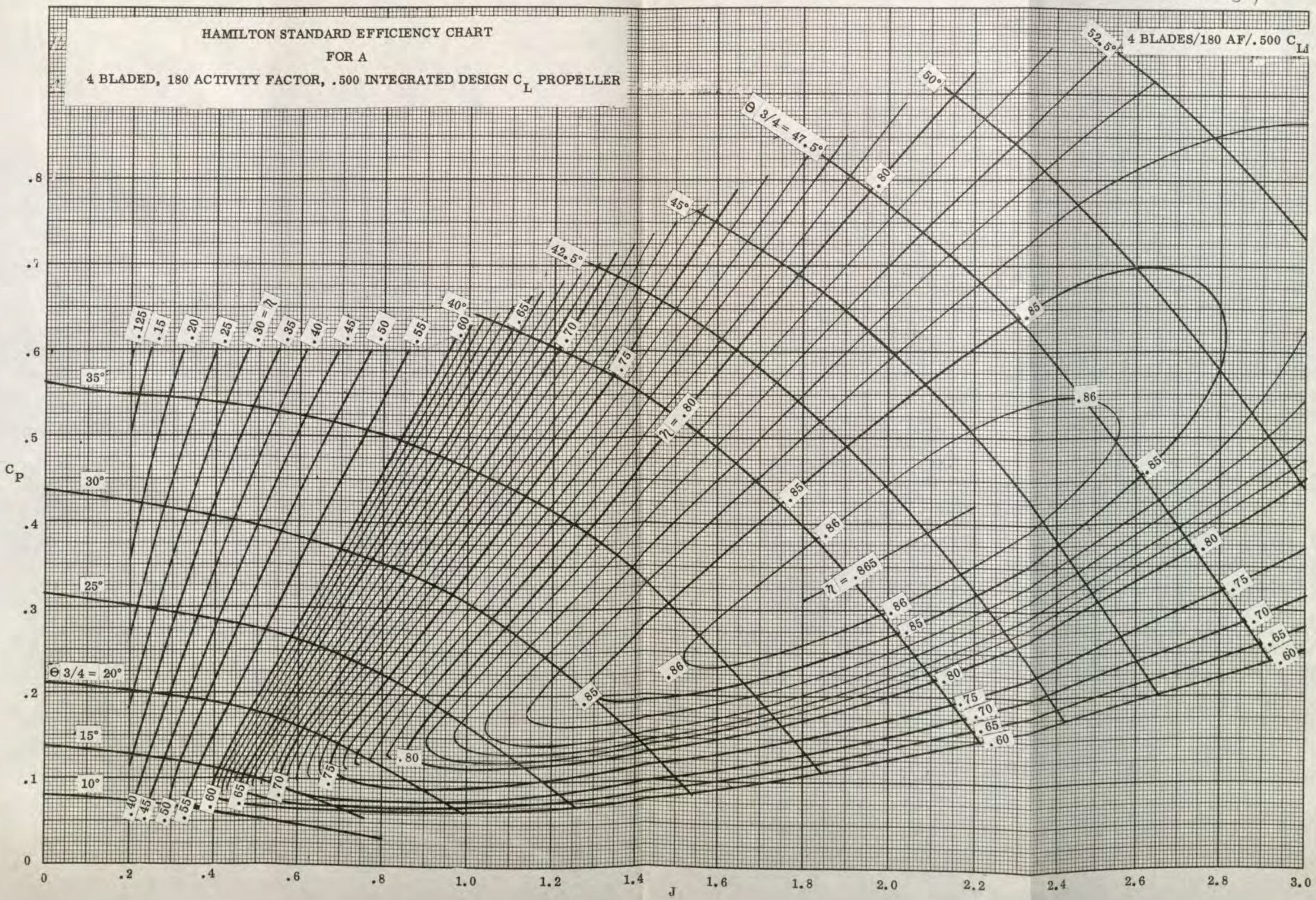
HAMILTON STANDARD EFFICIENCY CHART
FOR A
4 BLADED, 180 ACTIVITY FACTOR, .500 INTEGRATED DESIGN C_L PROPELLER
4 BLADES/180 AF/.500 C_L
C_P
J
Θ 3/4 = 20°
Θ 3/4 = 47.5°
η = .865

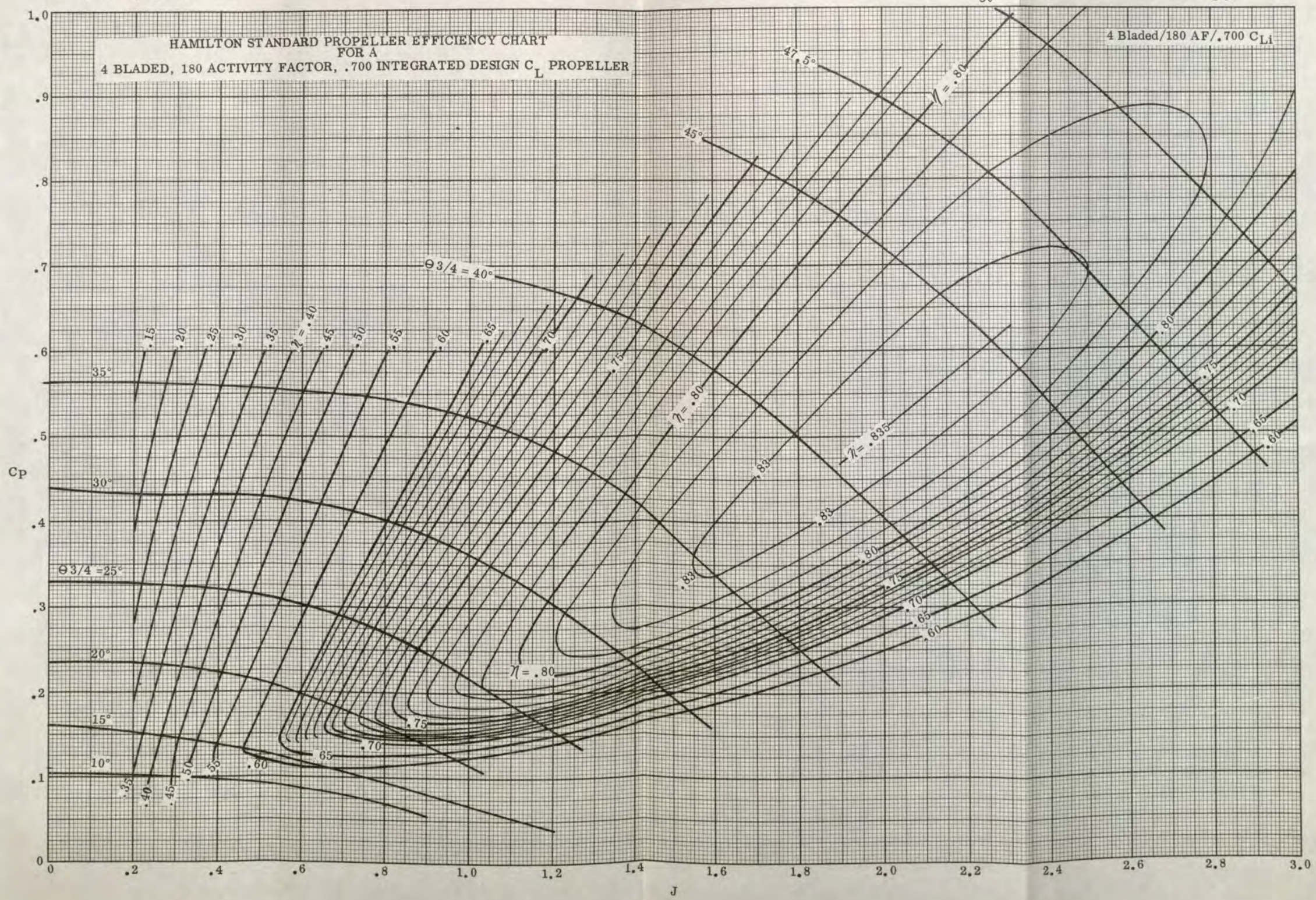
HAMILTON STANDARD PROPELLER EFFICIENCY CHART
FOR A
4 BLADED, 180 ACTIVITY FACTOR, .700 INTEGRATED DESIGN C_L PROPELLER
4 Bladed/180 AF/.700 C_{Li}
Cp
J
θ3/4 = 40°
θ3/4 = 25°
35°
30°
20°
15°
10°
45°
47.5°
50°
η = .80
η = .835
η = .40
.15
.20
.25
.30
.35
.45
.50
.55
.60
.65
.70
.75
.80
.83
0
.1
.2
.3
.4
.5
.6
.7
.8
.9
1.0
1.2
1.4
1.6
1.8
2.0
2.2
2.4
2.6
2.8
3.0

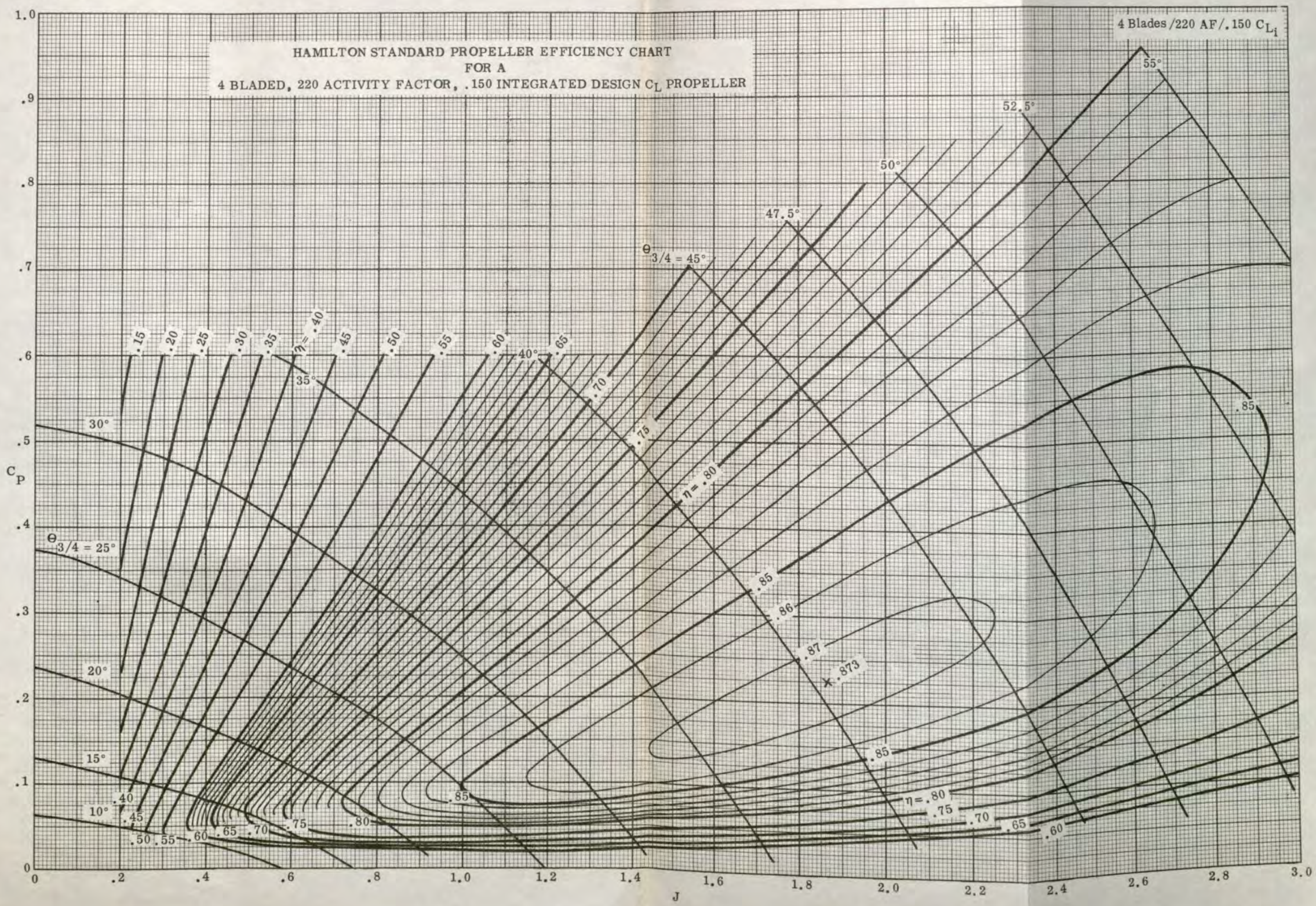
HAMILTON STANDARD PROPELLER EFFICIENCY CHART
FOR A
4 BLADED, 220 ACTIVITY FACTOR, .150 INTEGRATED DESIGN C_L PROPELLER
4 Blades /220 AF/.150 C_{L_i}
C_P
J
$\theta_{3/4} = 25°$
$\theta_{3/4} = 45°$
10°
15°
20°
30°
35°
40°
47.5°
50°
52.5°
55°
η = .40
.45
.50
.55
.60
.65
.70
.75
.80
.85
.86
.87
.873

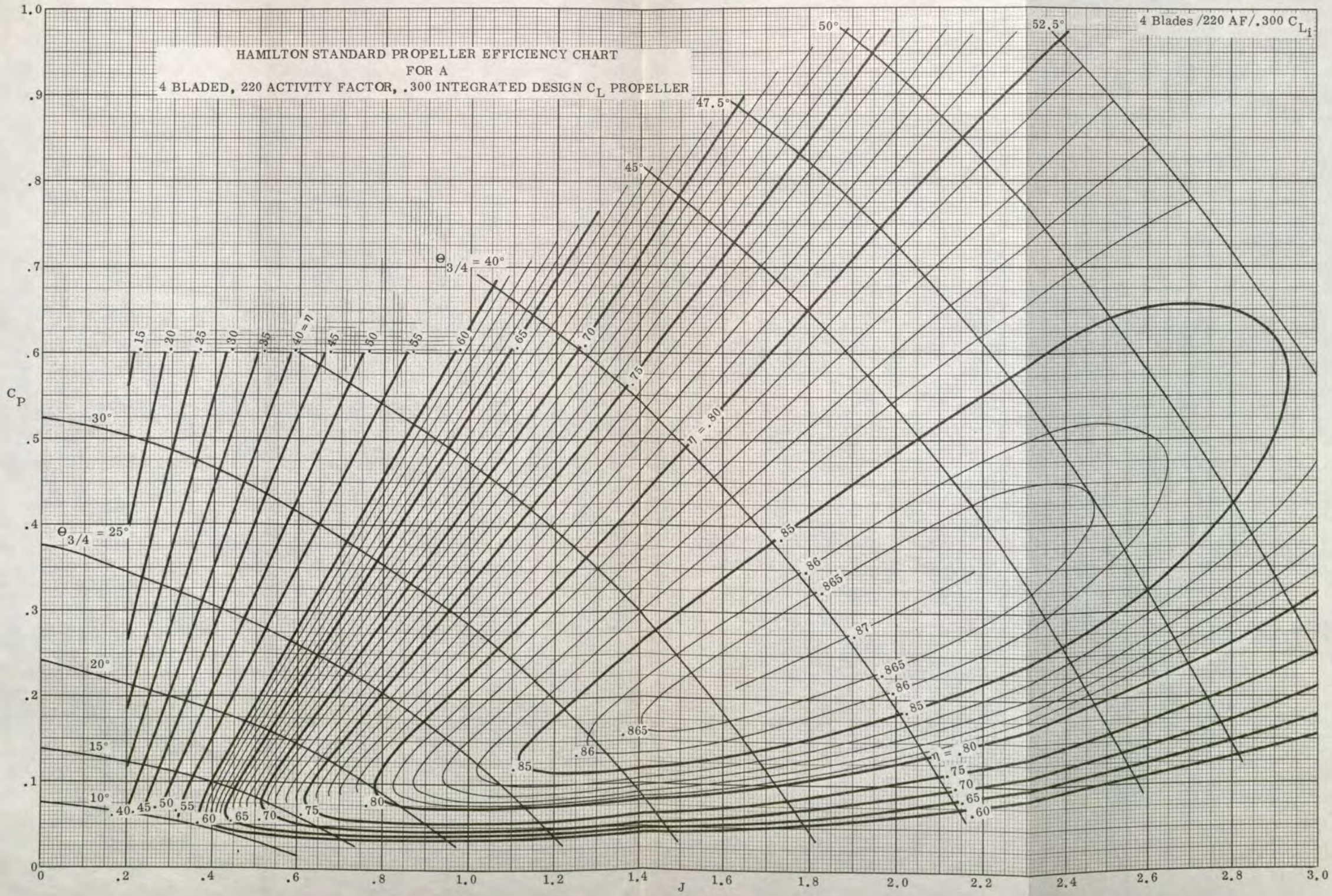
HAMILTON STANDARD PROPELLER EFFICIENCY CHART
FOR A
4 BLADED, 220 ACTIVITY FACTOR, .300 INTEGRATED DESIGN C_L PROPELLER
4 Blades /220 AF/.300 C_{L_i}
C_P
J
$\Theta_{3/4}$ = 40°
$\Theta_{3/4}$ = 25°
30°
20°
15°
10°
50°
52.5°
47.5°
45°
η = .80
η = .85
η = .86
η = .865
η = .87
η = .75
η = .70
η = .65
η = .60
η = .40
η = .45
η = .50
η = .55
η = .60
η = .65
η = .70
η = .75
η = .80
η = .85
η = .86
η = .865
η = .87
η = .865
η = .86
η = .85
η = .80
η = .75
η = .70
η = .65
η = .60
0
.1
.2
.3
.4
.5
.6
.7
.8
.9
1.0
0
.2
.4
.6
.8
1.0
1.2
1.4
1.6
1.8
2.0
2.2
2.4
2.6
2.8
3.0

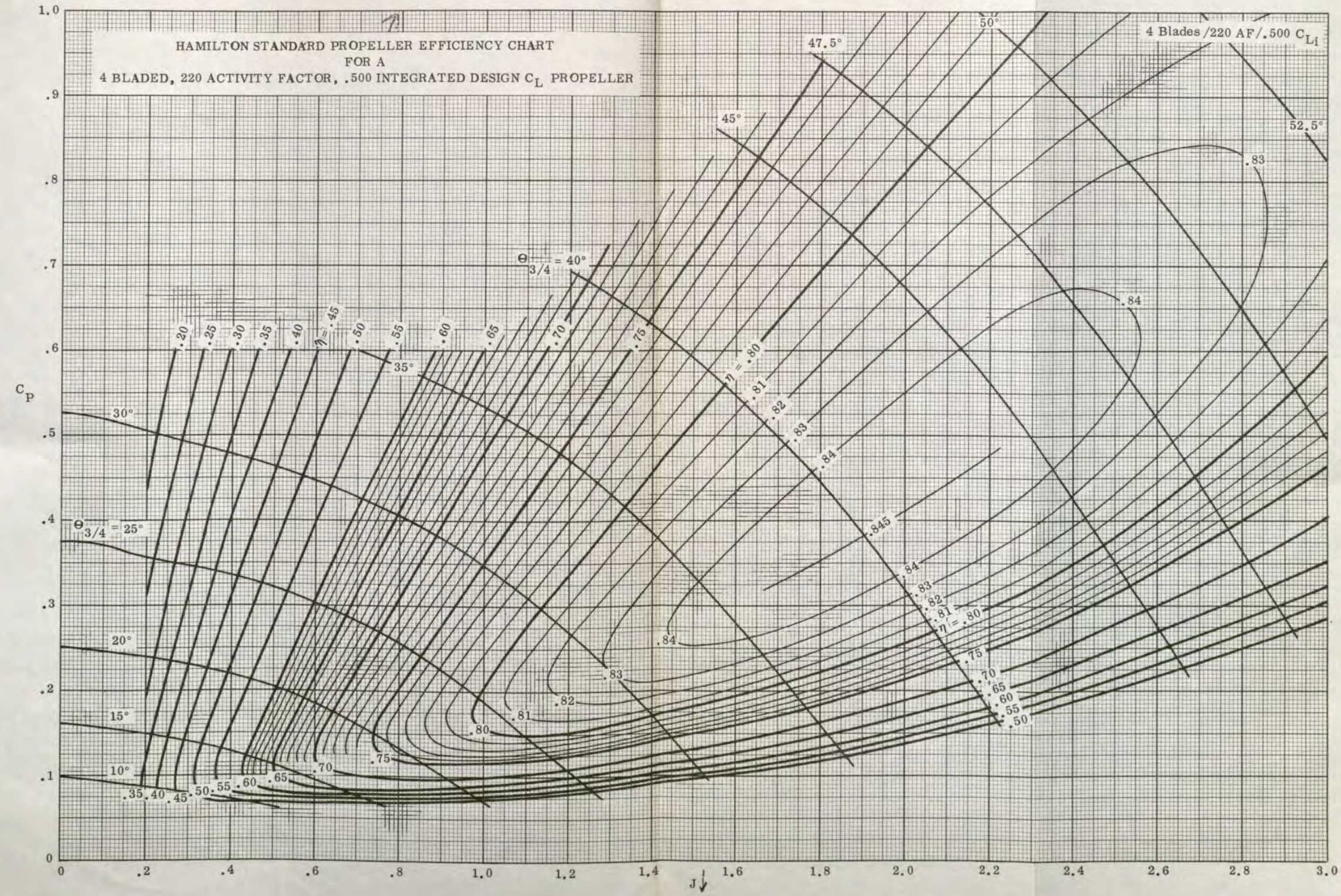
HAMILTON STANDARD PROPELLER EFFICIENCY CHART
FOR A
4 BLADED, 220 ACTIVITY FACTOR, .500 INTEGRATED DESIGN C_L PROPELLER
4 Blades /220 AF/.500 C_{L_i}
C_P
J
$\Theta_{3/4}$ = 40°
$\Theta_{3/4}$ = 25°
47.5°
50°
52.5°
45°
35°
30°
20°
15°
10°
η = .45
η = .80
.83
.84
.845
.20
.25
.30
.35
.40
.50
.55
.60
.65
.70
.75
.81
.82
.50

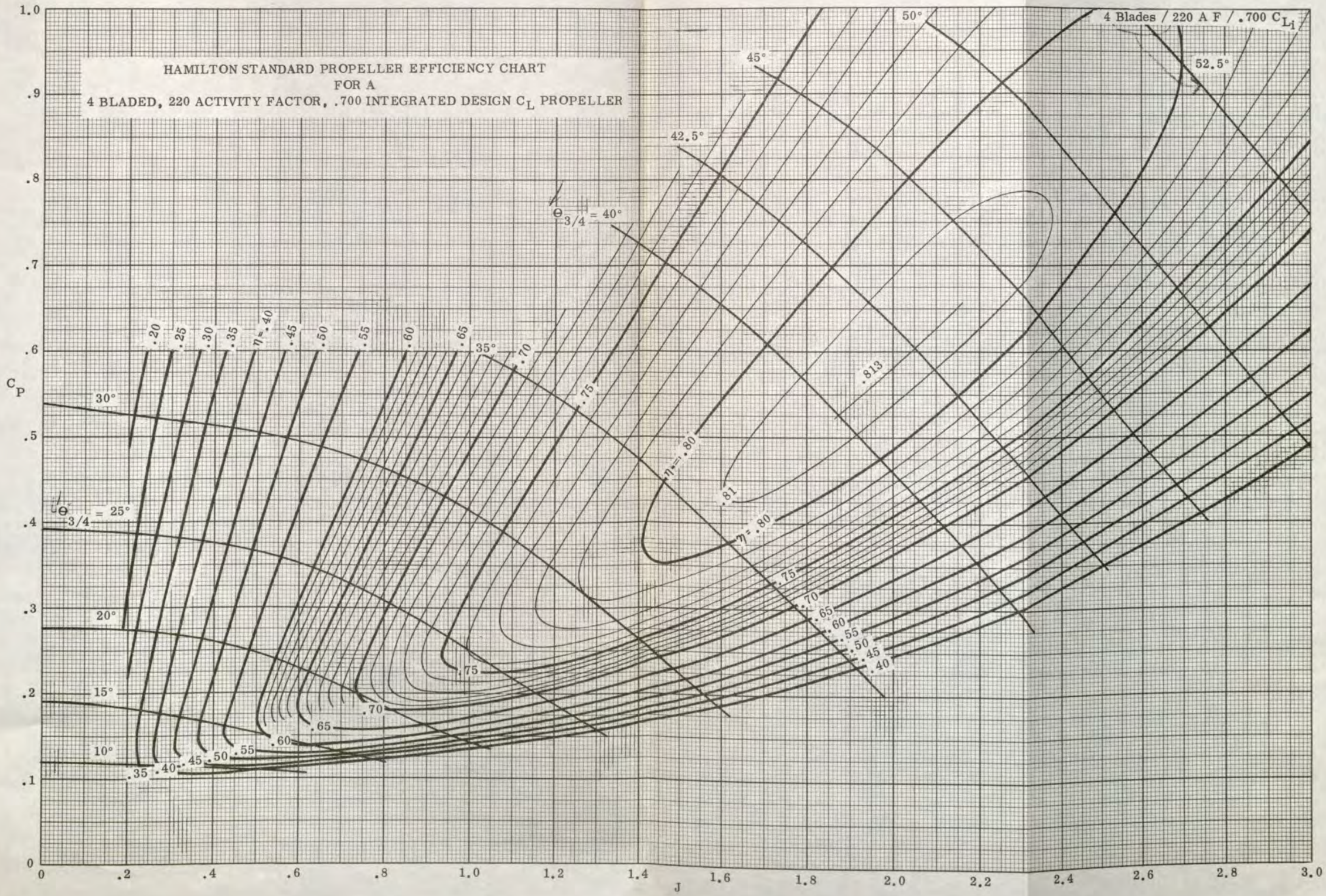
HAMILTON STANDARD PROPELLER EFFICIENCY CHART
FOR A
4 BLADED, 220 ACTIVITY FACTOR, .700 INTEGRATED DESIGN C_L PROPELLER
4 Blades / 220 A F / .700 C_{L_i}
C_P
J
$\theta_{3/4}$ = 40°
$\theta_{3/4}$ = 25°
30°
35°
45°
50°
42.5°
52.5°
20°
15°
10°
η = .40
η = .80
.20
.25
.30
.35
.40
.45
.50
.55
.60
.65
.70
.75
.81
.813

HAMILTON STANDARD GENERALIZED PROPELLER PERFORMANCE

Airplane _____ Date _____ Calc. No. _____

Engine _____ G. R. _____ Sheet No. _____

Reference _____ Calc. By _____ Checked By _____

Figure No.									
No. of Blades									
Diameter									
AF									
Int. Des. C_L									
Attitude									
BHP									
Engine RPM									
Altitude									
V_{Knots}									
ρ_o/ρ									
f_c									
N									
Mach No.									
ND x f_c									
C_P									
J									
η									
C_T/C_P									
Thrust									

SUPPLEMENTS TO PDB 6101

	TITLE	DATE
A.	PROPELLER WEIGHT GENERALIZATION	JANUARY 2, 1963
B.	GENERALIZED NACELLE BLOCKING AND COMPRESSIBILITY CORRECTIONS	JANUARY 11, 1963
C.	PROPELLER NOISE PREDICTION	FEBRUARY 5, 1963
D.		
E.		

HAMILTON STANDARD PROPELLER WEIGHT GENERALIZATION

JANUARY 2, 1963

HAMILTON STANDARD
DIVISION UNITED AIRCRAFT
CORPORATION

GENERALIZED METHOD OF PROPELLER WEIGHT ESTIMATION

An accurate weight generalization of modern aircraft propellers is difficult to achieve for many reasons. While a propeller may be described generally by several well known parameters, the actual design requirements can introduce a wide range of weights for several propellers all having the same well known parameters. For example, the type of control system required, the propeller environment, aircraft operating airspeeds, and attitudes all influence the propeller design and thus weight. In particular, blade weights vary greatly in spanwise distribution of thickness and, in the case of hollow blades, of wall thickness. These variations cannot be readily represented by a reasonable number of geometric parameters. Thus, only the gross geometric characteristics can be accounted for in any practical generalization.

It is recognized that, in conjunction with the use of generalized performance methods (e.g. Hamilton Standard PDB-6101 and PDB-6220) for preliminary propeller selection studies, there is a need for some means of estimating weight trends. This document has been prepared for that purpose - to estimate weight trends - and it must be recognized that the final weights may vary significantly after all factors have been considered.

The formulae in the upper portion of Figure 1 are the result of a recent effort to derive a geometric generalization of Hamilton Standard propeller weights for two classes of propellers:

1. Conventional shaft mounted turbo-props with solid aluminum alloy blades.

2. Lightweight propellers with fiberglass-shell, steel-spar blades and integral gearbox type hubs. (Weight of gearbox is provided by Figure 3).

The propeller geometric and operational parameters incorporated in these formulae are the ones which experience has shown to have the most predominant effect on propeller weight and the exponents have been established empirically to best fit the weight trends of current Hamilton Standard propeller constructions. This generalization represents the complete engine-mounted propeller weight including control, spinner, deicing and oil. It is seen that, for the majority of cases, the agreement with actual design weights is within ± 5% over a range of propeller sizes from 7 to 18 feet diameter.

For less detailed propeller selection studies where propeller geometry trends need not be defined, a much simpler weight generalization is possible, purely in terms

(Continued)

of the design operating conditions. The two most pertinent operational parameters are the airplane Mach number at the flight condition for which optimum propeller performance is required, and the disc power loading at take-off condition. These essentially establish the aerodynamic and structural shape requirements of the propeller and thus are sufficient to define specific weight (weight/SHP) for propellers tailored to these requirements. For example, with increase in design Mach number, the blades must have lower camber and therefore higher activity factor, wider tips, lower thickness ratios, and more bending stiffness to handle higher 1P excitations; all tending to increase the specific weight of the propeller. Similarly, increase in disc power loading calls for higher solidity and/or camber, higher tip speed, and higher torsional stiffness to cope with the increasing tendency of stall flutter; all tending to flatten out the normal trend of decreasing specific weight with increase in disc loading.

Although it was recognized that other factors might also influence propeller weight, it appeared that these might be secondary effects which could be neglected for a broad generalized presentation. Thus it was decided to examine the past and present weight history of all Hamilton Standard controllable pitch propellers in terms of just these two parameters: design Mach number and disc power loading. Except for a few freak cases which involved abnormal hub or blade weights for the particular installation, an excellent correlation was obtained for a broad spectrum of propeller sizes ranging from a 2-bladed, 7 foot diameter propeller to a 4-bladed 20 foot diameter propeller. The results of this generalization are presented in the form of the solid lines on Figure 2. These represent the weights of propellers with conventional blades (solid aluminum or hollow steel) and include control, spinner, deicing and oil. The weights of all recent Hamilton Standard turbo-prop installations (i.e. P3V, C-130B, AO-1 and Caribou II) agree with this generalization within ± 5 %.

The excellent representation of conventional propeller weights afforded by this form of generalization recommends it for application to weight presentations for the newer types of propeller construction (integral gearbox propeller, fiberglass-shell steel-core blades, variable camber propeller) now nearing production status at Hamilton Standard. Design weights are now available on a reasonable number of such propeller models, and these span a wide range of disc power loadings and design Mach numbers. Based on these design weights, the broken-lined curves on Figure 2 represent the weight characteristics of fixed camber light-weight propellers with fiberglass shell blades and integral gearbox type hubs. These weights include control, spinner, deicing and oil <u>but do not include the weight of the gearbox.</u> A separate generalization of gearbox weights is described subsequently and presented by Figure 3. A few design weights have also been established for variable camber propellers of the

(Continued)

integral gearbox type and with fiberglass shell blades. These are generalized in the form of the dotted line on Figure 2, and again do not include the weight of the gearbox. In the case of variable camber propellers, the steeper slope of the weight curves is due to the inability to decrease solidity with decrease in disc power loading as rapidly as can be done with fixed camber propellers of fewer number of blades.

The form of generalization presented in Figure 2 appears to be a fairly reliable representation of the weight of propellers which are of optimum design for given sets of operating conditions. In view of its simplicity, it is the preferred method of propeller weight estimation in aircraft preliminary design studies. However, where trade-off studies between propeller size, geometry, performance and weight are called for, it is obviously necessary to utilize the geometric weight generalization formula of Figure 1. It must be recognized, however, that neither of these generalizations can account for the effect of abnormal performance requirements, operational features, or environmental conditions imposed by a specific aircraft installation.

To supplement the weight generalization of the light weight fixed and variable camber propellers, there is need for a similar generalization of the associated gearbox weight. Since the basic intent of integrating the gearbox and propeller is to achieve minimum weight, the Hamilton Standard integral gearboxes represent a stepped weight reduction from previous shaft mount type gear boxes. This has been accomplished by such design approaches as carrying the propeller side loads and moments through the housing rather than the gear train, and careful sizing and support of each gear component relative to its imposed loads.

Two classes of gearboxes are of current interest: a single stage transmission (right angle drive through a spiral bevel set) with reduction ratios ranging from between 2.5:1 and 3.5:1 and a two stage transmission (with one planetary and prop shaft offset in relation to input) and with reduction ratios between 10:1 and 14:1. In examining the factors affecting the weight of such gearboxes, it becomes quite evident that, by far, the most predominant factor is the output torque of the gearbox. On this basis the design weights of several integral gearbox models have shown good correlation with available weight data on similar helicopter gearboxes. Accordingly, the generalized gearbox weight presentation in Figure 3 is believed to be quite representative for use in conjunction with the lightweight propeller data of Figure 3. For STOL/VTOL applications with cross-shafting, the output torque used to enter Figure 3 should be the maximum continuous torque transmitted to a single propeller. It should be noted however that the weights of Figure 3 do not include provision in the gearbox for cross shaft drive, declutching, or special accessory drives. Furthermore, it should be appreciated that unusual installation requirements may influence the gearbox

(Continued)

weight significantly. Thus the weight data of Figure 3 should be construed only to represent relative uncomplicated gearbox installations.

Accordingly, the addition of the gearbox weight from Figure 3 to a lightweight propeller value from Figures 1 or 2 will provide the complete weight of a representative Hamilton Standard integral gearbox propeller with fiberglass shell, steel-core blades.

FIG. 1

HAMILTON STANDARD PROPELLER WEIGHT GENERALIZATION

$$W = 355\left[\left(\frac{D}{10}\right)^{2.00}\left(\frac{B}{4}\right)^{0.70}\left(\frac{AF}{100}\right)^{0.75}\left(\frac{ND}{20000}\right)^{0.50}\left(M+1.0\right)^{0.50}\left(\frac{SHP/D^2}{10}\right)^{0.12}\right]$$ (CONVENTIONAL SOLID DURAL BLADES)

$$W = 285\left[\left(\frac{D}{10}\right)^{1.85}\left(\frac{B}{4}\right)^{0.70}\left(\frac{AF}{100}\right)^{0.60}\left(\frac{ND}{20000}\right)^{0.50}\left(M+1.0\right)^{0.50}\left(\frac{SHP/D^2}{10}\right)^{0.12}\right]$$ (LIGHT WEIGHT FIBERGLAS BLADES IGB HUB)

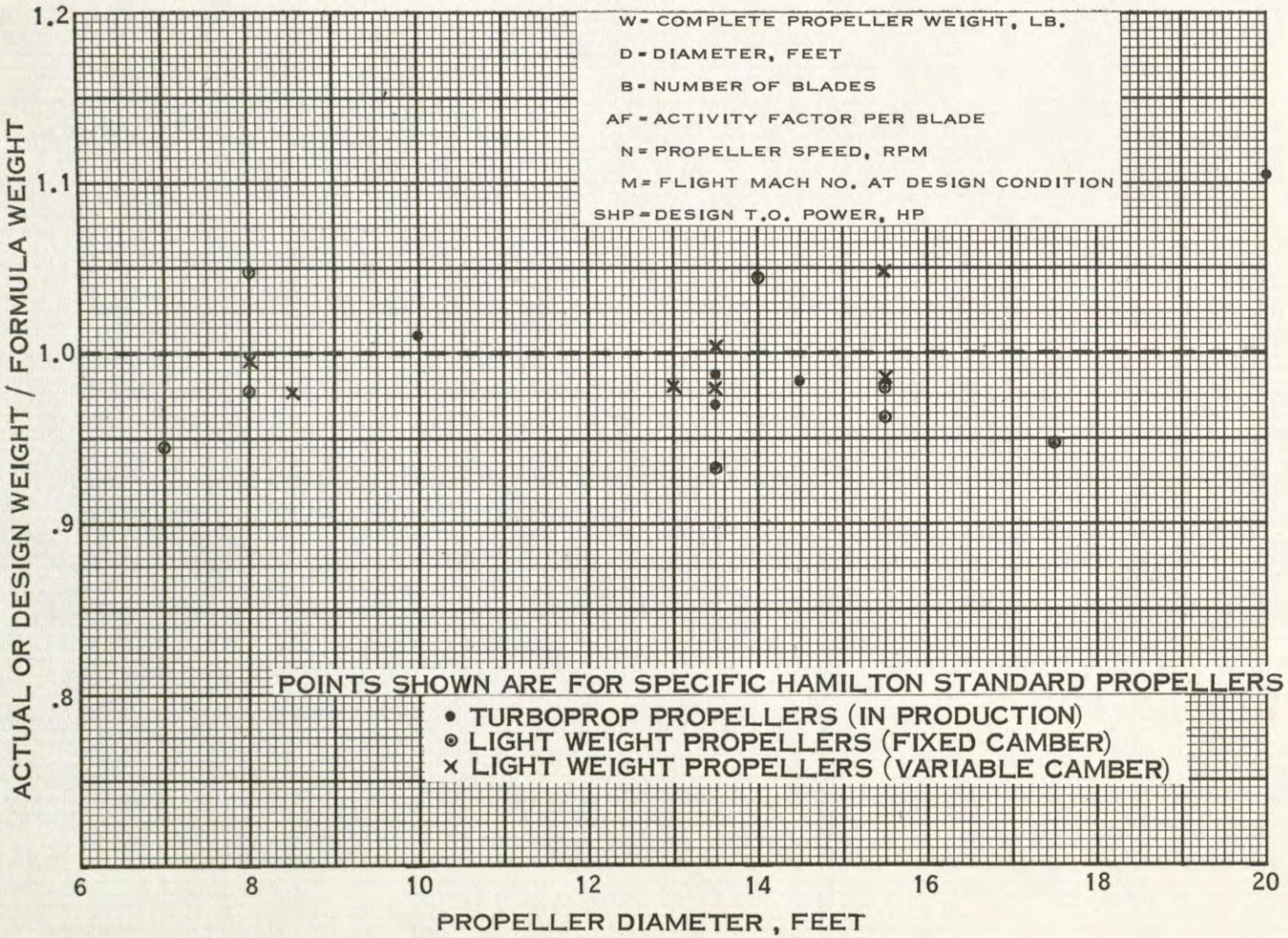

FIG. 2

HAMILTON STANDARD

PROPELLER WEIGHT GENERALIZATION

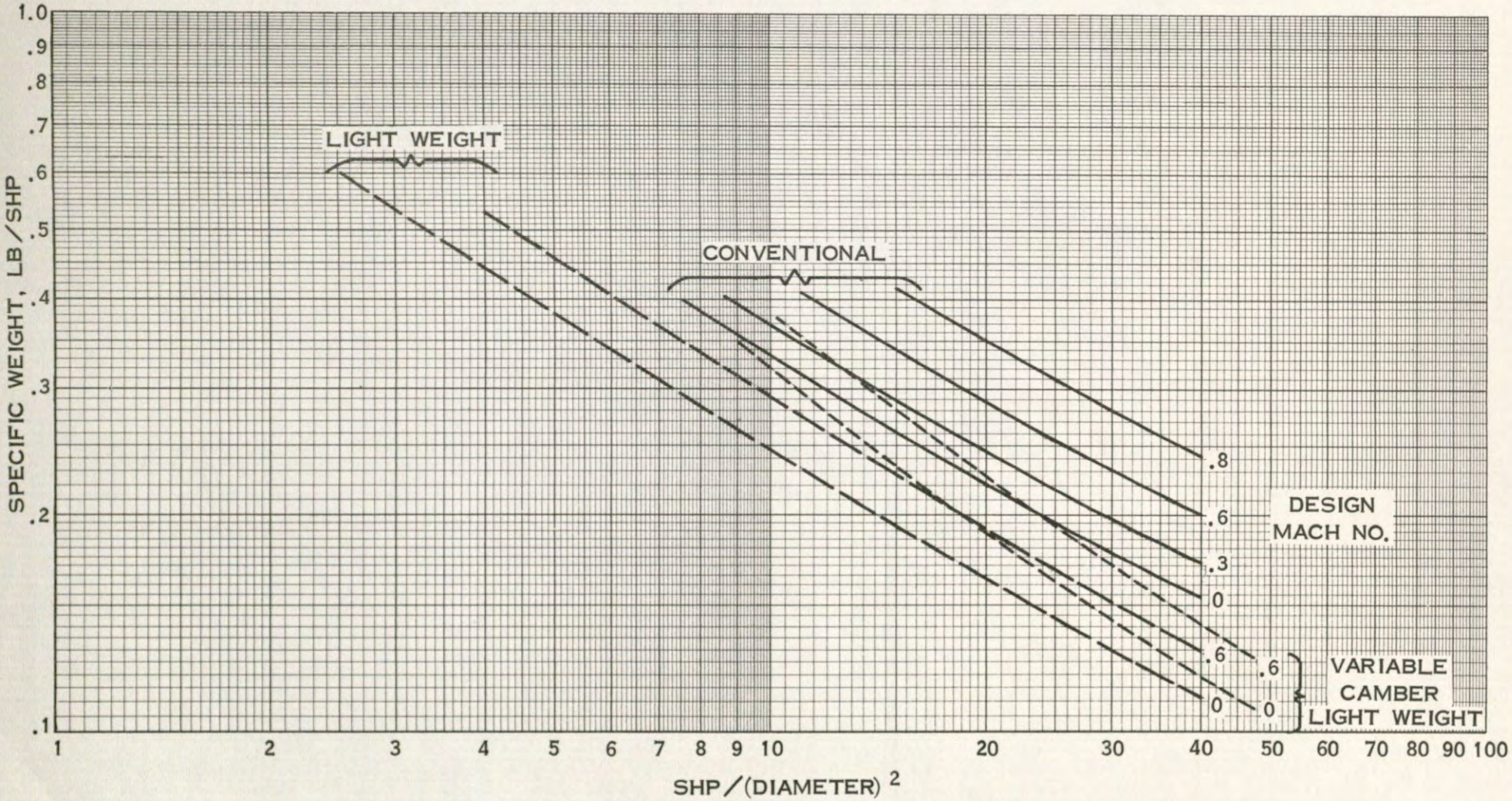

FIG. 3
HAMILTON STANDARD
GEAR BOX WEIGHT GENERALIZATION

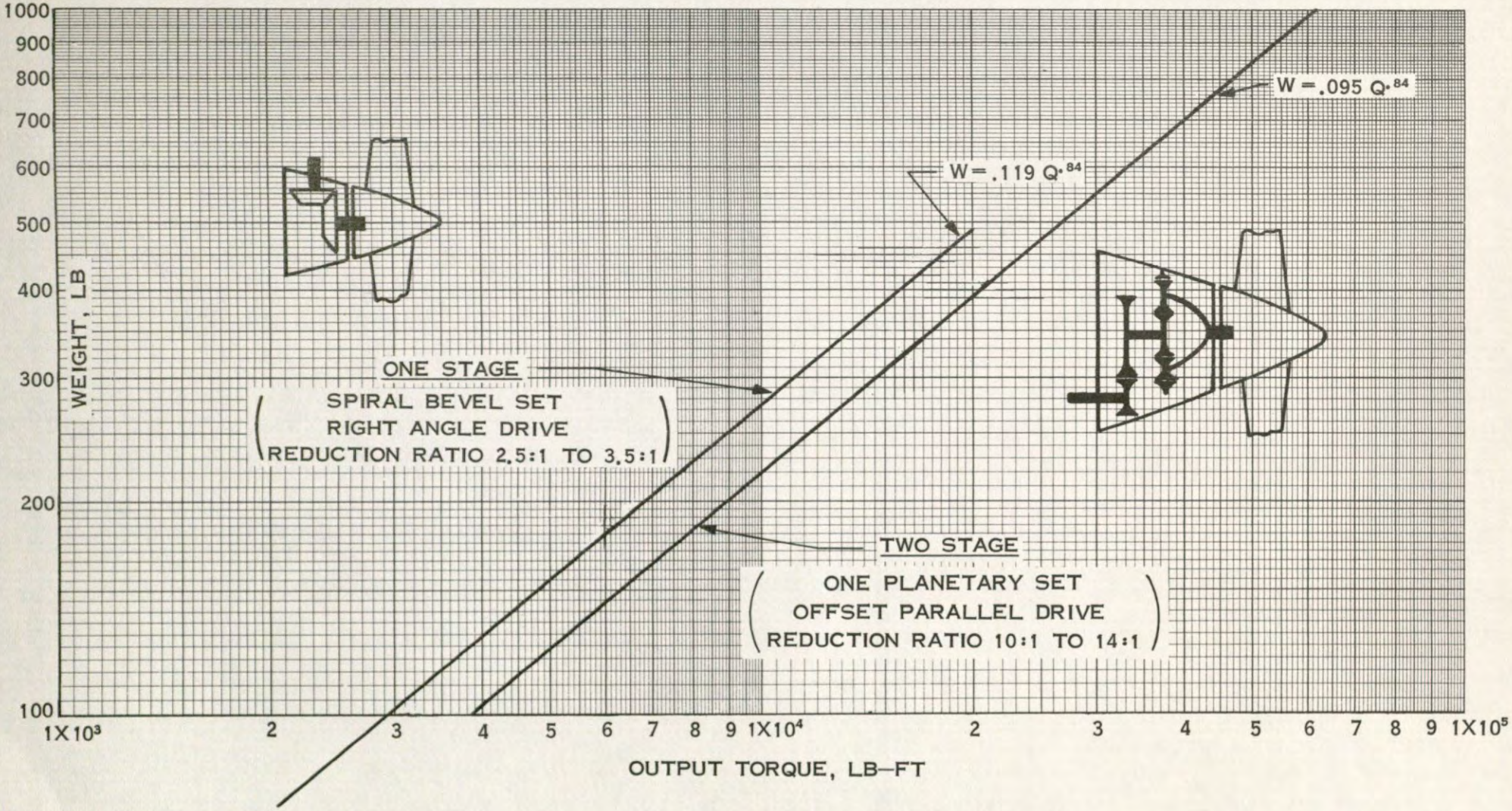

PDB 6101
SUPPLEMENT B

GENERALIZED NACELLE BLOCKING AND COMPRESSIBILITY CORRECTIONS

JANUARY 11, 1963

HAMILTON STANDARD
DIVISION UNITED AIRCRAFT
CORPORATION

NACELLE BLOCKING AND COMPRESSIBILITY CORRECTIONS

In the interests of providing a relatively simple but reliable generalized propeller performance method in the original PDB-6101 manual, certain limitations were imposed which were deemed not to be unduly restrictive. For example, the basic charts were limited to operating conditions (as defined by Figure 1 of PDB-6101) which would not introduce appreciable compressibility losses and were based on uniform axial velocity directly upstream of the propeller disc (no effect of nacelle blocking).

Several users of the manual have indicated a desire for some means, even if only approximate, to account for compressibility and nacelle effects. Accordingly, this supplement is aimed at providing generalized correction factors for compressibility and nacelle blocking effects which are consistent with the simplicity of the computing process of PDB-6101. It must be appreciated, however, that the reliability of these corrections cannot be as high as that of the basic method, but they will provide a proper order of magnitude of these effects.

Figures 1 and 2 present the generalized compressibility correction in terms of airplane Mach number, propeller advance ratio, and blade camber. The reliability of this correction is reasonably good for conditions near peak efficiency for a given advance ratio, but deteriorates somewhat with increase or decrease in power coefficient from this region. This correction presumes a blade design with levels of blade thickness ratio appropriate to a specific range of design Mach number.

The correction for nacelle blocking effect is presented in Figure 3 in terms of propeller advance ratio. A differentiation is made between symmetric annular-inlet nacelles and non-symmetric scoop-inlet nacelles. Obviously, there can be many nacelle shape permutations, but this type of simplified generalization cannot account for their individual effects. This correction adjusts isolated propeller efficiency to the so-called "apparent efficiency" of the propeller operating in front of a nacelle:

$$\eta_{app.} = \frac{\text{Shaft thrust (in presence of nacelle)} \times \text{Free stream velocity}}{\text{Power}}$$

It should be recognized that the propeller, in turn, applies a pressure and velocity increment to the nacelle and these must be accounted for by the airframe manufacturer.

The nacelle blocking effect represented by Figure 3 is purely that of the increase in shaft thrust due to the effective decrease in blade section advance angles with decrease in axial velocity. For high speed applications where the propeller blades may be subject to compressibility losses, the reduced axial velocities due to nacelle blocking also result in lower blade section Mach numbers. The corresponding reduction in blade compressibility losses can be quite significant and accordingly, the effect of representative nacelle blocking has been incorporated in the compressibility correction chart of Figure 1.

(Continued)

The application of these corrections to the efficiency values of PDB-6101 is quite straight forward in accordance with the following equation:

$$\eta_{corrected} = \eta_{PDB-6101} \times F_t \times F_b$$

FIG. 1

GENERALIZED COMPRESSIBILITY CORRECTION

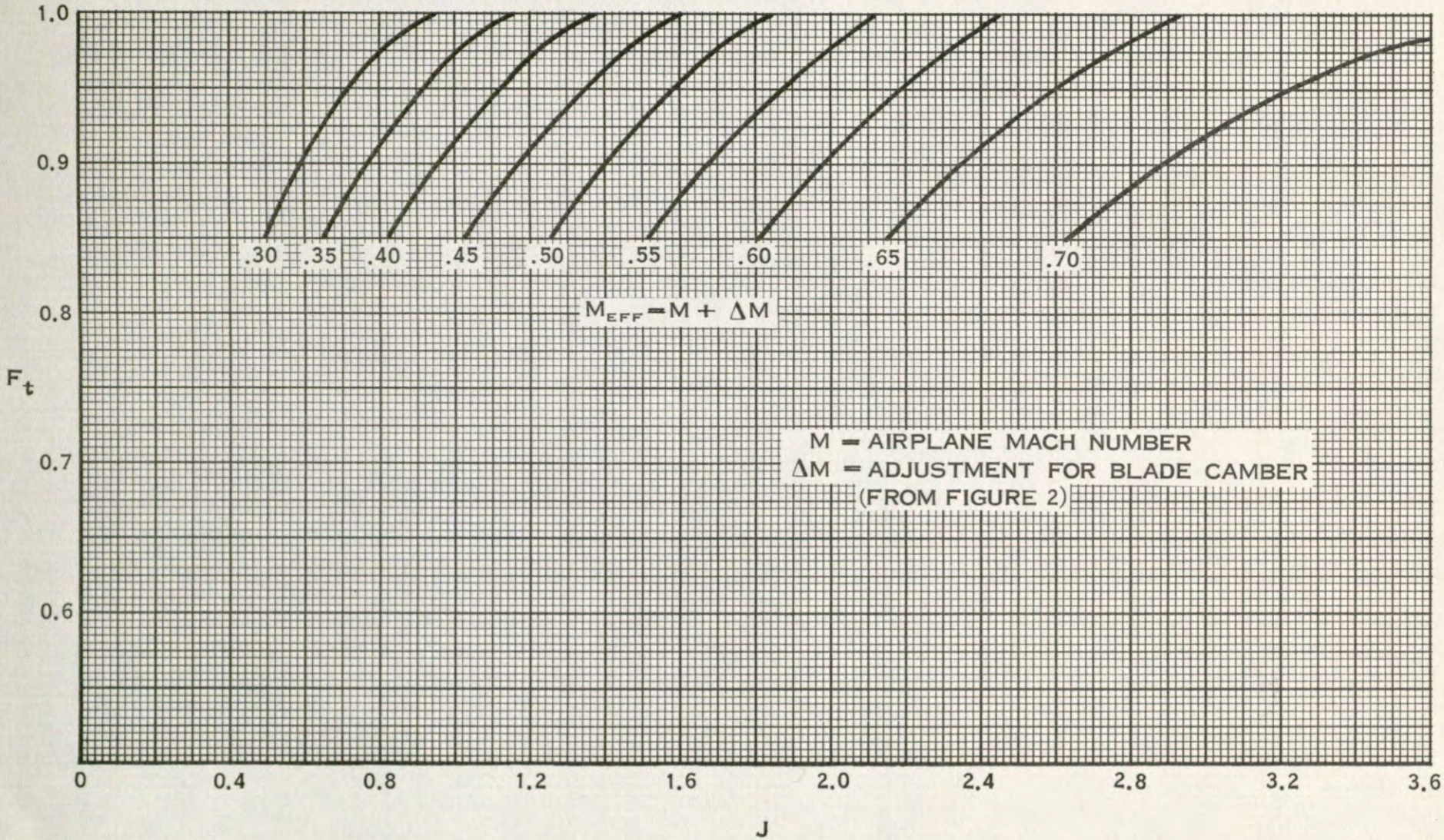

FIG. 2

MACH NUMBER ADJUSTMENT
FOR
EFFECT OF BLADE CAMBER

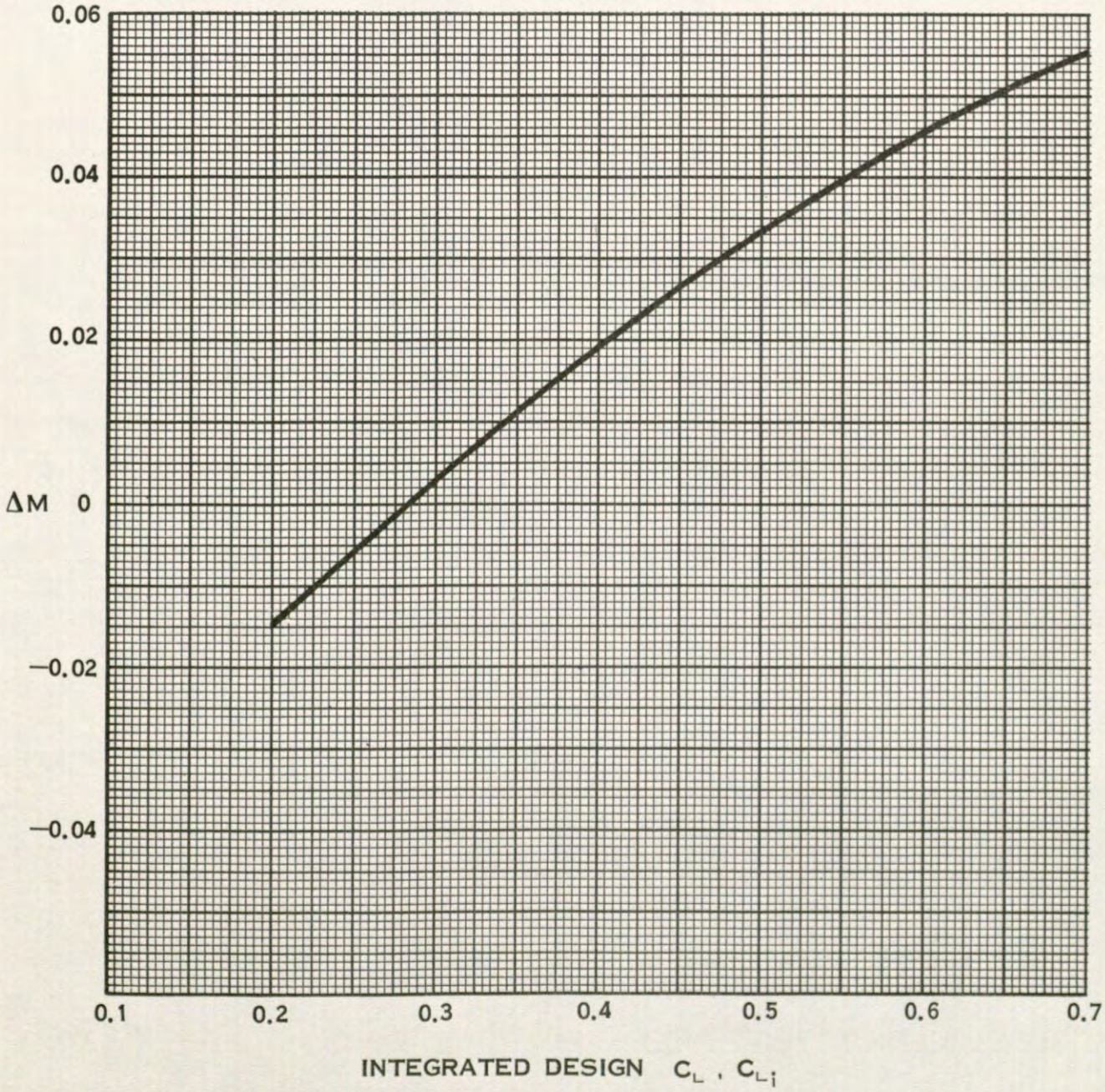

FIG. 3

GENERALIZED NACELLE BLOCKING CORRECTION
FOR
TYPICAL SCOOP AND ANNULAR INLET NACELLES

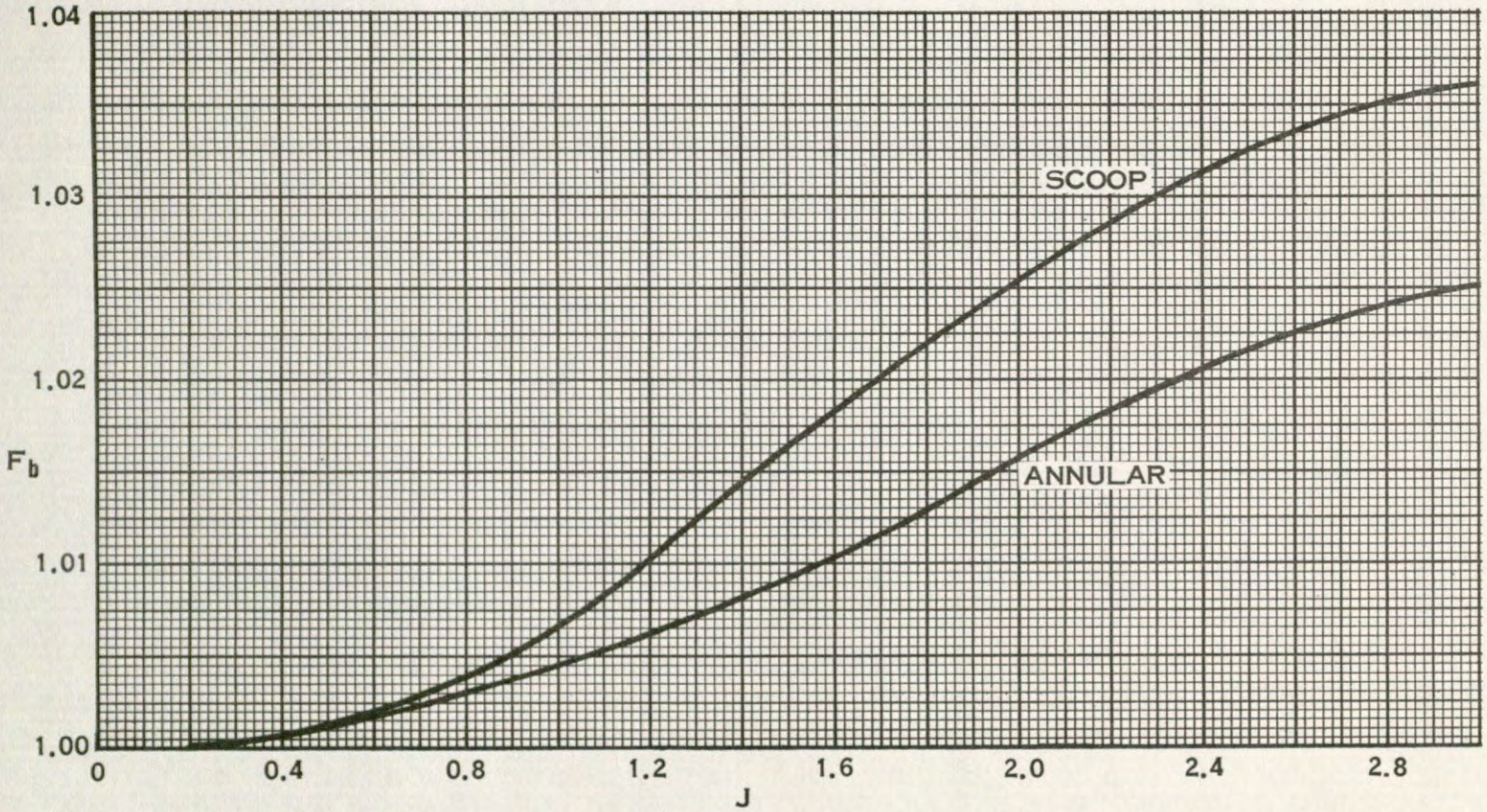

PDB 6101
SUPPLEMENT C

PROPELLER NOISE PREDICTION

FEBRUARY 5, 1963

HAMILTON STANDARD
DIVISION UNITED AIRCRAFT
CORPORATION

PROPELLER NOISE

Although the propeller is a major contributor to the alternating sound pressure fields generated by propeller-driven aircraft, noise considerations have never been important in the design and selection of propellers for a specific installation. This is due to the fact that the effective means of reducing propeller noise, such as reduction of tip speed, reduction in disc loading and increase in number of blades, entail penalties in performance and/or weight of such magnitude as are generally considered prohibitive. However, there has been need for assessment of propeller-generated sound pressure fields in aircraft design, and both theoretical and empirical methods are available for this purpose.

The classical Gutin propeller noise theory is still a reliable means for defining far field propeller noise at zero airspeed and a nomographic presentation of this theory is provided in Figure 1. The use of this chart is described in the attached sample calculation. Reasonable verification of this theory by experimental data has been demonstrated over the years.

Near field propeller noise has not been as convenient for theoretical treatment, and thus such empirical presentations as that presented in NACA Rep. 966 have been considered to be the more effective means of treating this specific area of propeller noise determination.

An experimental program recently conducted by Hamilton Standard on near field sound pressure measurements has shown good agreement with NACA Rep. 966. The test setup is shown in Figure 2 and some typical test results for the fundamental mode are plotted in Figure 3. Frequency spectrum analysis of the test data indicated a total sound pressure level, at the maximum noise point, approximately 4 db higher than that for the fundamental mode. From NACA Rep. 966, such test data can be extended for effects of variation in distance from propeller tip and power loading by factors derived from that report and shown on Figure 4.

These previously described methods are, however, limited to the condition of zero forward airspeed. A method is available (NACA TN 3018 & TN 3809) for calculating the effect of forward speed on the free-space sound pressure field around a propeller. The method involves an input of blade aerodynamic loading at a given operating condition, and computes the complete frequency spectrum of sound pressure generated at any point in the propeller field. The method is quite elaborate and, even when programmed on a high-speed digital computer, involves a considerable computing effort. Thus practical considerations dictate a limitation on the number of calculations to be performed to those conditions which are deemed of primary interest.

The following references are suggested as additional data sources for application in propeller noise prediction:

(Continued)

NACA TM 1195	"On the Sound Field of a Rotating Propeller", by L. Gutin, October 1948.
NACA TN 1354	"Comparison of Sound Emission From Two-Blade, Four-Blade, and Seven-Blade Propellers", by C. W. Hicks & H. H. Hubbard, July 1947.
NACA TN 2968	"Propeller Noise Charts for Transport Airplanes", by H. H. Hubbard, June 1953.
NACA TN 3018	"A Theoretical Study of Forward Speed on the Free-Space Sound Pressure Field Around Propellers", by I. E. Garrick & C. E. Watkins, October 1953.
NACA TN 3809	"A Method for the Calculation of Free-Space Sound Pressures Near a Propeller in Flight Including Considerations of Chordwise Blade Loading", by Watkins & Durling, 1956.
NACA Rep. 996	"Free-Space Oscillating Pressures Near the Tips of Rotating Propellers", by H. H. Hubbard & A. A. Regier, 1950.
NACA RM L51C27	"Sound from a Two-Blade Propeller at Supersonic Tip Speeds", by H. H. Hubbard & L. W. Lassiter, May 8, 1951.
R. A. E. Tech. Note MS19	"Some Propeller Noise Calculations" by K. V. Diprose, 1955.
OSRD Report 1543	"Principles of Sound Control in Airplanes", by L. L. Beranek, 1944.

Journal of the Acoustical Society of America, Volume 5, No. 3, May 1953.

"Handbook of Noise Control", edited by C. M. Harris, McGraw-Hill Book Co., 1957.

NOISE CALCULATION FOR STATIC PROPELLERS

Based upon the Gutin noise theory as presented in C. M. Harris and others.

$$Pm = \frac{169.3\, M_t R_t}{SA}\left(-T\cos\Theta + \frac{.76\, HP}{M_t^2}\right) \quad mBJ_{mB}(.8mBM_t \sin\Theta)$$

where:

M_t	=	tip rotational Mach number - π ND/60c c = speed of sound - fps.
R_t	=	Propeller radius - ft.
S	=	Distance of observer from propeller - ft.
A	=	Propeller disc area πR_t^2 - ft^2
T	=	Propeller static thrust - lbs.
Θ	=	Angular position of observer - degrees
HP	=	Horsepower supplied to propeller
B	=	Number of propeller blades
JmB ( )	=	Bessell function of first kind, order mB and argument ( )
Pm	=	Sound pressure - dynes/cm^2
m	=	Harmonic of sound (m = 1 is fundamental tone)

The total sound pressure = $\sqrt{\sum_{m=1}^{n} Pm^2}$. Usually values of Pm where m>3 do not affect P_{total}.

To convert P_{total} to decibels:

$$I\,(Db) = 20 \log_{10} \frac{P_{total}}{P_{reference}}$$

$P_{reference}$ is the sound pressure at the threshold of hearing (.0002 dynes/cm^2)

$$\text{or} \quad I\,(Db) = 74 + 20 \log_{10} P_{total}$$

To determine the noise level at any distance (S_x) based upon the calculated noise level at distance (S):

$$I_x(Db) = I - 20 \log_{10} \frac{Sx}{S}$$

This assumes no atmospheric attenuation.

(Continued)

For an airplane on the ground at zero airspeed, the sound pressure is doubled by ground reflection. When the sound pressure level (dynes/cm^2) is doubled, the sound level is increased by 6 decibels. This can be seen in the equation: I(Db) = 74 + 20 $\log_{10}$ P_{total} by doubling P_{total}.

Figure 1 is a nomographic presentation of the propeller noise level and is presented because of the length of time required to utilize Gutin's equation. For both the nomograph, and the equation, the 6 decibels mentioned above for ground reflection should be added.

A sample calculation to demonstrate use of propeller noise curve follows:

Propeller	- 4 blades, 15' dia.
Horsepower	- 5000
ND	- 15000
S	- 500'
Θ	- 90°

N_1 - read at 5000 HP and 15' = 40.95
N_3 - read at 500' = -4.45
N_2 - read at mb = 4, 8, 12 and ND = 15000
mb = 4, N_2 = 60.75
mb = 8, N_2 = 51.50
mb = 12, N_2 = 38.80

To obtain the total sound (decibels), each harmonic must be converted into dynes/cm^2 and the square root of the sum of the squares obtained. This total sound pressure is then converted back into decibels; i.e.

mB = 4, $N_1 + N_2 + N_3$ = 97.25 Db = 14.5* dynes/cm^2
mB = 8, $N_1 + N_2 + N_3$ = 88.00 Db = 5.0 dynes/cm^2
mB = 12, $N_1 + N_2 + N_3$ = 75.30 Db = 1.2 dynes/cm^2

* 20 $\log_{10}$ P (dynes/cm^2) = I(Db) -74

$$\therefore P_{total} = \sqrt{(14.5)^2 + (5.0)^2 + (1.2)^2} = 15.4 \text{ dynes/cm}^2$$

and $I_{total} = 74 + 20 \log_{10} 15.4$

$I_{total} = 97.8$ Db.

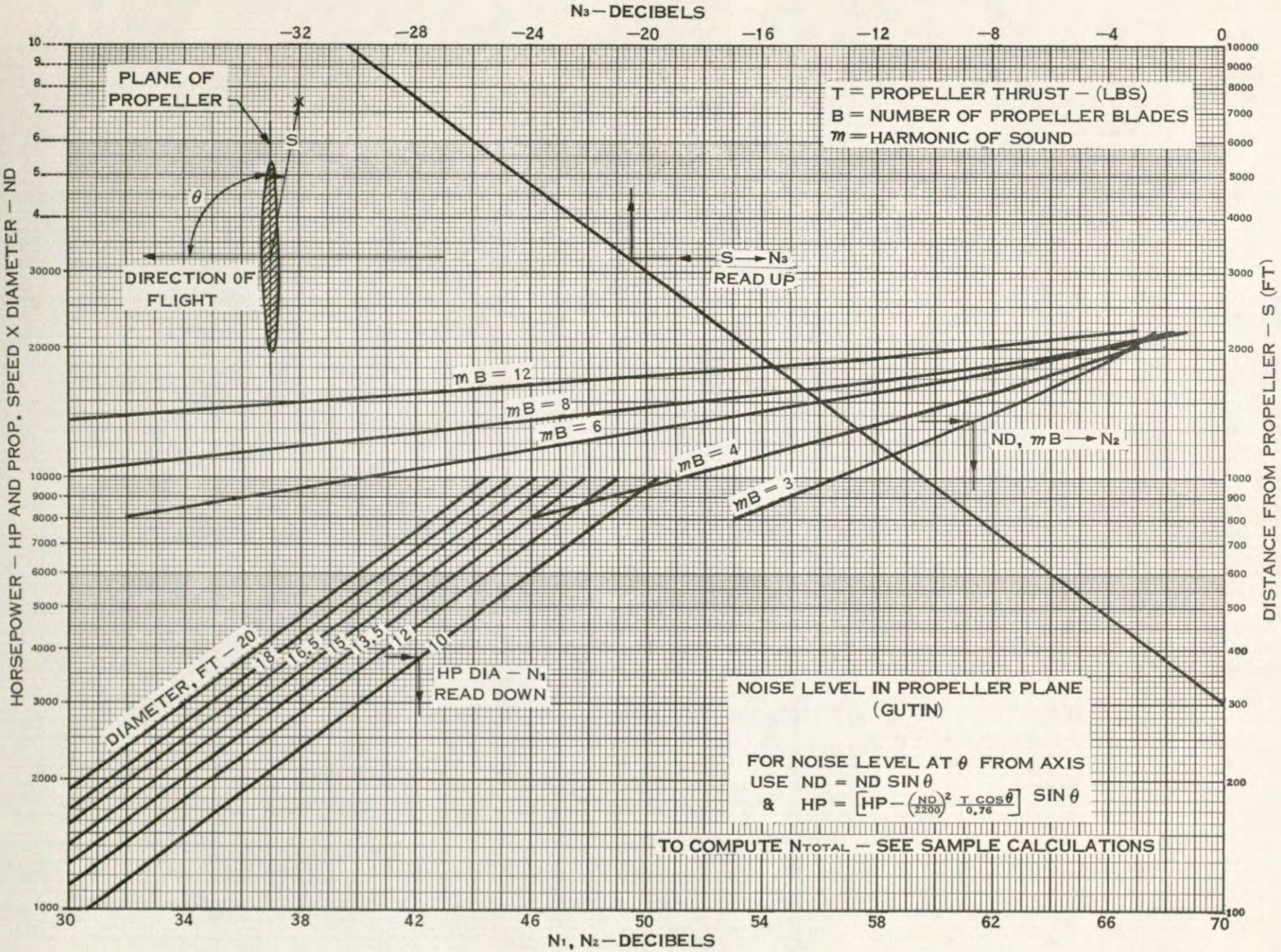
N3 — DECIBELS
−32
−28
−24
−20
−16
−12
−8
−4
0
PLANE OF PROPELLER
S
θ
DIRECTION OF FLIGHT
T = PROPELLER THRUST — (LBS)
B = NUMBER OF PROPELLER BLADES
m = HARMONIC OF SOUND
S → N3
READ UP
m B = 12
m B = 8
m B = 6
m B = 4
m B = 3
ND, m B → N2
DIAMETER, FT — 20
18
16.5
15
13.5
12
10
HP DIA — N1
READ DOWN
NOISE LEVEL IN PROPELLER PLANE
(GUTIN)
FOR NOISE LEVEL AT θ FROM AXIS
USE ND = ND SIN θ
& HP = [HP − (ND/2200)² (T COS θ / 0.76)] SIN θ
TO COMPUTE NTOTAL — SEE SAMPLE CALCULATIONS
HORSEPOWER — HP AND PROP. SPEED X DIAMETER — ND
DISTANCE FROM PROPELLER — S (FT)
N1, N2 — DECIBELS
30
34
38
42
46
50
54
58
62
66
70

FIGURE 1

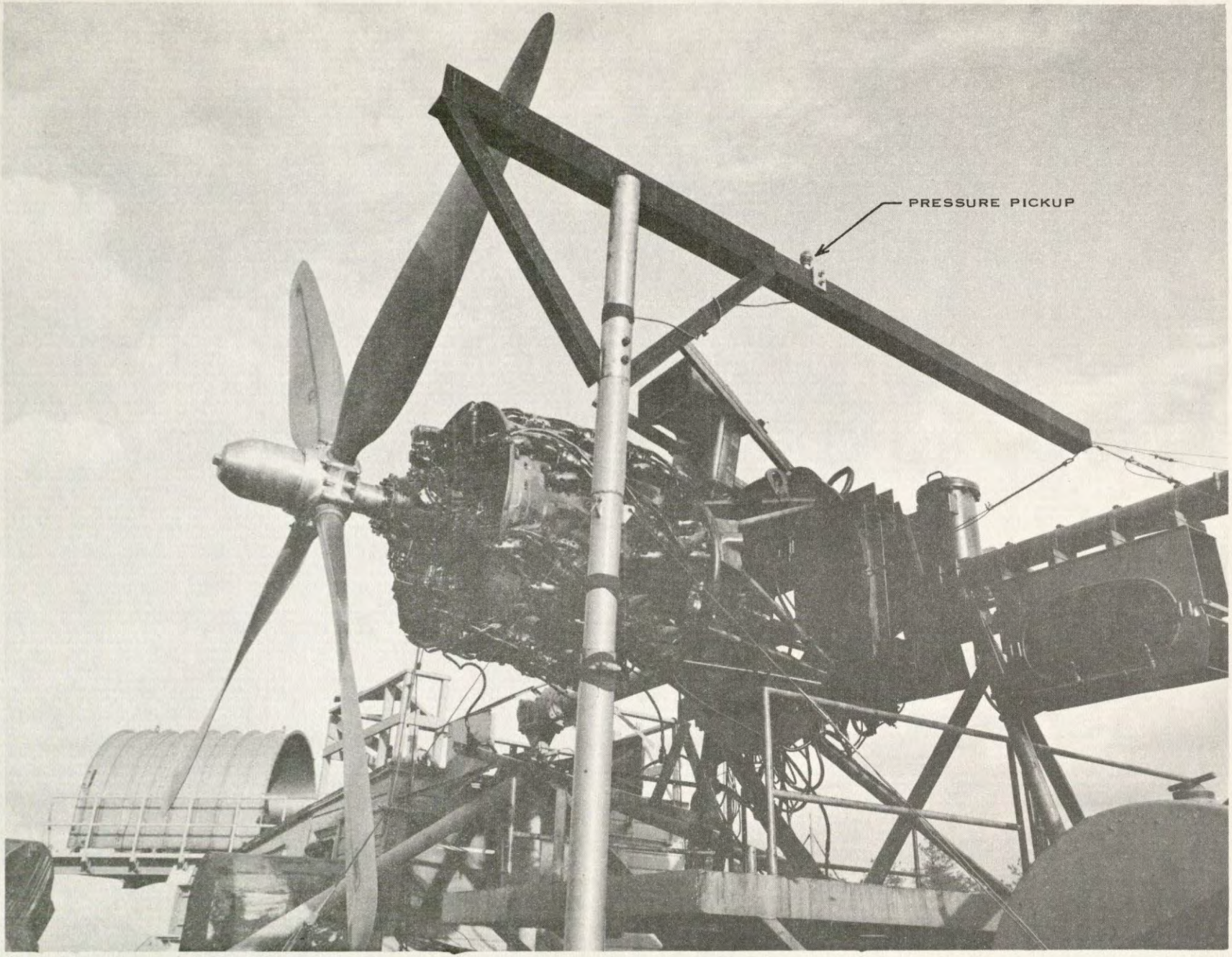

NEAR FIELD SOUND PRESSURE TEST
FIGURE 2

FULL SCALE PROPELLER NOISE MEASUREMENTS

AT BLADE PASSAGE FREQUENCY (4P)
ALONG LINE PARALLEL TO PROPELLER SHAFT
ONE FOOT FROM THE BLADE TIP
APPROX. 11 FEET ABOVE THE GROUND

PROPELLER: 4 – BLADED, 15.0′ DIAMETER
AF = 101.5, C_{Li} = .498
CONDITION: 2100 SHP, 1000 FT/SEC. TIP SPEED

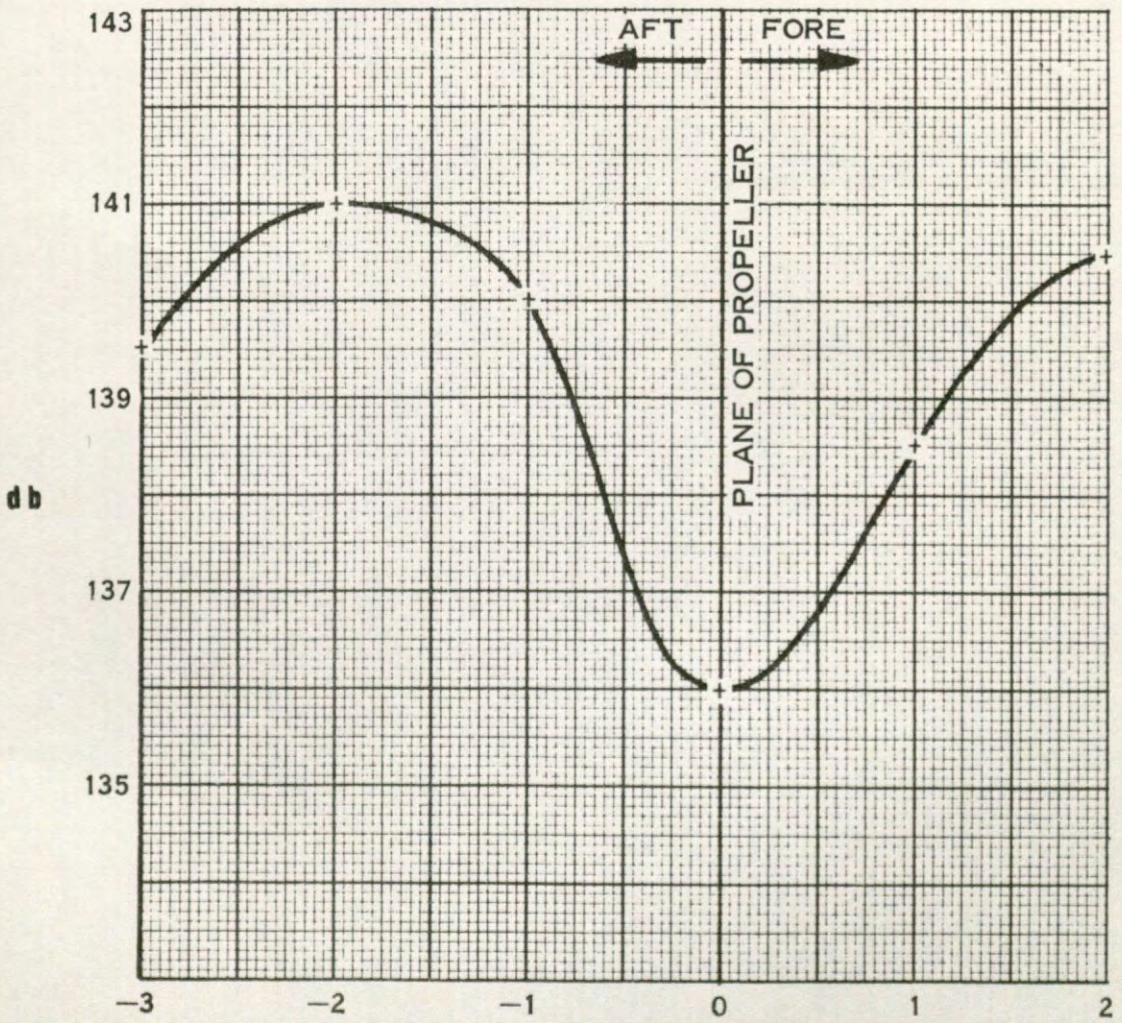

FORE AND AFT DISTANCE FROM PLANE OF PROPELLER, FEET

FIGURE 3

EFFECT OF VARIATION IN POWER LOADING
ON PROPELLER NOISE LEVEL

(FROM NACA TR 996)

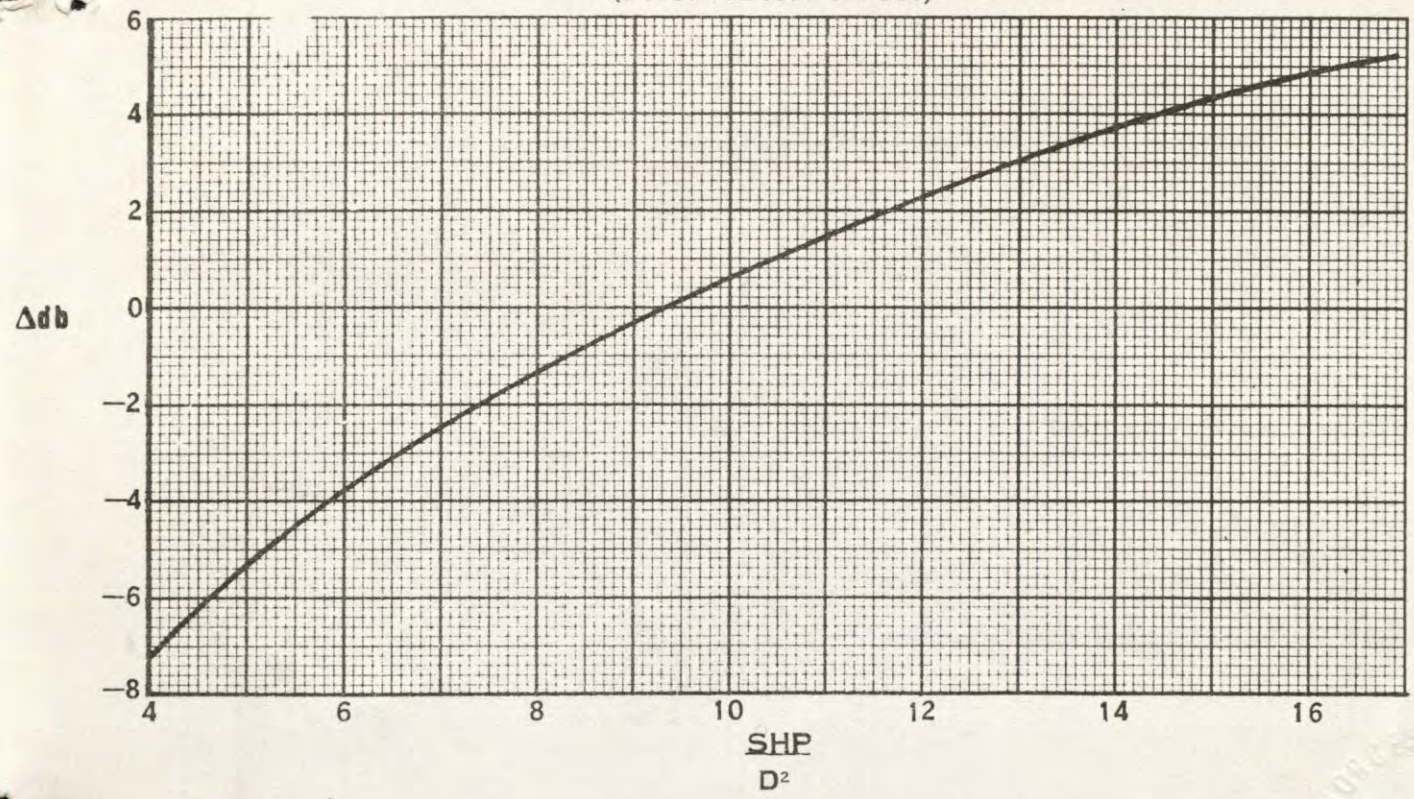

EFFECT OF VARIATION IN DISTANCE FROM BLADE TIP
ON PROPELLER NOISE LEVEL

(FROM NACA TR 996)

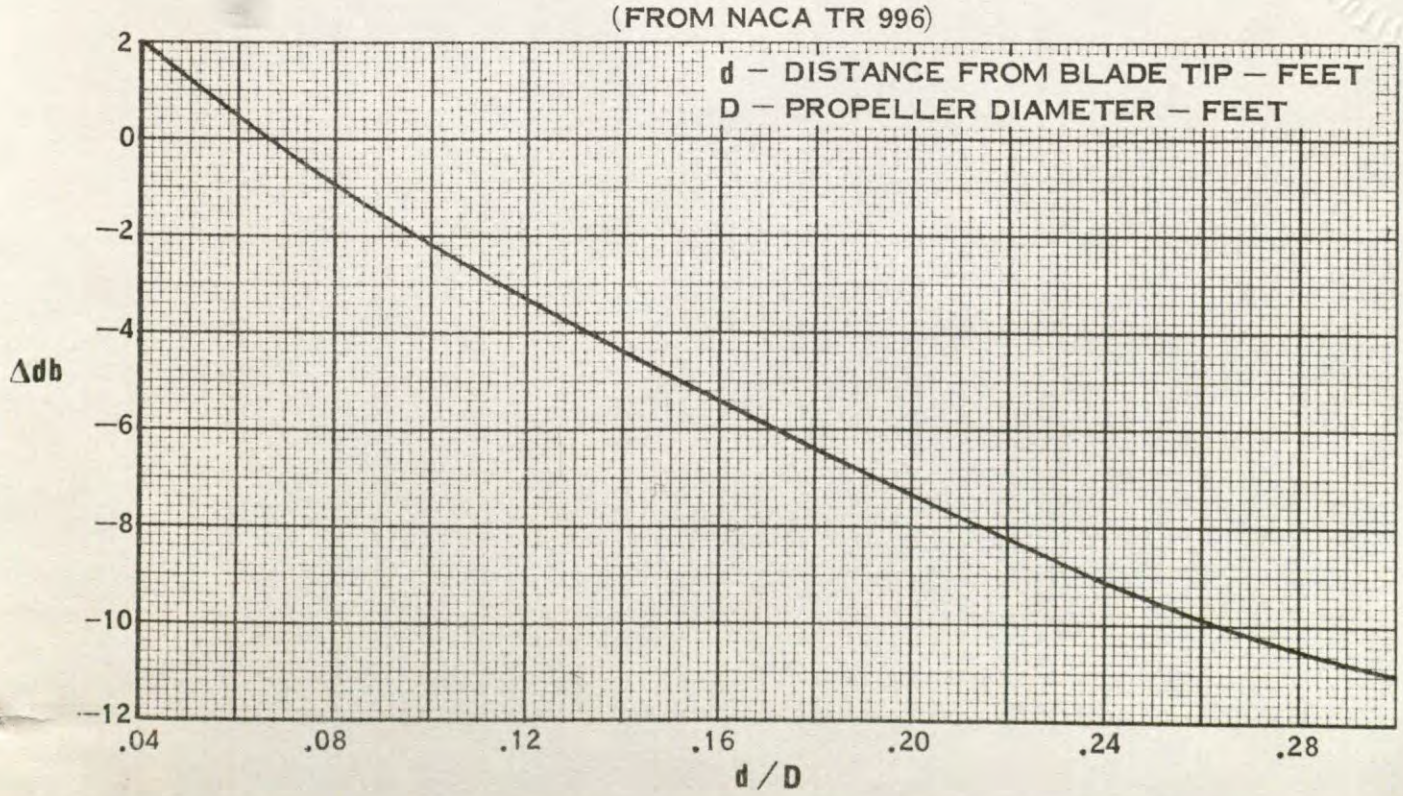

FIGURE 4

WORCESTER POLYTECHNIC INSTITUTE LIBRARY